INFORMATION TO USERS

This manuscript has been reproduced from the microfilm master. UMI films the text directly from the original or copy submitted. Thus, some thesis and dissertation copies are in typewriter face, while others may be from any type of computer printer.

The quality of this reproduction is dependent upon the quality of the copy submitted. Broken or indistinct print, colored or poor quality illustrations and photographs, print bleedthrough, substandard margins, and improper alignment can adversely affect reproduction.

In the unlikely event that the author did not send UMI a complete manuscript and there are missing pages, these will be noted. Also, if unauthorized copyright material had to be removed, a note will indicate the deletion.

Oversize materials (e.g., maps, drawings, charts) are reproduced by sectioning the original, beginning at the upper left-hand corner and continuing from left to right in equal sections with small overlaps.

ProQuest Information and Learning
300 North Zeeb Road, Ann Arbor, MI 48106-1346 USA
800-521-0600

University of Alberta

Early to Late Events in Peroxisome Biogenesis

by 

Yuen Yi Chris Tam

A thesis submitted to the Faculty of Graduate Studies and Research in partial fulfillment of the requirements for the degree of Doctor of Philosophy

Department of Cell Biology

Edmonton, Alberta

Fall 2005

ABSTRACT

Peroxisomes are organelles essential for normal human development and physiology. This fact is underscored by the lethality of a group of disorders collectively called the peroxisome biogenesis disorders in which peroxisomes fail to assemble properly. Peroxins are proteins required for peroxisome assembly and are encoded by the *PEX* genes. This thesis describes the identification and characterization of Pex24p and Pex27p of the yeasts *Yarrowia lipolytica* and *Saccharomyces cerevisiae*, respectively, and the initiation of peroxisome formation from a subdomain of the ER by Pex3p in *S. cerevisiae*.

PEX24 was identified by functional complementation of a peroxisome assembly mutant with a genomic library. It encodes Pex24p, a protein of 550 amino acids, with a predicted molecular mass of 61,100 Da. Pex24p is an integral membrane protein of peroxisomes, and its levels are significantly increased by incubation of cells in oleic acid-containing medium. Mutations in *PEX24* lead to mislocalization of peroxisomal proteins to the cytosol and accumulation of membrane structures that contain subsets of peroxisomal proteins. These results suggest a role for Pex24p in the import of peroxisomal matrix and membrane proteins.

PEX27 was uncovered by database mining based on *PEX25*, which was identified previously by transcriptome profiling. Pex27p is a homolog of Pex25p. Both proteins share sequence similarities to a previously identified peroxin, Pex11p. Unlike Pex11p and Pex25p, Pex27p is constitutively expressed in wild-type cells grown in oleic acid-containing medium. Peroxisomes are greatly enlarged in cells harboring either single or

double deletions of *PEX11/PEX25/PEX27*. Yeast two-hybrid analyses showed that Pex27p interacts with Pex25p and itself, Pex25p interacts with Pex27p and itself, and Pex11p interacts only with itself. Overexpression of *PEX27*, *PEX25* or *PEX11* led to peroxisome proliferation and the formation of small peroxisomes. Together these data demonstrate a role for Pex27p in controlling peroxisome size and number in *S. cerevisiae*.

The *de novo* formation of peroxisomes was also studied. The amino-terminal 46 amino acids of Pex3p can target to a subdomain of the endoplasmic reticulum (ER) in cells lacking peroxisomes. Confocal video microscopy showed that this ER compartment can import both peroxisomal matrix and membrane proteins leading to the formation of *bona fide* peroxisomes through the continued activity of full-length Pex3p. This process is dependent on *PEX14* and *PEX19*, which are required for the targeting of peroxisomal matrix and membrane proteins, respectively. These results point to a direct role for the ER in *de novo* peroxisome formation.

ACKNOWLEDGEMENTS

I deeply thank Dr. Rick Rachubinski for giving me an excellent opportunity to work in his laboratory. It is a great honour for me to be the 16th Ph.D. graduate of Rick's. He values my ideas and allows me to work independently. His constant encouragement and enthusiasm have led me through the graduate program. I have learned tremendously from him. I am a better person and scientist because of him. He really is the best supervisor I have ever had (I have had more than two!). Rick has put together a world-class Cell Biology department. I feel extremely lucky to be able to meet and/or work with many talented scientists.

I would also like to thank the Department of Cell Biology, the Alberta Heritage Foundation for Medical Research, the Faculty of Graduate Studies and Research, and the Faculty of Medicine and Dentistry for the financial support provided throughout my studies.

I am grateful to our excellent technical staff, Honey Chan, Hanna Kroliczak, Rick Poirier, Elena Savidov and Dwayne Weber. They have eased my life both in and outside the lab. I especially thank Hanna and Honey for sharing many of my problems. I am going to miss them a lot.

It has been a pleasure to work with the fellow students and postdocs in the lab, both past and present, Roger Bascom, Jenny Chang, Melissa Dobson, Andrei Fagarasanu, Monica Fagarasanu, Cleofe Hurtado, Barbara Knoblach, Gareth Lambkin, David Lancaster, Martine Ooms (I call her Miss Yap or YQ), Oleh Petriv (I call him James sometimes and he knows why), Jennifer Smith, Vladimir Titorenko, Juan Carlos Torres

and Franco Vizeacoumar. Juan Carlos and Jennifer, two very nice people, taught me many things. I am lucky to have them as my teachers. I owe them a lot.

Finally, I am extremely grateful to my family. My grandparents have given me tremendous support, even though they have no clue what I am doing. My parents and sisters have supported me financially. I especially thank Joyce for her support and encouragement everyday. She contributed a lot to Figure 4-4 H. She measured the area of over 700 cells during her Christmas holiday. I certainly don't want to leave out my cat who has accompanied me from Montreal to this boring land.

TABLE OF CONTENTS

LIST OF TABLES

LIST OF FIGURES

LIST OF SYMBOLS AND ABBREVIATIONS

20KgP	pellet obtained from centrifugation at 20,000 × *g*
20KgS	supernatant obtained from centrifugation at 20,000 × *g*
250KgP	pellet obtained from centrifugation at 250,000 × *g*
250KgS	supernatant obtained from centrifugation at 250,000 × *g*
4D	four dimensional
AAA	ATPase associated with various cellular activities
AOX	acyl-CoA oxidase
bp	base pair
BSA	bovine serum albumin
Ca	*Candida albicans*
Cb	*Candida boidinii*
CFP	cyan fluorescent protein
CHO	Chinese Hamster Ovary
CoA	coenzyme A
COP	coat protein
Da	dalton
DMF	N,N-Dimethylformamide
dNTP	deoxyribonucleoside triphosphate
DsRed	*Discosoma sp.* red fluorescent protein
ECL	Enhanced Chemiluminescence
ER	endoplasmic reticulum
g	gram
g	gravitational force
G6PDH	glucose-6-phosphate dehydrogenase
GFP	green fluorescent protein
h	hour
HRP	horseradish peroxidase
Hp	*Hansenula polymorpha*
Hsp	heat shock protein
ICL	isocitrate lyase
IgG	immunoglobulin G
IPTG	isopropyl β-D-thiogalactoside
MBP	maltose binding protein
mPTS	membrane protein peroxisomal targeting signal
mRFP	monomeric red fluorescent protein
OD	optical density
OLE	ability to use oleic acid as the sole carbon source
ole	inability to use oleic acid as the sole carbon source
ORF	open reading frame
pA	protein A
PAGE	polyacrylamide gel electrophoresis

PBD	peroxisome biogenesis disorder
PCR	polymerase chain reaction
PEX#	wild-type gene encoding Pex#p
pex#	mutant *PEX#* gene
PMP	peroxisomal membrane protein
PNS	post-nuclear supernatant
Pp	*Pichia pastoris*
PTS	peroxisome targeting signal
RNase	ribonuclease
Sc	*Saccharomyces cerevisiae*
SDS	sodium dodecyl sulphate
sec	second
TCA	Trichloroacetic acid
THI	thiolase
TPR	tetratricopetide repeat
U	unit of enzyme activity
v	volume
w	weight
X-gal	5-bromo-4-chloro-3-indolyl-β-D-galactopyranoside
YFP	yellow fluorescent protein
Yl	*Yarrowia lipolytica*

CHAPTER 1

INTRODUCTION

1.1 Peroxisomes

Peroxisomes were first described as spherical microbodies by electron microscopy of mouse kidney cells (Rhodin, 1954). Later, these organelles were isolated by de Duve and Baudhuin using density gradient centrifugation and shown to contain oxidases and catalase to break down hydrogen peroxide to water and molecular oxygen (de Duve and Baudhuin, 1966). These organelles were renamed peroxisomes based on the chemical reactions that take place inside them. Since then, the biochemistry of peroxisomes and their roles in human physiology have been increasingly defined. Peroxisomes belong to the microbody family of organelles, which also includes the glyoxysomes of plants and the glycosomes of trypanosomes. They are roughly spherical with a diameter of 0.1 to 1 μm, are delimited by a single membrane and house more than 50 different enzymes (reviewed in Lazarow and Fujiki, 1985; Subramani, 1998; Purdue and Lazarow, 2001; Titorenko and Rachubinski, 2001; Brosius and Gärtner, 2002; Eckert and Erdmann, 2003). Peroxisomes do not contain DNA nor any protein synthesis machinery. Therefore, all peroxisomal proteins are encoded by nuclear genes, synthesized on free polysomes in the cytosol and imported into peroxisomes post-translationally.

1.2 Functions of peroxisomes

Peroxisomes perform a diverse set of functions in eukaryotic cells depending on the cell type (reviewed in Purdue and Lazarow, 2001; Titorenko and Rachubinski, 2001; Eckert and Erdmann, 2003). Two well conserved functions are hydrogen peroxide respiration and fatty acid β-oxidation (Figure 1-1). In yeast, peroxisomes have roles in the

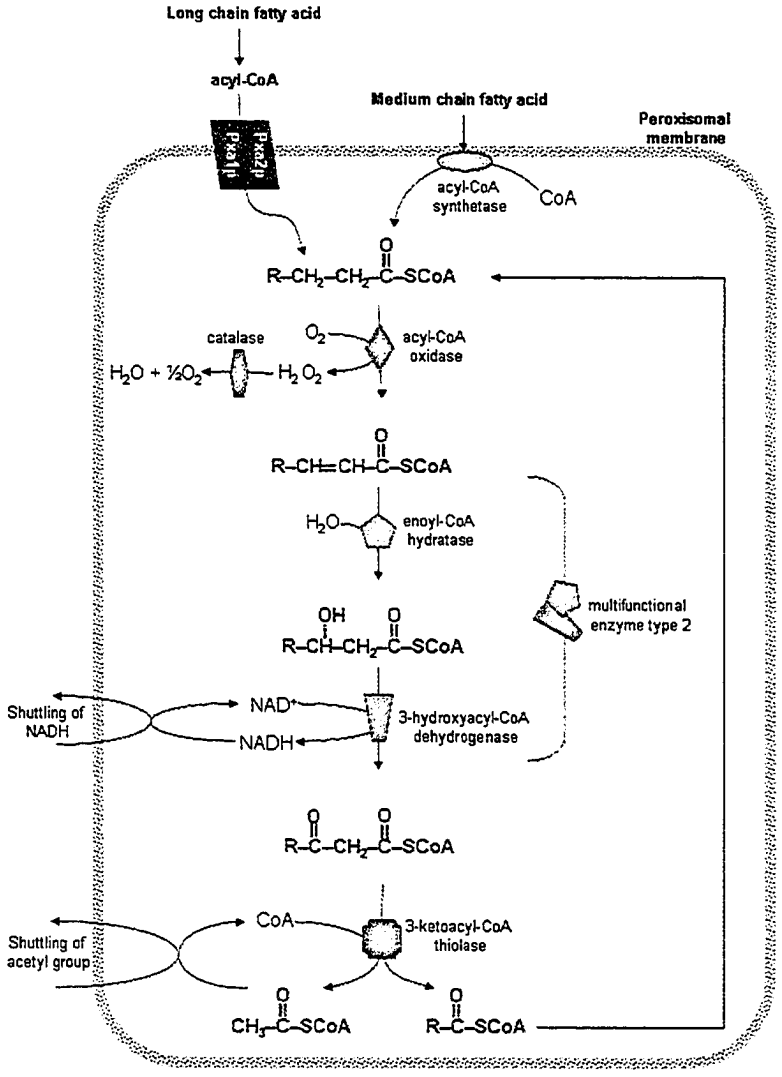

Figure 1-1. Schematic representation of β-oxidation in yeast peroxisomes. Note that multifunctional enzyme type 2 contains enoyl-CoA hydratase and 3-hydoxyacyl-CoA dehydrogenase activities.

biosynthesis of lysine, the catabolism of amino acids and methanol, and the glyoxylate cycle. In mammals, peroxisomes take part in the biosynthesis of plasmalogens, polyunsaturated fatty acids, cholesterol and bile acids, and the degradation of amino acids, purines and polyamines. In plants, peroxisomes play roles in photorespiration and the glyoxylate cycle. In fungi, peroxisomes are involved in the biosynthesis of penicillin and also the glyoxylate cycle.

Peroxisomes exhibit remarkable flexibility to cope with its various functions. Their size, number and enzyme content vary with different environmental conditions and metabolic needs. When yeast cells are transferred from culture medium containing glucose to culture medium containing a carbon source such as oleic acid (*Candida albicans*, *Candida boidinii*, *Pichia pastoris*, *Saccharomyces cerevisiae* and *Yarrowia lipolytica*) or methanol (*Hansenula polymorpha*, *C. boidinii* and *P. pastoris*), the metabolism of which requires peroxisomes, the cells respond to this change by increasing the synthesis of peroxisomal proteins (Veenhuis and Harder, 1987; van der Klei and Veenhuis, 1997). This result is always accompanied by an increase in peroxisome size and number. Also, the administration of peroxisome proliferators such as hypolipidemic drugs, plasticizers, fatty acid analogs, herbicides, industrial solvents and anti-inflammatory drugs to rats can lead to increases in the size and number of peroxisomes and to elevated levels of peroxisomal proteins (Reddy and Mannaerts, 1994).

1.3 Peroxisomal disorders

The importance of peroxisomes to human physiology and development is underscored by the severity and often lethality of a group of inherited disorders in which

peroxisomes of affected individuals are compromised. One in 20,000 to 100,000 newborn babies is diagnosed with one of these disorders (Gould *et al.*, 2001). These disorders are grouped into two major categories (Lazarow and Moser, 1994; Gould *et al.*, 2001; Brosius and Gärtner, 2002; Weller *et al.*, 2003). The first category is the peroxisome biogenesis disorders (PBDs), which include Zellweger syndrome, neonatal adrenoleukodystrophy, infantile Refsum disease, rhizomelic chondrodysplasia punctata and hyperpipecolic acidemia. Patients suffering from these diseases have multiple defects in peroxisome function and do not survive beyond their first few years. Their clinical phenotypes are usually craniofacial abnormalities, severe hypotonia, global developmental delay, and neurological and hepatic dysfunctions. Biochemical phenotypes include high levels of phytanic acid and very-long chain fatty acids, mislocalization of peroxisomal matrix enzymes to the cytosol and reduced levels of plasmalogens (Brosius and Gärtner, 2002; Weller *et al.*, 2003). Individual *PEX* genes are affected in PBDs. So far, there are at least 12 complementation groups identified indicating that at least 12 *PEX* genes are responsible for PBDs (Table 1-1) (Brosius and Gärtner, 2002; Weller *et al.*, 2003; Matsumoto *et al.*, 2003).

The second category is the single-enzyme deficiencies in which an individual peroxisomal enzyme is defective, but overall peroxisome assembly is unaffected. Examples of this category include X-linked adrenoleukodystrophy, adult Refsum disease and deficiencies in individual enzymes of the β-oxidation pathway. This category is characterized by a range of milder symptoms depending on the gene affected (Lazarow and Moser, 1994; Brosius and Gärtner, 2002).

1.4 Pathways of peroxisome assembly

Peroxisome assembly can be defined conceptually to be composed of three pathways, namely the formation of the peroxisomal membrane, the import of proteins into peroxisomes and the proliferation of peroxisomes. A total of 32 *PEX* genes have been identified in yeasts, plants, mammals and humans that encode 32 proteins called peroxins. Theses peroxins all play different roles in the pathway of peroxisome assembly. Their characteristics and proposed functions are listed in Table 1-1.

Table 1-1. Peroxins and their proposed functions

Peroxin	Characteristics and functions	PBD group
Pex1p	Cytosolic and/or peripherally associated with peroxisomal precursors. Member of the AAA-ATPase family. Interacts with Pex6p. Required for fusion of early peroxisomal precursors.	1
Pex2p	Integral to peroxisomal membrane. Member of the RING-finger complex. Required for peroxisomal matrix protein import.	10
Pex3p	Integral to peroxisomal membrane. Interacts with Pex19p. Required for assembly of peroxisomal membrane.	12
Pex4p	Ubiquitin conjugating enzyme. Peripherally associated with outer face of peroxisomal membrane. Interacts with Pex22p. Required for peroxisomal matrix protein import.	
Pex5p	Cytosolic and peroxisome-associated. PTS1 receptor. Contains TPR motifs at its carboxyl terminus.	2
Pex6p	Cytosolic and peripherally associated with peroxisomal precursors. Member of the AAA-ATPase family. Interacts with Pex1p. Required for fusion of early peroxisomal precursors.	4
Pex7p	Cytosolic and peroxisome-associated. PTS2 receptor. Member of WD-40 family.	11
Pex8p	Peroxisomal matrix and peripherally associated with inner face of peroxisomal membrane. Interacts with Pex5p. Required for peroxisomal matrix protein import.	
Pex9p	Integral to peroxisomal membrane. Required for peroxisomal matrix protein import.	

Pex10p	Integral to peroxisomal membrane. Member of the RING-finger complex. Interacts with itself, Pex4p, Pex12p and Pex22p. Required for peroxisomal matrix protein import.	7
Pex11p	Peripherally associated with peroxisomal membrane. Interacts with itself and Pex19p. Has similarity to *S. cerevisiae* Pex25p and Pex27p. Required for peroxisome proliferation.	
Pex12p	Integral to peroxisomal membrane. Member of the RING-finger complex. Interacts with Pex5p, Pex10p, Pex13p and Pex14p. Required for peroxisomal matrix protein import.	3
Pex13p	Integral to peroxisomal membrane. Contains SH3 domain. Part of receptor docking complex. Interacts with Pex5p, Pex7p and Pex14p. Required for peroxisomal matrix protein import.	13
Pex14p	Peripherally associated with peroxisomal membrane. Part of receptor docking complex. Interacts with Pex5p, Pex7p, Pex13p and Pex17p. Required for peroxisomal matrix protein import.	
Pex15p	Integral to peroxisomal membrane. Interacts with Pex6p. Required for peroxisomal matrix protein import.	
Pex16p	Integral to peroxisomal membrane. Required for peroxisome proliferation and/or assembly of peroxisome membrane.	9
Pex17p	Peripherally associated with outer face of peroxisomal membrane. Part of receptor docking complex. Interacts directly with Pex14p. Required for peroxisomal matrix protein import.	
Pex18p	Cytosolic and peroxisome-associated. Involved in PTS2 pathway. Functionally redundant with Pex21p. Interacts with Pex7p. Has similarity to *Y. lipolytica* Pex20p.	
Pex19p	Cytosolic and peroxisome-associated. Farnesylated. Interacts with Pex3p. Required for stability and import of numerous peroxisomal membrane proteins and/or assembly of peroxisomal membrane.	14
Pex20p	Cytosolic and peroxisome-associated. Interacts with Pex8p. Required for thiolase oligomerization and import.	
Pex21p	Cytosolic and peroxisome-associated. Involved in PTS2 pathway. Functionally redundant with Pex18p. Interacts with Pex7p. Has similarity to *Y. lipolytica* Pex20p.	
Pex22p	Integral to peroxisomal membrane. Anchors Pex4p on peroxisomal membrane. Required for peroxisomal matrix protein import.	
Pex23p	Integral to peroxisomal membrane. Required for peroxisomal matrix protein import. Has similarity to *S. cerevisiae* Pex30p, Pex31p and Pex32p.	

Pex24p	Integral to peroxisomal membrane. Required for peroxisomal matrix and membrane protein import. Has similarity to *S. cerevisiae* Pex28p and Pex29p.	
Pex25p	Peripherally associated with peroxisomal membrane. Interacts with itself and Pex27p. Has similarity to Pex11p and Pex27p. Required for peroxisome proliferation.	
Pex26p	Integral to peroxisomal membrane. Associates with Pex1p and Pex6p to recruit them to peroxisomal membrane.	8
Pex27p	Peripherally associated with peroxisomal membrane. Interacts with itself and Pex25p. Has similarity to Pex11p and Pex25p. Required for peroxisome proliferation.	
Pex28p	Integral to peroxisomal membrane. Has similarity to Pex29p and *Y. lipolytica* Pex24p. Required for peroxisome morphology and distribution.	
Pex29p	Integral to peroxisomal membrane. Has similarity to Pex28p and *Y. lipolytica* Pex24p. Required for peroxisome morphology and distribution.	
Pex30p	Integral to peroxisomal membrane. Has similarity to Pex31p, Pex32p and *Y. lipolytica* Pex23p. Interacts with itself, Pex29p, Pex31p and Pex32p. Functions as a negative regulator of peroxisome size.	
Pex31p	Integral to peroxisomal membrane. Has similarity to Pex30p, Pex32p and *Y. lipolytica* Pex23p. Interacts with itself and Pex30p. Functions as a negative regulator of peroxisome size.	
Pex32p	Integral to peroxisomal membrane. Has similarity to Pex30p, Pex31p and *Y. lipolytica* Pex23p. Interacts with itself and Pex30p and Pex28p. Functions as a negative regulator of peroxisome size.	

1.4.1 Protein import into peroxisomes

Peroxisomal matrix and membranes proteins are encoded by nuclear genes, synthesized on free polysomes in the cytosol and imported into peroxisomes post-translationally via different molecular mechanisms involving different proteins (Lazarow and Fujiki, 1985; Subramani, 1993, 1998; Subramani *et al.*, 2000; Purdue and Lazarow,

2001; Eckert and Erdmann, 2003). A schematic representation of peroxisome division and protein import into peroxisomes is shown in Figure 1-2.

1.4.1.1 Import of matrix proteins

Most matrix proteins are targeted to the peroxisome by one of two types of peroxisome targeting signal (PTS). PTS1 is a carboxyl-terminal tripeptide with the consensus sequence (S/A/C)(K/R/H)(L/M/F) (Gould *et al.*, 1988, 1989, 1990; Aitchison *et al.*, 1991; Swinkels *et al.*, 1992) and is found in the majority of matrix proteins. PTS2 is a sometimes cleaved amino-terminal nonapeptide with the consensus motif (R/K)(L/V/I)X_5(H/Q)(L/A), which is found in a smaller subset of matrix proteins (Osumi *et al.*, 1991; Swinkels *et al.*, 1991; Glover *et al.*, 1994; Waterham *et al.*, 1994).

Pex5p and Pex7p are the receptors for PTS1- and PTS2-containing proteins, respectively. Pex5p contains tetratricopetide (TPR) repeats, which are direct repeats of a 34-amino acid TPR motif and thought to mediate protein-protein interactions. In fact, it has been reported that the TPR domain of Pex5p binds to the PTS1 of cargo proteins (Brocard *et al.*, 1994; Dodt *et al.*, 1995; Szilard and Rachubinski, 2000; Gatto *et al.*, 2000). Pex7p, on the other hand, contains WD repeats, which are 40-amino acid repeats of tryptophan-aspartate motif and act as a site for protein-protein interaction. Pex5p and Pex7p interact with their respective substrates or cargos in the cytosol and then target them to the peroxisomes. Interestingly, the receptor for a PTS2-containing enzyme, thiolase, in *Y. lipolytica* is Pex20p (Titorenko *et al.*, 1998). The role of Pex7p in this yeast is yet to be determined. Unlike in the PTS1 pathway in which the receptor-cargo complex is composed of Pex5p and its cargo only, formation of a competent receptor-cargo

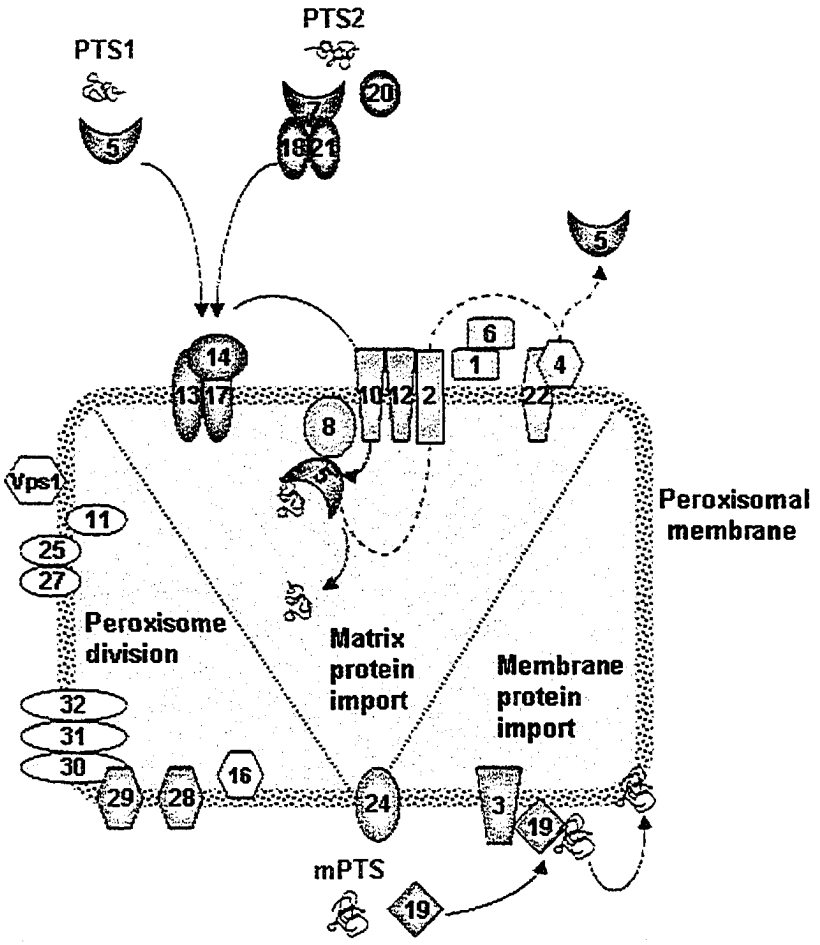

Figure 1-2. Schematic representation of peroxisome division and protein import into peroxisomes. Peroxins are shown by their Pex number. Solid arrows represent paths of protein targeting to peroxisomes. The broken arrow represents the receptor recycling pathway. Note that only the recycling of the PTS1 receptor is shown. This diagram includes two novel peroxins, Pex24p and Pex27p, described in this thesis.

complex for the PTS2 pathway apparently requires Pex18p and Pex21p, which have been shown to interact with Pex7p in *S. cerevisiae* (Purdue *et al.*, 1998; Stein *et al.*, 2002).

The receptor-cargo complex binds to components of the docking machinery at the peroxisomal membrane. The docking machinery consists of the integral membrane proteins Pex13p and Pex14p, and the peripheral membrane protein Pex17p (reviewed by Subramani, 1998; Hettema *et al.*, 1999; Terlecky and Fransen, 2000; Purdue and Lazarow, 2001; Titorenko and Rachubinski, 2001). Both Pex5p and Pex7p bind to Pex13p and Pex14p (Albertini *et al.*, 1997; Girzalsky *et al.*, 1999). The interaction between Pex14p and Pex5p or Pex7p is direct, suggesting that the PTS1 and PTS2 import pathways are not independent but overlapping and converge at Pex14p at the peroxisomal membrane (Albertini *et al.*, 1997).

The next step in the import pathway for matrix proteins is the translocation of the receptor-cargo complex across the peroxisomal membrane into the peroxisomal matrix and the recycling of the receptor back to the cytosol. Members of the RING-finger family – Pex2p, Pex10p and Pex12p – have been speculated to act as a translocon (Dodt and Gould, 1996; Chang *et al.*, 1999a; Okumoto *et al.*, 2000; Otera *et al.*, 2000). Pex12p has been shown to interact with Pex10p and Pex5p (Chang *et al.*, 1999a; Okumoto *et al.*, 2000). Mammalian cells bearing mutation in Pex12p (Dodt and Gould, 1996; Otera *et al.*, 2000) or Pex2p (Otera *et al.*, 2000) accumulate Pex5p inside peroxisomes. Other proteins are likely to be involved in recycling of the receptor. *H. polymorpha* cells deleted for *PEX4* display an accumulation of Pex5p inside peroxisomes (van der Klei *et al.*, 1998). Also, it is believed that Pex22p recruits and anchors Pex4p on the peroxisomal membrane (Koller *et al.*, 1999). Epistasis studies in *P. pastoris* indicate that Pex1p and Pex6p also

function in the translocation machinery upstream of Pex4p and Pex22p (Collins *et al.*, 2000). Pex8p, an intraperoxisomal protein, also has a role in receptor recycling. It interacts with Pex5p in *S. cerevisiae*, and the absence of Pex8p abolishes both PTS1 and PTS2 protein import (Rehling *et al.*, 2000). It also interacts with Pex20p in *Y. lipolytica*, and cells lacking Pex8p show association of usually cytosolic Pex20p with peroxisomes (Smith and Rachubinski, 2001).

It should be mentioned that a few peroxisomal matrix proteins are targeted by internal PTSs, which remain largely uncharacterized (Purdue *et al.*, 1990; Kragler *et al.*, 1993; Elgersma *et al.*, 1995). Recently, *S. cerevisiae* and *H. polymorpha* acyl-CoA oxidases have been demonstrated to target to the peroxisomal matrix via a Pex5p-dependent mechanism that does not require the TPR domains of Pex5p (Klein *et al.*, 2002; Gunkel *et al.*, 2004).

1.4.1.2 Import of membrane proteins

The pathway of targeting peroxisomal membrane proteins (PMPs) to the peroxisomal membrane is less well defined; however, it appears to be independent of the pathway for matrix protein targeting. The targeting signals of PMPs (mPTSs) that target and insert PMPs into the peroxisomal membrane have been elucidated for a few proteins in various organisms. They could be generalized as motifs consisting of stretches of basic amino acids or a mixture of basic and hydrophobic residues (McCammon *et al.*, 1994; Dyer *et al.*, 1996; Elgersma *et al.*, 1997; Pause *et al.*, 2000; Baerends *et al.*, 2000). Pex19p has been a candidate for the import receptor and/or chaperone of PMPs, as it interacts with and is required for the stability of a number of PMPs in different organisms

(Sacksteder *et al.*, 2000; Snyder *et al.*, 2000; Fransen *et al.*, 2001; Hettema *et al.*, 2000; Rottensteiner *et al.*, 2004). Recently, two classes of mPTSs have been proposed (Jones *et al.*, 2004). Class 1 mPTSs are bound by Pex19p and function in import in a Pex19p-dependent manner, whereas Class 2 mPTSs are not bound by Pex19p and function in targeting PMPs to peroxisomes independently of Pex19p. The only protein that contains a Class 2 mPTS is Pex3p (Jones *et al.*, 2004). Based on this distinctive feature of Pex3p, the same authors have further found that Pex3p functions as a docking factor for Pex19p. They showed that Pex3p interacts specifically with Pex19p and is required for recruitment of Pex19p to the peroxisomal membrane and other heterologous organelles (Fang *et al.*, 2004). How exactly PMPs are inserted into the peroxisomal membrane and if other yet unidentified proteins are involved in this process remain to be elucidated.

1.4.2 Peroxisome division

Peroxisome division can be categorized into two types: constitutive division and regulated division (Marshall *et al.*, 1996). Peroxisomes undergo constitutive division to maintain a proper number of peroxisomes in cells. New peroxisomes have to be made when the cell divides, as well as when old peroxisomes are turned over by pexophagy. In contrast, peroxisomes undergo regulated division when external stimuli are present. External stimuli can be a carbon source such as oleic acid and methanol for yeasts or peroxisome proliferators for mammals (see Section 1.2). Peroxisomes have to increase in number in order to accommodate the elevated levels of peroxisomal enzymes or proteins that are induced by these stimuli. Little is known about the mechanisms regarding the constitutive division of peroxisomes; however, several molecular players and how they

might act in the regulated division of peroxisomes have been proposed in animals and yeasts.

Pex11 protein members including yeast Pex11p and mammalian Pex11α, β and γ are not required for the import of matrix proteins. But cells lacking Pex11p have fewer but larger peroxisomes than normal (Erdmann and Blobel, 1995; Marshall *et al.*, 1995; Sakai *et al.*, 1995; Schrader *et al.*, 1998; Li and Gould, 2002; Li *et al.*, 2002). Also, oversynthesis of Pex11p leads to the formation of numerous small peroxisomes (Marshall *et al.*, 1995; Schrader *et al.*, 1998; Li and Gould, 2002; Li *et al.*, 2002). These observations strongly suggest that Pex11p acts as a positive regulator of peroxisome division. A model was proposed as to how Pex11p might control division (Marshall *et al.*, 1996). In *S. cerevisiae*, Pex11p is a monomer sitting on the inner side of the peroxisomal membrane of dividing peroxisomes, but it homodimerizes in mature peroxisomes. By switching between these two protein states, Pex11p might activate peroxisome division in its monomeric form by promoting membrane fission from inside the organelle and stop the process in its dimeric form, which could result from the rearrangement of the environment inside the mature peroxisome (Marshall *et al.*, 1996).

Other proteins in the yeast *S. cerevisiae* have also been implicated in controlling peroxisome size and number. Cells lacking the dynamin-related protein Vps1p (Hoepfner *et al.*, 2001) or the peroxin Pex25p (Smith *et al.*, 2002) contain fewer and enlarged peroxisomes. Peroxisomes in cells deleted for *PEX28* and/or *PEX29* are more in number and smaller in size than wild-type peroxisomes, and are often clustered together (Vizeacoumar *et al.*, 2003). In cells lacking Pex30p, number of peroxisomes is increased, but the morphology of peroxisomes appears to be normal. Also, peroxisomes in cells

deleted for *PEX31* or *PEX32* exhibit enlarged peroxisomes (Vizeacoumar *et al.*, 2004). How they function in peroxisome division is still not clear.

In *Y. lipolytica*, peroxisome division is negatively regulated by Pex16p (Eitzen *et al.*, 1997). Cells deleted for *PEX16* lack morphologically recognizable peroxisome, but cells overproducing Pex16p contain enlarged peroxisomes (Eitzen *et al.*, 1997). Recently, a mechanism involving Pex16p and the peroxisomal matrix enzyme, acyl-CoA oxidase (AOX), has been proposed for peroxisome division in *Y. lipolytica* (Guo *et al.*, 2003). AOX is imported into the matrix of peroxisomes. When the peroxisome grows to reach a certain size, AOX is redistributed to the peroxisomal membrane where it interacts with Pex16p. It is believed that the interaction between Pex16p and AOX removes the inhibition effect of Pex16p on peroxisome division, thereby allowing mature peroxisomes to divide (Guo *et al.*, 2003).

Metabolic processes also have an effect on peroxisome division. Loss of the enzymatic activity of AOX (van Roermund *et al.*, 2000; Chang *et al.*, 1999b), fatty acyl-CoA synthetase (van Roermund *et al.*, 2000), and/or multifunctional enzyme (MFE2) (Chang *et al.*, 1999b; Smith *et al.*, 2000) leads to marked alterations in peroxisome size and number. The molecular mechanism underlying the metabolic control of peroxisome division remains to be elucidated.

1.4.3 Formation of the peroxisomal membrane

Under normal conditions in wild-type cells, it is widely accepted that peroxisomes form from budding or division of existing peroxisomes. Little is known about the very early events of peroxisome biogenesis, particularly the formation of the peroxisome

membrane in cells which are devoid of any existing peroxisomes. Out of the 32 peroxins, only Pex3p, Pex16p and Pex19p have been shown to have specific roles in the biogenesis of the peroxisome membrane. Human cells lacking any of these peroxins contain neither peroxisomes nor peroxisome remnants (Honsho *et al.*, 1998; Matsuzono *et al.*, 1999; South and Gould, 1999; Ghaedi *et al.*, 2000; Sacksteder *et al.*, 2000), while cells of *S. cerevisiae* deleted for either *PEX3* or *PEX19* appear to lack any type of identifiable peroxisomal structure (Höhfeld *et al.*, 1991; Götte *et al.*, 1998). Functional peroxisomes that were considered to form by *de novo* peroxisome synthesis were observed upon reintroduction of the *PEX3*, *PEX16* and *PEX19* genes into their respective mutant cells (Matsuzono *et al.*, 1999; South and Gould 1999; Sacksteder *et al.*, 2000; South *et al.*, 2000; 2001); however, the ultimate source of these newly made peroxisomes remains undefined.

So from where could the peroxisomal membrane derive? Evidence implicating the endoplasmic reticulum (ER) in peroxisome biogenesis has increased in recent years (reviewed in Tabak *et al.*, 1999; Titorenko and Rachubinski, 2001; Eckert and Erdmann, 2003). The amino-terminal 16 amino acids of the peroxisomal integral membrane protein Pex3p of *H. polymorpha* were shown to be sufficient to target a reporter protein to the ER (Baerends *et al.*, 1996), while treatment of cells of this yeast with Brefeldin A led to the accumulation of newly synthesized peroxisomal membrane and matrix proteins at the ER (Salomons *et al.*, 1997). In the yeast *Y. lipolytica*, the peroxisomal membrane proteins Pex2p and Pex16p were shown to traffic through the ER and to acquire core *N*-linked glycosylation (Titorenko *et al.*, 1997). Findings supporting *de novo* peroxisome biogenesis in close association with the ER were obtained in cells of *Y. lipolytica*

temperature-sensitive for Pex3p function (Bascom *et al.*, 2003), and studies in the plant *Arabidopsis* showed that peroxisomal ascorbate peroxidase localized to a subdomain of rough ER that could serve as a compartment for post-translational sorting to peroxisomes (Lisenbee *et al.*, 2003). In mouse dendritic cells, the peroxisomal membrane proteins Pex13p and PMP70 were found in subdomains of the ER that extended to a peroxisomal reticulum from which mature peroxisome arose (Geuze *et al.*, 2003).

In contrast to the above lines of evidence pointing to the ER as a source of the peroxisomal membrane, experiments in mammalian cells have shown that the targeting of the membrane proteins Pex2p, Pex3p and Pex16p to peroxisomes was unaffected in cells blocked in COPI- or COPII-mediated vesicular transport (South *et al.*, 2000; Voorn-Brouwer *et al.*, 2001). Furthermore, inactivation of the ER translocation machinery components Sec61p and Ssh1p in *S. cerevisiae* cells did not have an effect on peroxisome biogenesis (South *et al.*, 2001). Therefore, the source of the peroxisomal membrane in cells lacking any pre-existing peroxisomes remains an open question and a subject of debate.

1.5 Approaches to study peroxisome assembly

Molecular players involved in peroxisome assembly have been identified using several approaches in various model organisms.

1.5.1 *In vitro* assays

In vitro assays have provided some insights into the targeting and import of proteins into yeast peroxisomes (Thieringer *et al.*, 1991), mammalian peroxisomes

(Imanaka *et al.*, 1987; Walton *et al.*, 1995) and plant glyoxysomes (Baker, 1996; Brickner *et al.*, 1997; Crookes and Olsen, 1998; Pool *et al.*, 1998). These assays usually employ isolated peroxisomes of rat liver cells, semi-permeabilized mammalian cells or microinjection of mammalian cells (Terlecky and Fransen, 2000). These techniques have unveiled energy and cytosolic requirements for protein import into peroxisomes. For example, Pex14p, Hsp70 and Hsp90 were shown to be involved in peroxisomal protein import in plants (Lopez-Huertas *et al.*, 1999; Crookes and Olsen, 1998). Also, *in vitro* import assays have demonstrated that unfolding of import substrates is not necessary for peroxisomal protein import (Walton *et al.*, 1995). However, these *in vitro* import assays have so far failed to work well in yeasts. A major difficulty is the fragility of yeast peroxisomes.

1.5.2 Genetic screens

Genetic screens of cultured Chinese Hamster Ovary (CHO) and yeast mutants to identify genes involved in peroxisome assembly have been a great success. Cultured CHO mutant cells affected in plasmalogen synthesis were initially shown to be defective in peroxisome assembly (Tsukamoto *et al.*, 1990). Tsukamoto and co-workers developed a method to identify the underlying affected genes that were responsible for the mutant phenotypes (Tsukamoto *et al.*, 1991). They transfected CHO mutant cells with a genomic library and then assayed for the complementation of the plasmalogen deficiency. The complementing gene was then isolated and its sequence determined.

A similar approach has been taken using various yeasts. It was reported that the proliferation of peroxisomes was induced by growth of *S. cerevisiae* cells on medium

containing oleic acid (Veenhuis *et al.*, 1987). Unlike mammalian cells, the only site for β-oxidation in yeasts is peroxisomes (Figure 1-1) (Kunau *et al.*, 1988). Therefore, growth of yeast cells on medium containing a sole carbon source which undergoes β-oxidation in peroxisomes provides a simple and rapid measurement for possible peroxisomal abnormalities. Yeast mutants are isolated by their inability to grow on oleic acid or methanol. Mutants affected in peroxisome assembly are then selected based on abnormal peroxisome morphology and/or mistargeting of peroxisomal proteins. The first peroxisome assembly mutants were identified using this method by Erdman *et al.*, (1989). Complementation analysis as described above for CHO cells is then employed to identify the affected genes. Genetic screening was extended to the use of different yeasts such as *H. polymorpha*, *P. pastoris* and *Y. lipolytica*. To date, 20 *PEX* genes were identified using this method.

1.5.3 Genomics and proteomics

A proteomic approach has been used to identify novel peroxisomal proteins. *S. cerevisiae* Pex11p and Pex13p were identified by isolation of a subcellular fraction enriched for peroxisomal membranes and partial sequencing of the abundant proteins present in that fraction (Erdmann and Blobel, 1995; Marshall *et al.*, 1995; Erdmann and Blobel, 1996).

Upon completion of the *S. cerevisiae* genome, global biology or high throughput approaches have facilitated and accelerated studies in various aspects of yeast biology. Transcriptome profiling of cells incubated in oleic acid-containing medium, which allows for the proliferation of peroxisomes, versus cells incubated in glucose-containing

medium, which suppresses peroxisome proliferation, has been used to predict gene involvement in peroxisome biogenesis or function (Smith *et al.*, 2002). This study uncovered a novel gene, *PEX25*, involved in the regulation of peroxisome size and number. This gene could not have been identified by a classical genetic screen of mutant cells defective in oleic acid metabolism, because cells deleted for *PEX25* display only a minor growth defect on medium containing oleic acid as the sole carbon source (Smith *et al.*, 2002).

Recently, a study combined classical subcellular fractionation and large-scale quantitative mass spectrometry to provide a quantitative assessment of the contribution of proteins to peroxisomal subcellular fractions of *S. cerevisiae* (Marelli *et al.*, 2004). This revealed the involvement of Rho1p in peroxisome biogenesis, specifically in actin organization on the peroxisomal membrane. Although Rho1p is known to associate with membranes in the secretory pathway, it is recruited to the membrane of peroxisomes whose proliferation is induced (Marelli *et al.*, 2004).

Global analysis of protein localization also provides insights into the identification of novel potential peroxisomal proteins. O'Shea and co-workers constructed and examined a collection of yeast strains expressing full-length proteins fused at their carboxyl terminus with green fluorescent protein (GFP) from their endogenous gene promoters (Huh *et al.*, 2003). This study provided localization information for 70% of proteins whose localization was previously unknown. Among these proteins, one protein of unknown function, Ymr204p, was shown to be peroxisomal. Characterization of this protein is currently in progress in our laboratory.

1.5.4 Modern fluorescent microscopy

GFP, its variants yellow fluorescent protein (YFP) and cyan fluorescent protein (CFP), and *Discosoma* sp. red fluorescent protein (DsRed) have been used extensively as reporters in cell biology research and revolutionized the study of cellular dynamics. These fluorescent proteins have some problems that could affect the interpretation of cellular observations. For example, GFP variants homodimerize (Ward, 1998), and DsRed requires a long maturation time and form homotetramers (Baird *et al.*, 2000). New and improved fluorescent proteins have become available over the last couple of years, such as fast-maturing DsRed (Bevis and Glick, 2002), monomeric red fluorescent protein (mRFP) (Campbell *et al.*, 2002), a more photostable mRFP and different hues of mRFP (Shaner *et al.*, 2004).

Three-dimensional time lapse (4D) live cell imaging has become a routine experimental tool in cell biology (Hammond and Glick, 2000). Using fluorescent proteins as reporters, a stack of fluorescence and/or confocal images of a sample is captured at each time point in a 4D experiment. A video is generated by combining stacks of images sequentially. This powerful tool has been used recently to show *de novo* formation of transitional ER sites in *P. pastoris* (Bevis *et al.*, 2002). Our laboratory is currently using this technique to study peroxisome inheritance, an important process of peroxisome biogenesis.

1.6 Using yeasts as a model system

Yeasts are excellent model systems in which to study peroxisome assembly for a number of reasons. The molecular components and interactions that make up a cell are

conserved between yeasts and humans; therefore, experiments using yeasts can provide tremendous insights into human biology. The manipulation of yeasts is easy. Both genetic and biochemical tools for studying yeasts are very well established. The completion of the *S. cerevisiae* and *Y. lipolytica* genomes has facilitated global gene and protein analyses. The *Saccharomyces* Genome Deletion Project (Winzeler *et al.*, 1999) has constructed a unique library of gene-disruption mutants covering 96% of the yeast genome. This collection of knock-out strains provides a unique tool for the functional analysis of the yeast genome. Also, collections of *S. cerevisiae* strains that express full-length proteins tagged with either a high-affinity epitope or GFP from their endogenous gene promoters have been made to facilitate global protein analyses (Ghaemmaghami *et al.*, 2003; Huh *et al.*, 2003). These collections are available commercially. Lastly, yeasts can be grown rapidly in large quantities at a much lower cost than maintaining mammalian cell cultures. For these reasons, the yeasts *Y. lipolytica* and *S. cerevisiae* have been chosen to be the systems of choice to study peroxisome assembly in this thesis.

1.7 Focus of this thesis

The aim of this thesis is to study various processes in the assembly of peroxisomes. This thesis uses different approaches including classical genetic screening, DNA microarray analysis combined with bioinformatics and modern fluorescence microscopy to examine from early to late events in the assembly of peroxisomes in the yeasts *Y. lipolytica* and *S. cerevisiae*. Early, intermediate and late events in peroxisome assembly can be viewed as the formation of the peroxisomal membrane, the import of proteins into peroxisomes and the division of peroxisomes, respectively. The work

presented herein describes the identification and characterization of two novel peroxins, Pex24p and Pex27p, involved in peroxisomal protein import and peroxisome division, respectively, and a role for Pex3p in initiating the formation of a peroxisomal precursor from the ER membrane.

CHAPTER 2

MATERIALS AND METHODS

2.1 Materials

2.1.1 List of chemicals and reagents

2-(*N*-Morpholino)ethanesulfonic acid (MES)	Sigma
2,4,6,-tri-(dimethylaminomethyl) phenol (DMP 30)	Marivac
3-(*N*-Morpholino)propanesulfonic acid (MOPS)	EM Science
5-bromo-4-chloro-3-indolyl-β-D-galactoside (X-gal)	Rose Scientific
acetone	Fisher
acrylamide	Roche
agar	Difco
agarose, UltraPure	Invitrogen
albumin, bovine serum (BSA)	Roche
ammonium bicarbonate (NH_4HCO_3)	Sigma
ammonium chloride (NH_4Cl)	EM Science
ammonium persulfate	BDH
ammonium sulfate ($(NH4)_2SO_4$)	BDH
ampicillin	Sigma
anhydrous ethyl alcohol	Commercial Alcohols
antipain	Roche
aprotinin	Roche
benzamidine hydrochloride	Sigma
biotin	Sigma
boric acid	EM Science
Brij 35	EM Science
bromophenol blue	BDH
calcium pantothenate	Sigma
chloroform	Fisher
Complete Protease Inhibitor Cocktail	Roche
complete supplement mixture (CSM)	BIO 101
Coomassie Brilliant Blue R-250	ICN
cytochrome *c*, horse heart	Sigma
D-(+)-galactose	EM Science
D-(+)-glucose	EM Science
D-(+)-raffinose	Sigma
dithiothreitol (DTT)	Fisher
ethylenedinitrilo-tetraacetic acid (EDTA)	EM Science
formaldehyde, 37% (v/v)	Biochemicals
Geneticin	Invitrogen
glass beads	Sigma
glutaldehyde, 25% EM grade	Ted Pella
glycerol	EM Science
glycine	Roche
hydrogen peroxide solution, 30% (w/v)	Sigma
myo-inositol	Sigma

isoamyl alcohol	Fisher
isopropyl β-D-thiogalactopyranoside (IPTG)	Roche
lanolin	Alfa Aesar
leupeptin	Roche
L-histidine	Sigma
lithium acetate	Sigma
L-leucine	Sigma
L-lysine	Sigma
magnesium sulfate ($MgSO_4$)	Sigma
maltose	Sigma
methyl nadic anhydride	Marivac
MitoTracker CMXRos	Molecular Probes
N,N,N',N'-tetramethylethylenediamine (TEMED)	EM Science
N,N'-dimethyl formamide (DMF)	BDH
N,N'-methylene bisacrylamide	Sigma
N-propyl gallate	Sigma
Nycodenz	BioLynx
oleic acid	Fisher
paraffin	Fisher
Pefabloc SC	Roche
pepstatin A	Sigma
peptone	Difco
phenol, buffer saturated	Invitrogen
phenylmethylsulphonylfluoride (PMSF)	Roche
poly *L*-lysine	Sigma
polyethylene glycol, M.W. 3350 (PEG)	Sigma
Ponseau S	Sigma
potassium acetate	BDH
potassium chloride	BDH
potassium permanganate ($KMnO_4$)	BDH
potassium phosphate, dibasic (K_2HPO_4)	EM Science
potassium phosphate, monobasic (KH_2PO_4)	EM Science
pyridoxine-HCl	Sigma
salmon sperm DNA, sonicated	Sigma
Sephadex G25	Amersham
skim milk	Carnation
sodium acetate	EM Science
sodium cacodylate	Fisher
sodium carbonate (Na_2CO_3)	BDH
sodium chloride	EM Science
sodium dithionite ($Na_2S_2O_4$)	BDH
sodium dodecyl sulfate (SDS)	Bio-Rad
sodium fluoride (NaF)	Sigma
sodium periodate ($NaIO_4$)	Sigma
sodium phosphate, dibasic (Na_2HPO_4)	BDH

sodium sulphite (Na_2SO_3)	Sigma
sorbitol	EM Science
specially distilled DDSA	Marivac
sucrose	EM Science
TAAB 812 resin	Marivac
thiamine-HCl	Sigma
trichloroacetic acid (TCA)	EM Science
tris(hydroxymethyl)aminomethane (Tris)	Roche
Triton X-100	VWR
tryptone	Difco
Tween 20	Sigma
Tween 40	Sigma
uracil	Sigma
vaseline	Vaseline
xylene cyanol FF	Sigma
yeast extract	Difco
yeast nitrogen base without amino acids (YNB)	Difco
β-mercaptoethanol	BioShop

2.1.2 List of enzymes

CIP (calf intestinal alkaline phosphatase)	NEB
Platinum *Pfx* DNA polymerase	Invitrogen
restriction endonucleases	NEB
Quick T4 DNA ligase	NEB
RNase A (ribonuclease A), bovine pancreas	Sigma
T4 DNA ligase	NEB
Zymolyase 20T	ICN
Zymolyase 100T	ICN

2.1.3 Molecular size standards

1 kb DNA ladder (500-10,000 bp)	NEB
1 kb DNA ladder (75-12,216 bp)	Invitrogen
100 bp DNA ladder (100-1,517 bp)	NEB
prestained protein marker, broad range (6-175 kDa)	NEB

2.1.4 Multicomponent systems

BigDye Terminator Cycle Sequencing Ready Reaction Kit	Applied Biosystems
Matchmaker Two-Hybrid System	Clontech
pGEM-T Vector System	Promega
pMAL Protein Fusion and Purification System	NEB
QIAprep Spin Miniprep Kit	Qiagen
QIAquick Gel Extraction Kit	Qiagen
QIAquick PCR Purification Kit	Qiagen
Ready-To-Go PCR Beads	Amersham Biosciences

2.1.5 Plasmids

pBluescript II SK(-)	Stratagene
pGEM-7Zf	Promega
pGEM-T	Promega
pINA445 (*Y. lipolytica*/*E. coli* shuttle vector)	Dr. Claude Gaillardin
pMAL-c2	NEB
pRS315	NEB
YEp13	Broach *et al.*,1979
pUB4(*Y. lipolytica*/*E. coli* shuttle vector)	Dr. Stefan Kerscher

2.1.6 Antibodies

The antibodies used in this study are described in Table 2-1 and 2-2.

Table 2-1. Primary antibodies

Specificity	Type	Name	Dilution[a]	Reference
carboxyl-terminal SKL	rabbit	16-final	1:3000	Aitchison *et al.*, 1992
His6GFP[b]	rabbit	His6GFP	1:2000	Jun *et al.*, 2004
mouse IgG	rabbit	IgG	1:3000	ICN
S. cerevisiae G6PDH	rabbit	G6PDH	1:20,000	Sigma-Aldrich

S. cerevisiae Pex3p	rabbit	P84-final	1:4000	This study
S. cerevisiae Kar2p	guinea pig	P41-1[b]	1:4000	This study
S. cerevisiae Sdh2p[c]	rabbit	Sdh2	1:5000	Dibov *et al.*, 1998
Y. lipolytica Aox5p[d]	rabbit	Aox5	1:5000	Wang *et al.*, 1999
Y. lipolytica ICL	rabbit	E405-1[b]	1:5000	Eitzen *et al.*, 1996
Y. lipolytica Kar2p[e]	rabbit	Kar2	1:10,000	Titorenko *et al.*, 1997
Y. lipolytica Pex16p	guinea pig	SOAP-2[b]	1:7500	Eitzen *et al.*, 1997
Y. lipolytica Pex19p	guinea pig	194-final	1:10,000	Lambkin and Rachubinski 2001
Y. lipolytica Pex24p	rabbit	L257-3[b]	1:2500	This study
Y. lipolytica Pex2p	guinea pig	Pay5-NN	1:7500	Eitzen *et al.*, 1996
Y. lipolytica thiolase	guinea pig	N-3[b]	1:10,000	Eitzen *et al.*, 1996

[a]Dilutions are for use in immnunoblotting. Dilutions used in microscopy were at ten-fold higher concentrations.
[b]A gift of Dr. Gary Eitzen (University of Alberta, Edmonton, Canada).
[c]A gift of Dr. Bernard Lemire (University of Alberta, Edmonton, Canada).
[d]A gift of Dr. Jean-Marc Nicaud (Laboratoire de Génétique des Microorganismes, Thiverval-Grignon, France)
[e]A gift of Dr. Joel Goodman (University of Texas, Dallas, Texas).

Table 2-2. Secondary antibodies

Specificity	Type	Dilution	Source
horseradish peroxidase-conjugated anti-rabbit IgG	donkey	1:30,000	Amersham Biosciences
horseradish peroxidase-conjugated anti-guinea pig IgG	goat	1:30,000	Sigma-Aldrich
fluorescein isothiocyanate-conjugated anti-rabbit IgG	donkey	1:250	Jackson Immunoresearch Laboratories
rhodamine-conjugated anti-guinea pig IgG	donkey	1:250	Jackson Immunoresearch Laboratories

2.1.7 Oligonucleotides

The oligonucleotides used in this study are described in Table 2-3. They were either synthesized on an Oligo 1000M DNA Synthesizer (Beckman) or by Sigma-Genosys (Oakville, Ontario).

Table 2-3. Oligonucleotides

Name	Sequence[a,b,c]	Application
AA0975	5'-ATTGAATTCAGTACCAGTACATGAAAGATC-3'	pΔPEX24, pUB4-PEX24
AA0976	5'-TGTATAAAGTCGACGTGTGCGGGTGGTTGTGT-3'	pΔPEX24
AA0977	5'-GCACACGTCGACTTTATACAACATTGTCGAGCG-3'	pΔPEX24
AA0984	5'-ATTAAGCTTGTCGCGTGTCGAGAC-3'	pΔPEX24
AA0978	5'-ATTGAATTCGTCGCGTGTCGAGACGC-3'	pUB4-PEX24
AA0972	5'-ATTGAATTCATGTTCCGACGACTCACTGG-3'	pMAL-PEX24
AA0973	5'-ATTTCTAGATTAAACCAGGCCCAACAACTCC-3'	pMAL-PEX24
0636SG	5'-ATTGGATCCACAGTGACGTACACAGTATC-3'	pMAL-PEX3C
0420SG	5'-ATTGGATCCTTAAGGCTTGAAGGAAAACGA-3'	pMAL-PEX3C
0041SG	5'-ATTGAATTCATGACATCCGATCCTGTTAA-3'	pGAD424-PEX27, pGBT9-PEX27
0042SG	5'-ATTGAATTCTCAAACAGCGCTTGTATGTT-3'	pGAD424-PEX27, pGBT9-PEX27
0043SG	5'-ATTGAATTCATGAGTCAGTTTGGCACGAC-3'	pGAD424-PEX25, pGBT9-PEX25
0044SG	5'-ATTGAATTCTCAATCTTTTGAAGAGCAAAG-3'	pGAD424-PEX25, pGBT9-PEX25
0045SG	5'-ATTGGATTCATGGTCTGTGATACACTGGT-3'	pGAD424-PEX11, pGBT9-PEX11
0046SG	5'-ATTGGATTCCTATGTAGCTTTCCACATGT-3'	pGAD424-PEX11, pGBT9-PEX11

0082SG	5'-ATTCTCGAGAGCATAGGCGCTACCATG-3'	YEp-PEX27
0083SG	5'-ATTCTCGAGCAGAACTAGATGATTCCGA-3'	YEp-PEX27
0084SG	5'-ATTAGATCTCGTAAATTGGATATACGGTA-3'	YEp-PEX25
0085SG	5'-ATTAGATCTATCTGCTATGTCAATTGAAG-3'	YEp-PEX25
0473QC	5'-ATTGGATCCTCTCTGAATAAGTACTGACACTCAC-3'	pRS315-T
0474QC	5'-ATTCTCGAGAGACCGAACATTGGGCACGGG-3'	pRS315-T
0383SG	5'-ATTTCTAGATGTGCATCGGCATCTGAAT-3'	p20aa-GFP, p46aa-GFP, pFull_length-GFP
0436QC	5'-ATTGGATCCAATGAGTACCTTTCCTCGAT-3'	p20aa-GFP
0464QC	5'-ATTGGATCCCTGTTTATACAACCATCTCTT-3'	p46aa-GFP
0465QC	5'-ATTGGATCCAGGCTTGAAGGAAAACGAG-3'	pFull_length-GFP
0467QC	5'-ATTGGATCCATGTCTAAAGGTGAAGAATTATT-3'	p20aa-GFP, p46aa-GFP, pFull_length-GFP
0395SG	5'-ATTGGATCCTTATTTGTACAATTCATCCATAC-3'	p20aa-GFP, p46aa-GFP, pFull_length-GFP
0324QC	5'-TGTTTCGAAATATGGCCTCCTCCGAGGACGTA-3'	pmRFP-SKL
0356SG	5'- ATTGGATCCAATCTAAAGCTTTGAGGCGCCGGT GGAGTGGC -3'	pmRFP-SKL
0501QC	5'-ATTGAATTCATGGTGAGCAAGGGCGAGGA-3'	pTC3-mRFP$^{1.5}$SKL
0502QC	5'-ATTGAATTCCTAAAGCTTTGACTTGTACAGCTC GTCCATG-3'	pTC3-mRFP$^{1.5}$SKL, pmRFP$^{1.5}$SKL(HIS5)
0503QC	5'-ATTGAATTCATGGACCGACTTAACAACCT-3'	pTC3-THIGFP^{+}
0504QC	5'-GCTAGCCATCTCGGCAACAACCAGAGAA-3'	pTC3-THIGFP^{+}
0505QC	5'-GTTGTTGCCGAGATGGCTAGCAAAGGAGAAGA-3'	pTC3-THIGFP^{+}
0506QC	5'-ATTGAATTC TTATTTGTAGAGCTCATCCATG-3'	pTC3-THIGFP^{+}
0456QC	5'-ATTGAATTCGGTGAAGCTCAAAAACTTAATGGT GGTATGGTGAGCAAGGGCGAG-3'	pmRFP$^{1.3}$(HIS5), pmRFP$^{1.5}$HDEL(HIS5), pmRFP$^{1.5}$SKL(HIS5)
0457QC	5'-ATTGAATTCTTACTTGTACAGCTCGTCCA-3'	pmRFP$^{1.3}$(HIS5)
0740SG	5'-ATTGAATTCCTACAATTCGTCGTGCTTGTACAG CTCGTCCATG-3'	pmRFP$^{1.5}$HDEL(HIS5),

s*Eco*RI GFP	5'-GGGAATTCGGCGGTGGCGGTGGCGGTGAAGCT CAAAAACTTAATGAAGGAGATATACATATGGCTA G-3'	pGFP$^+$HDEL(HIS5), pGFP$^+$SKL(HIS5)
0732SG	5'-ATTGAATTCCTACAATTCGTCGTGTTTGTAGAG CTCATCCATGC-3'	pGFP$^+$HDEL(HIS5)
0588SG	5'-ATTGAATTCCTAAAGCTTTGATTTGTAGAG CTCATCCATGC-3'	pGFP$^+$SKL(HIS5)
0863SG	5'-*ATCAATTTGAAAACTCAAGTAAAACAGAGAAGTTG TAAGGTGAATAAGGA*AGATTGTACTGAGAGTGCAC-3'	*PEX14* deletion
0864SG	5'-*GTTACAATTACAATTTCCGTTAAAAAACTAATTACT TACATAGAATTGCG*CTGTGCGGTATTTCACACCG-3'	*PEX14* deletion
0865SG	5'-*GAAGAAAGAATTACAAATTGTGGGAACCGAAGTA TTGACGGAAAGAAGAA*AGATTGTACTGAGAGTGC AC-3'	*PEX19* deletion
0866SG	5'-*TGAACTACTTTTTTTTTTTTTTTTTACTGTTATCA TAAATATATATACC*CTGTGCGGTATTTCACACCG-3'	*PEX19* deletion
0198SG	5'-*GTTATTCGACTTATATGAGCATGGGGTATATTAT TGAGGTAGTTAATACT*GAATTCGAGCTCGTTTAA AC-3'	*GAL1* promoter introduction
0199SG	5'-*ACCTTTCCTCGATGTCTCTGCAGAAGCGAACGTG ATCTTTGATTTGGGGC*CATTTTGAGATCCGGGTTT T-3'	*GAL1* promoter introduction
YOR193w-PTAF	5'-*CTCCTTAAGCTATGGAACCGAGCCAAAGTCACT TCGGCTAATGAACATACAAGCGCTGTT*GGTGAAG CTCAAAAACTTAAT-3'	*PEX27-pA* construction
AA1543	5'-*ATAGAAATGACTACACATTCCAAAAAGCTCAAG TGGAAGCGGAGTGGGTATAACTAAATC*GCTGAC GGTATCGATAAGCTT-3'	*PEX27-pA* construction
YDR329c-3WebA	5'-*GATCTGAGCGCCAGCGTATACAGCAACTTTGGC GTCTCCAGCTCGTTTTCCTTCAAGCCT*GGTGAAG CTCAAAAACTTAAT-3'	*PEX3-GFP* construction
YDR329c-3WebB	5'-*TCAATATATCAACCTATTTCTTCCCTTTCTCTTCT TTTCTCCAAGACGCCCGTTAAATC*GCTGACGGTA TCGATAAGCTT-3'	*PEX3-GFP, 46aa-GFP* construction
YIL160c-3WebA	5'-*GGGGTTGTTAGTATGTGTATCGGTACTGGTATGG GTGCCGCCGCCATCTTTATTAAAGAA*GGTGAAGCT CAAAAACTTAAT-3'	*POT1-mRFP* construction

YIL160c-3WebB	5'-*AAATATTGAAAATGGAAAATTATAAACAAATTGA TAAACTACGTAATAGCTTTTACAAA*GCTGACGGTA TCGATAAGCTT-3'	*POT1-mRFP* construction
0560SG	5'-*GCTTTATTTACCACAGGGTCGGTGGTAGTGTTTT TCGTGAAGAGATGGTTGTATAAACAG*GGTGAAGC TCAAAAACTTAAT-3'	*46aa-GFP* construction
0614SG	5'-*GATACGACCAGAAACGTCATTGTATTGGATAACG CCGCTGTAAAACTATCGCAGGCAAAA*GGTGAAGCT CAAAAACTTAAT-3'	*GAL1PEX3/FOX2-mRFP-SKL* construction
0615SG	5'-*ACACATGACAAAAAAGTTGCGTCCGTAAAGAAAA AGTACTTAAAATGGGTAGGTTAGTTA*GCTGACGGT ATCGATAAGCTT -3'	*GAL1PEX3/FOX2-mRFP-SKL* construction
0751SG	5'-*GGTTCTGGTGCCGCTGATTATGACGACGAAGAT GAAGATGACGATGGTGATTATTTCGAA*GGTGAAGC TCAAAAACTTAAT -3'	*KAR2-mRFP-HDEL* construction
0752SG	5'-*CAGTATAATCTCCTCGAAAATTGTATGAAGCTCG AAGTTTGAATTAGCTATGCATGTATT*GCTGACGGT ATCGATAAGCTT -3'	*KAR2-mRFP-HDEL* construction

[a]Restriction endonuclease recognition sites are underlined.
[b]Additional modifications are colored in green.
[c]Sequences for homologous recombination are italicized.

2.1.8 Standard buffers and solutions

The compositions of commonly used buffered solutions are described in Table 2-4.

Table 2-4. Common solutions

Solution	Composition	Reference
1 × PBS	137mM NaCl, 2.7 mM KCl, 8 mM Na_2HPO_4, 1.5 mM K_2HPO_4, pH 7.3	Pringle *et al.*, 1991
1 × protease inhibitor (PIN) cocktail	1 μg/ml each of antipain, aprotinin, leupeptin, pepstatin, 0.5 mM benzamidine hydrochloride, 5 mM NaF, 1 mM PMSF or 0.5 mg Pefabloc SC/ml	Smith, 2000

1 × TBST	20 mM Tris-HCl, pH 7.5, 150 mM NaCl, 0.05% (w/v) Tween 20	Huynh *et al.*, 1988
1 × Transfer buffer	20 mM Tris-HCl, 150 mM glycine, 20% (v/v) methanol	Towbin *et al.*, 1979; Burnette, 1981
5 × SDS-PAGE running buffer	0.25 M Tris-HCl, pH 8.8, 2 M glycine, 0.5% SDS	Ausubel *et al.*, 1989
10 × TBE	0.89 M Tris-borate, 0.89 M boric acid, 0.02 M EDTA	Maniatis *et al.*, 1982
2× sample buffer	20% (v/v) glycerol, 167 mM Tris-HCl, pH 6.8, 2% SDS, 0.005% bromophenol blue	Ausubel *et al.*, 1989
6 × DNA loading dye	0.25% bromophenol blue, 0.25% xylene cyanol, 30% (v/v) glycerol	Maniatis *et al.*, 1982
Breakage buffer	2% (v/v) Triton X-100, 1% SDS, 100 mM NaCl, 10 mM Tris-HCl, pH 8.0, 1 mM EDTA, pH 8.0	Ausubel *et al.*, 1989
Disruption buffer	20 mM Tris-HCl, pH 7.5, 0.1 mM EDTA, pH 7.5, 100 mM KCl, 10% (w/v) glycerol	Eitzen, 1997
Ponceau stain	0.1% Ponceau S, 1% TCA	Szilard, 2000
Solution B	100 mM KH_2PO_4, 100 mM K_2HPO_4, 1.2 M sorbitol	Pringle *et al.*, 1991
TE	10 mM Tris-HCl, pH 7.0-8.0 (as needed), 1 mM EDTA	Maniatis *et al.*, 1982

2.2 Microorganisms and culture conditions

2.2.1 Bacterial strains and culture conditions

The *Escherichia coli* strains and culture media used in this study are described in Tables 2-5 and 2-6, respectively. Bacteria were grown at 37°C. Cultures of 5 ml or less were grown in culture tubes in a rotary shaker at 200 rpm. Cultures greater than 5 ml were grown in flasks in a rotary shaker at 250 rpm. Culture volumes were approximately 20% of flask volumes.

Table 2-5. *E. coli* strains

Strain	Genotype	Source
DH5α	F⁻, Φ80d*lac*ZΔM15, Δ(*lac*ZYA-*arg*F), U169, *rec*A1, *end*A1, *hsd*R17(r_k^-, m_k^+), *pho*A, *sup*E44, λ⁻, *thi*-1, *gyr*A96, *rel*A1	Invitrogen
BLR-DE3	F⁻, *omp*T, *hsd*SB(r_B^- m_B^-) *gal*, *dcm*, (DE3), Δ(*srl-recA*)*306*::Tn*10* (Tet^R)	Novagen

Table 2-6. Bacterial culture media

Medium	Composition	Reference
LB[a,b]	1% tryptone, 0.5% yeast extract, 1% NaCl	Maniatis *et al.*, 1982
SOB	2% tryptone, 0.5% yeast extract, 10 mM NaCl, 2.5 mM KCl	Maniatis *et al.*, 1982
TYP[a]	1.6% tryptone, 1.6% yeast extract, 0.5% NaCl, 0.25% K_2HPO_4	Promega Protocols and Applications Guide, 1989/1990

[a]Ampicillin was added to 100 μg/ml for plasmid selection when necessary.
[b]For solid media, agar was added to 1.5%.

2.2.2 Yeast strains and culture conditions

The *Y. lipolytica* and *S. cerevisiae* strains used in this study are listed in Tables 2-7 and 2-8, respectively. Yeast culture media are described in Table 2-9. Yeasts were grown at 30°C, unless otherwise indicated. Cultures of 10 ml or less were grown in 16 × 150 mm glass tubes in a rotating wheel. Cultures greater than 10 ml were grown in flasks in a rotary shaker at 250 rpm. Culture volumes were approximately 20% of flask volumes.

Table 2-7. *Y. lipolytica* strains

Strain	Genotype	Reference
E122	*MATA, ura3-302, leu2-270, lys8-11*	Barth and Gaillardin, 1997
mut1-1	*MATA, ura3-302, leu2-270, lys8-11, ole*	This study
pex24KOA	*MATA, ura3-302, leu2-270, lys8-11, pex24::URA3*	This study
P24TR	*MATA, ura3-302, leu2-270, lys8-11, pUB4(HygBR)PEX24*	This study

[a]A gift of Dr. Claude Gaillardin (Laboratoire de Génétique Moléculaire et Cellulaire, Thiverval-Grignon, France).

Table 2-8. *S. cerevisiae* strains

Strain	Genotype	Reference
BY4742	*MATα, his3Δ1, leu2Δ0, lys2Δ0, ura3Δ0*	Giaever et al., 2002
DF5α	*MATα, ura3-52, his3-200, trp1-1, leu2-3, 112, lys2-801*	Finley *et al.*, 1987
DF5a	*MATa, ura3-52, his3-200, trp1-1, leu2-3, 112, lys2-801*	Finley *et al.*, 1987
SFY526	*MATa, ura3-52, his3-200, ade2-101, lys2-801, trp1-901, leu2-3, 112, gal4-542, gal80-538, LYS2::GAL1*$_{UAS}$-*GAL1*$_{TATA}$-*lacZ, MEL1*	Harper *et al.*, 1993
pex27Δ	*MATα, his3Δ1, leu2Δ0, lys2Δ0, ura3Δ0, yor193w::KanMX4*	Giaever *et al.*, 2002
pex25Δ	*MATα, his3Δ1, leu2Δ0, lys2Δ0, ura3Δ0, pex25::KanMX4*	Giaever *et al.*, 2002
pex11Δ	*MATα, his3Δ1, leu2Δ0, lys2Δ0, ura3Δ0, pex11::KanMX4*	Giaever *et al.*, 2002
pex27Δ/pex25Δ	*MATa, his3Δ1, leu2Δ0, ura3Δ0, yor193w::KanMX4, pex25::KanMX4*	This study
pex27Δ/pex11Δ	*MATα, his3Δ1, leu2Δ0, met15Δ0, ura3Δ0, yor193w::KanMX4, pex11::KanMX4*	This study
pex25Δ/pex11Δ	*MATα, his3Δ1, leu2Δ0, ura3Δ0, pex25::KanMX4, pex11::KanMX4*	This study
pex27Δ-HD	*MATa/MATα, his3Δ1/his3Δ1, leu2Δ0/leu2Δ0, met15Δ0/+, +/lys2Δ0, ura3Δ0/ura3Δ0, yor193w::KanMX4*	Giaever *et al.*, 2002

pex25Δ-HD	*MATa/MATα, his3Δ1/his3Δ1, leu2Δ0/leu2Δ0, met15Δ0/+, +/lys2Δ0, ura3Δ0/ura3Δ0, pex25::KanMX4*	Giaever *et al.*, 2002
pex27Δ-A	*MATa, his3Δ1, leu2Δ0, met15Δ0, ura3Δ0, yor193w::KanMX4*	This study
pex25Δ-A	*MATa, his3Δ1, leu2Δ0, met15Δ0, ura3Δ0, pex25::KanMX4*	This study
27-25-HetD	*MATa/MATα, his3Δ1/his3Δ1, leu2Δ0/leu2Δ0, met15Δ0/+, +/lys2Δ0, ura3Δ0/ura3Δ0, yor193w::KanMX4/+, +/pex25::KanMX4*	This study
27-11-HetD	*MATa/MATα, his3Δ1/his3Δ1, leu2Δ0/leu2Δ0, met15Δ0/+, +/lys2Δ0, ura3Δ0/ura3Δ0, yor193w::KanMX4/+, +/pex11::KanMX4*	This study
25-11-HetD	*MATa/MATα, his3Δ1/his3Δ1, leu2Δ0/leu2Δ0, met15Δ0/+, +/lys2Δ0, ura3Δ0/ura3Δ0, pex25::KanMX4/+, +/ pex11::KanMX4*	This study
PEX27-pA	*MATα, his3Δ1, leu2Δ0, lys2Δ0, ura3Δ0, yor193w::YOR193w-protA (HIS5)*	This study
PXA1-pA	*MATα, his3Δ1, leu2Δ0, lys2Δ0, met15Δ0, ura3Δ0, pxa1::PXA1-protA (HIS5)*	This study
PEX17-pA	*MATα, his3Δ1, leu2Δ0, lys2Δ0, ura3Δ0, pex17::PEX17-protA (HIS5)*	Vizeacoumar *et al.*, 2003
BY4741	*MATa, his3Δ1, leu2Δ0, met15Δ0, ura3Δ0*	Giaever *et al.*, 2002
pex3Δ	*MATα, his3Δ1, leu2Δ0, lys2Δ0, ura3Δ0, pex3::KanMX4*	Giaever *et al.*, 2002
pex19Δ	*MATα, his3Δ1, leu2Δ0, lys2Δ0, ura3Δ0, pex19::KanMX4*	Giaever *et al.*, 2002
46aa-GFP	*MATa, his3Δ1, leu2Δ0, met15Δ0, ura3Δ0, pex3::46aa-GFP (HIS5)*	This study
PEX3-GFP	*MATa, his3Δ1, leu2Δ0, met15Δ0, ura3Δ0, pex3::PEX3-GFP (HIS5)*	This study
GAL1PEX3	*MATα, his3Δ1, leu2Δ0, lys2Δ0, met15Δ0, ura3Δ0, pex3::GAL1PEX3 (KanMX6)*	This study
GAL1PEX3/POT1-mRFP	*MATα, his3Δ1, leu2Δ0, lys2Δ0, met15Δ0, ura3Δ0, pex3::GAL1PEX3 (KanMX6), pot1::POT1-mRFP (HIS5)*	This study
POT1-mRFP	*MATa, his3Δ1, leu2Δ0, met15Δ0, ura3Δ0, pot1::POT1-mRFP (HIS5)*	This study
GAL1PEX3/FOX2-mRFP-SKL	*MATα, his3Δ1, leu2Δ0, lys2Δ0, ura3Δ0, pex3::GAL1PEX3 (KanMX6), fox2::FOX2-mRFP-SKL (HIS5)*	This study

GAL1PEX3-mRFP	*MATα, his3Δ1, leu2Δ0, lys2Δ0, ura3Δ0, pex3::GAL1PEX3 (KanMX6), pex3::PEX3-mRFP (HIS5)*	This study
KAR2-mRFP-HDEL	*MATα, his3Δ1, leu2Δ0, lys2Δ0, ura3Δ0, kar2::KAR2-mRFP-HDEL (HIS5)*	This study
46aa-GFP/KAR2-mRFP-HDEL	*MATa, his3Δ1, leu2Δ0, lys2Δ0, ura3Δ0, pex3::46aa-GFP (HIS5), kar2::KAR2-mRFP-HDEL (HIS5)*	This study
B59P	*MATa/MATα, his3Δ1/his3Δ1, leu2Δ0/leu2Δ0, met15Δ0/met15Δ0, +/lys2Δ0, ura3Δ0/ura3Δ0, pex3::46aa-GFP (HIS5)/pex3::GAL1PEX3 (KanMX6), pot1::POT1-mRFP (HIS5)/+*	This study
B523F	*MATa/MATα, his3Δ1/his3Δ1, leu2Δ0/leu2Δ0, met15Δ0/+, +/lys2Δ0, ura3Δ0/ura3Δ0, pex3::46aa-GFP (HIS5)/pex3::GAL1PEX3 (KanMX6), fox2::FOX2-mRFP-SKL (HIS5)/+*	This study
B5P3	*MATa/MATα, his3Δ1/his3Δ1, leu2Δ0/leu2Δ0, met15Δ0/+, +/lys2Δ0, ura3Δ0/ura3Δ0, pex3::46aa-GFP (HIS5)/pex3::GAL1PEX3-mRFP (HIS5)*	This study
B59P-pex14Δ	*MATa/MATα, his3Δ1/his3Δ1, leu2Δ0/leu2Δ0, met15Δ0/met15Δ0, +/lys2Δ0, ura3Δ0/ura3Δ0, pex14::URA3/pex14::URA3, pex3::46aa-GFP (HIS5)/pex3::GAL1PEX3 (KanMX6), pot1::POT1-mRFP (HIS5)/+*	This study
B59P-pex19Δ	*MATa/MATα, his3Δ1/his3Δ1, leu2Δ0/leu2Δ0, met15Δ0/met15Δ0, +/lys2Δ0, ura3Δ0/ura3Δ0, pex19::URA3/pex19::URA3, pex3::46aa-GFP (HIS5)/pex3::GAL1PEX3 (KanMX6), pot1::POT1-mRFP (HIS5)/+*	This study
B5P3-pex14Δ	*MATa/MATα, his3Δ1/his3Δ1, leu2Δ0/leu2Δ0, met15Δ0/+, +/lys2Δ0, ura3Δ0/ura3Δ0, pex14::URA3/pex14::URA3, pex3::46aa-GFP (HIS5)/pex3::GAL1PEX3-mRFP (HIS5)*	This study
B5P3-pex14Δ	*MATa/MATα, his3Δ1/his3Δ1, leu2Δ0/leu2Δ0, met15Δ0/+, +/lys2Δ0, ura3Δ0/ura3Δ0, pex19::URA3/pex19::URA3, pex3::46aa-GFP (HIS5)/pex3::GAL1PEX3-mRFP (HIS5)*	This study

Table 2-9. Yeast culture media

Medium	Composition[a,b]	Reference
GIM (galactose induction medium)	0.67% YNB, 0.5% yeast extract, 0.5% peptone, 0.5% (w/v) Tween 40, 2% galactose, 0.5% (v/v) oleic acid, 1 × CSM	This study
Non-fluorescent medium	6.61 mM KH_2PO_4, 1.32 mM K_2HPO_4, 4.06 mM $MgSO_4 \cdot 7H_20$, 26.64 mM $(NH_4)SO_4$, 1 × CSM, 0.5% (w/v) Tween 40, 0.1% glucose, 1% agarose, 2% galactose	This study
RIM (raffinose induction medium)	0.67% YNB, 0.5% yeast extract, 0.5% peptone, 0.5% (w/v) Tween 40, 0.1% raffinose, 0.5% (v/v) oleic acid, 1 × CSM	This study
SCIM	0.67% YNB, 0.5% yeast extract, 0.5% peptone, 0.5% Tween (w/v) 40, 0.1% glucose, 0.15% (v/v) oleic acid, 1 × CSM	Erdmann *et al.*, 1989
Sporulation medium	1% potassium acetate, 0.1% yeast extract, 0.05% glucose	Rose *et al.*, 1988
SM	0.67% YNB, 2% glucose, 1× CSM without leucine, uracil, or tryptophan as required	This study
YEPA	1% yeast extract, 2% peptone, 2% sodium acetate	Brade, 1992
YEPD	1% yeast extract, 2% peptone, 2% glucose	Rose *et al.*, 1988
YEPR	1% yeast extract, 2% peptone, 2% raffinose	Rose *et al.*, 1988
YNA[c]	0.67% YNB, 2% sodium acetate	Brade, 1992
YND[c]	0.67% YNB, 2% glucose	Rose *et al.*, 1988
YNO[c]	0.67% YNB, 0.05% (w/v) Tween 40, 0.1% (v/v) oleic acid	Nuttley *et al.*, 1993
YPBO	0.3% yeast extract, 0.5% peptone, 0.5% K_2HPO_4, 0.5% KH_2PO_4, 0.2% (w/v) Tween 40 or 1% (v/v) Brij 35, 1% (v/v) oleic acid	Kamiryo *et al.*, 1982

[a]For solid media, agar was added to 2%.
[b]Glucose, galactose, oleic acid and geneticin were added after autoclaving.
[c]Supplemented with histidine, leucine, lysine or uracil, each at 50 µg/ml, as required.

2.2.3 Mating, sporulation and tetrad dissection of *S. cerevisiae*

S. cerevisiae strains were mated by the method of Rose *et al.*, 1988. Haploid strains of opposite mating types were streaked in single straight line on separate YEPD

agar and incubated overnight. They were then replica plated on the same fresh YEPD agar in such a way that streaks of cells of opposite mating types were perpendicular to each other and incubated overnight. Cells on this YEPD agar were then replica plated on YND agar supplemented with the auxotrophic requirements of the diploid strain. Diploid cells appeared after overnight incubation.

Sporulation and tetrad dissection of *S. cerevisiae* strains was performed according to Rose *et al.*, 1988 with modifications. An individual diploid strain was grown overnight in 5 ml of YND medium supplemented with its auxotrophic requirements. Cells were harvested by centrifugation and washed twice with 10 ml of water. 5 µl of cell pellet was transferred to and incubated in 3 ml of sporulation medium for 3 to 7 days. Formation of tetrads was examined by light microscopy. When approximately 10% or more cells formed tetrads, 1 ml of cells was transferred to a microcentrifuge tube and washed twice with water. The cell pellet was resuspended in 1 ml of water. 10 µl of cells was transferred to 1 ml of water containing 3 to 5 µg of Zymolyase 20T and incubated at 30°C in a rotating wheel for 15 min. 20 µl of spheroplasted cells was spread in a single line near the edge of a thin YEPD plate. Tetrads were dissected using a Zeiss Axioskop 40 microscope equipped with a Tetrad Manipulator System (Carl Zeiss). Isolated spores were incubated for 2 days at 30°C.

2.3 Introduction of DNA into microorganisms

2.3.1 Chemical transformation of *E. coli*

Plasmid DNA was introduced into Subcloning Efficiency, chemically competent *E. coli* DH5α cells, as recommended by the manufacturer (Invitrogen). Essentially, 1 to 2 µl of ligation reaction (Section 2.5.7) or 0.5 µl (0.25 µg) of plasmid DNA was added to 25 µl of cells. The mixture was incubated on ice for 30 min, subjected to a 20 sec heat shock at 37°C, and chilled on ice for 2 min. 1 ml of LB medium (Table 2-6) was added, and the cells were incubated in a rotary shaker for 45 to 60 min at 37°C. Cells were spread onto LB agar plates containing ampicillin (Table 2-6) and incubated overnight at 37°C. 100 µl of 2% X-gal in DMF and 50 µl of 100 mM IPTG were added to agar plates to allow for blue/white selection of colonies carrying recombinant plasmids when necessary.

2.3.2 Electroporation of *E. coli*

For high efficiency transformation of *E. coli* DH5α or BLR-DE3 cells with plasmid DNA, cells were made electrocompetent as recommended by Invitrogen. Cells were grown overnight in 10 ml of SOB medium (Table 2-6). 0.5 ml of this overnight culture was transferred to and incubated in 500 ml of SOB until the culture reached an OD_{600} (optical density at a wavelength of 600 nm) of 0.5. Cells were harvested by centrifugation at 2,600 × *g* for 15 min at 4°C, washed twice with 500 ml of ice-cold 10% (v/v) glycerol, and resuspended in a minimal amount of 10% (v/v) glycerol. Cells were either used immediately or frozen as 100 µl aliquots by immersion in a dry ice/ethanol bath and stored at -80°C. For transformation, 1 µl of ligation reaction or 0.5 µl of plasmid

DNA was added to 20 µl of cells. The mixture was placed between the bosses of an ice-cold disposable micro-electroporation chamber (width ~0.15 cm) (Whatman Biometra) and submitted to an electrical pulse of 395 V (amplified to ~2.4 kV) at a capacitance of 2 µF and a resistance of 4 kΩ using a Cell-Porator connected to a Voltage Booster (Whatman Biometra). Cells were then immediately transferred to 1ml of LB, incubated in a rotary shaker at 37°C for 45 to 60 min, and spread on LB agar plates containing ampicillin.

2.3.3 Chemical transformation of yeast

Plasmid DNA was introduced into yeast according to Gietz and Woods (2002). Essentially, 25 µl of cells was scraped from a plate not more than one week old with a sterile toothpick and resuspended in 1 ml of water. Cells were harvested by centrifugation, resuspended in 1 ml of 100 mM lithium acetate, and incubated at 30°C for 5 min. Cells were again harvested by centrifugation, and the following components were added on top of the cell pellet in this order: 240 µl of 50% (w/v) PEG, 36 µl of 1 mM lithium acetate, 50 µl of 2 mg sheared salmon sperm DNA/ml, 1 µl of plasmid DNA and 20 µl of water. The mixture was vortexed vigorously for 1 min and incubated at 42°C for 20 min. Cells were harvested by centrifugation, resuspended gently in 200 µl of water and plated onto YNA (*Y. lipolytica* cells only), SM or YND agar (Table 2-9). Plates were incubated at 30°C for 3 days for colony formation.

2.3.4 Electroporation of yeast

Yeast cells were made electrocompetent as recommended by Ausubel *et al.* (1989). *Y. lipolytica* and *S. cerevisiae* cells were handled in the same manner except that growth of *Y. lipolytica* and *S. cerevisiae* cells was in YEPA and YEPD, respectively. Cells were grown overnight in 10 ml of YEPA or YEPD (Table 2-9). 5 ml of overnight culture was transferred to 45 ml of YEPA or YEPD, and incubated for 4 to 5 h or until the culture reached an OD_{600} of ~1.0. Cells were then harvested by centrifugation at 2,000 × *g*, resuspended in 50 ml TE 7.5 (Table 2-4) containing 100 mM lithium acetate, and incubated for 30 min at room temperature or 30°C with gentle agitation. DTT was added to a final concentration of 20 mM, and the incubation was continued for another 15 min. Cells were harvested by centrifugation at 2,000 × *g*, washed once with 50 ml each of room-temperature water, ice-cold water, and ice-cold 1 M sorbitol. Cells were resuspended in a minimal volume of ice-cold 1 M sorbitol. 20 µl of cells was mixed with 1 µl of plasmid DNA or 100 to 150 ng of purified DNA fragment, placed between the bosses of an ice-cold micro-electroporation chamber (width ~0.15 cm) (Whatman Biometra), submitted to an electrical pulse of 250 V (amplified to ~1.6 kV) at a capacitance of 2 µF and a resistance of 4 kΩ Cell-Porator connected to a Voltage Booster (Whatman Biometra). Cells were immediately resuspended in 100 µl of ice-cold 1 M sorbitol and plated onto YNA (*Y. lipolytica* cells only), SM or YND agar plates (Table 2-9). Plates were incubated at 30°C for 3 to 5 days for colony formation.

2.3.5 Isolation of DNA from microorganisms

2.3.6 Isolation of plasmid DNA from bacteria

Single bacterial colonies were inoculated into 2 ml of LB (Table 2-6) containing ampicillin and incubated overnight at 37°C. Cells were harvested by centrifugation in a microcentrifuge tube, and plasmid DNA was isolated by using a QIAprep Spin Miniprep Kit according to the manufacturer's instructions (Qiagen). This method is based on the alkaline lysis of bacterial cells, followed by adsorption of DNA onto silica in the presence of high salt and elution of DNA in low salt buffer. Plasmid DNA was usually eluted in 50 µl of the supplied elution buffer.

2.3.7 Isolation of chromosomal DNA from yeast

Yeast genomic DNA was prepared as recommended by Ausubel *et al.* (1989). Cells were grown overnight in 10 ml of YEPD (Table 2-9), harvested by centrifugation for 5 min at 2,000 × *g*, washed twice in 10 ml of water, and transferred to a 2.0 ml microcentrifuge tube. 200 µl each of breakage buffer (Table 2-4), glass beads and phenol/chloroform/isoamyl alcohol (25:24:1) were added to the cells. The mixture was vortexed for 3 to 5 min at 4°C to simultaneously break yeast cells and separate nucleic acids from proteins. 200 µl of TE 8.0 (Table 2-4) was added, and the mixture was vortexed briefly. The organic and aqueous phases were separated by centrifugation at 16,000 × *g* for 5 min at room temperature. The aqueous phase was extracted once against an equal volume of phenol/chloroform/isoamyl alcohol (25:24:1). DNA was precipitated by the addition of 2.5 volumes of absolute ethanol and centrifugation at 16,000 × *g* for 5 min at room temperature. The pellet was washed once with 1 ml 70% (v/v) ethanol, dried

in a rotary vacuum desiccator and dissolved in 50 µl of TE 8.0 containing 100 µg RNase A/ml. DNA was incubated at 37°C for 1 to 2 h to allow for digestion of RNA.

2.4 DNA manipulation and analysis

Unless otherwise indicated, reactions were carried out in 1.5 ml microcentrifuge tubes, and microcentrifugation was performed in an Eppendorf microcentrifuge at 16,000 × *g*.

2.4.1 Amplification of DNA by the polymerase chain reaction (PCR)

PCR was used to amplify specific DNA sequences or to introduce modifications in the amplified DNA sequence. Primer design, reaction components and cycling conditions were performed following standard protocols (Innis and Gelfand, 1990; Saiki, 1990). A reaction usually contained 0.1 to 0.5 µg of yeast genomic DNA or 100 to 200 ng of plasmid DNA, 20 pmol of each primer, 0.25 mM of each dNTP, 1 mM Mg_2SO_4, and 1.25 U of Platinum *Pfx* DNA polymerase in 50 µl of the supplied reaction buffer (Invitrogen). Reactions were performed in 0.6 ml microcentrifuge tubes in a Robocycler 40 with a Hot Top attachment (Stratagene). Alternatively, Ready-to-Go PCR Beads were used as recommended by the manufacturer (Amersham Biosciences).

2.4.2 Digestion of DNA by restriction endonucleases

In general, 1 to 2 µg of plasmid DNA or purified DNA was digested by restriction endonucleases for 1 to 1.5 h according to the manufacturer's instructions. Digestion was

immediately terminated by agarose gel electrophoresis of the DNA fragments, except for plasmid DNA, which required dephosphorylation.

2.4.3 Dephosphorylation of 5' ends

Plasmid DNA linearized by one restriction endonuclease was subjected to dephosphorylation at its 5' end to prevent intramolecular ligations. After digestion of plasmids, reactions were mixed with 10 U of CIP (NEB) and incubated at 37°C for 30 min. The dephosphorylation reaction was terminated by agarose gel electrophoresis of the DNA fragments.

2.4.4 Separation of DNA fragments by agarose gel electrophoresis

DNA fragments in solution were mixed with 0.2 volume of 6 × DNA loading dye (Table 2-4) and separated by electrophoresis in 1% agarose gels in 1 × TBE (Table 2-4) containing 0.5 μg of ethidium bromide/ml. Gels were subjected to electrophoresis at 10 V/cm in 1 × TBE, and DNA fragments were subsequently visualized on an ultraviolet transilluminator (Photodyne, Model 3-3006).

2.4.5 Purification of DNA fragments from agarose gel

A DNA fragment of interest was excised from the agarose gel using a razor blade. DNA was extracted from the agarose slice by using the QIAquick Gel Extraction Kit according to manufacturer's instructions (Qiagen). This method is based on the dissolution of agarose gel and adsorption of DNA to the silica-membrane in the presence of a high concentration of chaotropic salts, followed by washing and elution of DNA in

the presence of low salts. DNA was usually eluted in 30 to 50 µl of the supplied elution buffer.

2.4.6 Purification of DNA from solution

Contaminants (small oligonucleotides, salts, enzymes, *etc.*) were removed from a DNA solution by using the QIAquick PCR Purification Kit as described by the manufacturer (Qiagen). The principle of this method is similar to that of the QIAquick Gel Extraction Kit (Section 2.5.5), except that no dissolution of agarose gel was involved. DNA was usually eluted in 30 to 50 µl of the supplied elution buffer.

2.4.7 Ligation of DNA fragments

DNA fragments treated with restriction endonucleases (Section 2.5.2) and purified as described in Section 2.5.6 were ligated using 1 µl of T4 DNA ligase in the buffer supplied by the manufacturer (NEB). The reaction was typically in a volume of 10 µl, with the molar ratio of plasmid to insert being between 1:3 and 1:10, and incubated overnight at 16°C. Alternatively, 1 µl of Quick T4 DNA ligase (NEB) in 1 × Quick Ligation Buffer was used in a reaction volume of 20 µl. The reaction was incubated at room temperature for 10 min.

Occasionally, PCR products after purification by agarose gel electrophoresis (Section 2.5.5) were ligated with the vector pGEM-T using the pGEM-T Vector System according to the manufacturer's instructions (Promega).

2.4.8 DNA sequencing

DNA sequencing was performed using the BigDye Terminator v1.1/3.1 Cycle Sequencing Ready Reaction Kit as described by the manufacturer (Applied Biosystems). This method is based on the method of Sanger *et al.* (1977) and involves the random incorporation of fluorescent dideoxy terminators during the elongation of DNA sequences with a modified version of *Taq* DNA polymerase. Essentially, a reaction contained 1 µl of plasmid DNA, 3.2 pmol of primer, 3 µl of Terminator Ready Reaction Mix, and 2.5 µl of the supplied 5 × buffer in a total volume of 20 µl. The reaction was subjected to cycle sequencing using the Robocycler 40 with a Hot Top attachment (Stratagene) and the following conditions: 1 cycle at 96°C for 2 min; 25 cycles at 96°C for 46 sec, 50°C for 51 sec and 60°C for 4 min 10 sec; 1 cycle at 6°C to hold until ready to purify. Reaction products were precipitated with 80 µl of 75% isopropanol for 20 min at room temperature, subjected to microcentrifugation at 16,000 × *g* for 20 min, washed twice with 250 µl of 75% isopropanol, dried in a rotary vacuum dessicator and resuspended in 15 µl of Template Suppression Reagent. They were then heated at 95°C for 2 min and immediately cooled on ice. Finally, they were separated by capillary electrophoresis, and fluorescence was detected and recorded by an ABI 310 Genetic Analyzer (Applied Biosystems).

2.5 Protein manipulation and analysis

2.5.1 Preparation of yeast whole cell lysates

Yeast lysates were prepared by disruption with glass beads (adapted from Needleman and Tzagoloff, 1975). Cells were harvested by centrifugation at 2, 000 × *g* for

5 min, washed twice with 10 ml of water, and resuspended in an equal volume of ice-cold Disruption Buffer (Table 2-4) containing 1 × PIN (Table 2-4) and 1 mM DTT. Ice-cold glass beads were added until they reached the meniscus of the cell suspension. The mixture was vortexed for 5 min at 4°C, and glass beads were pelleted by microcentrifugation for 20 sec at 4°C. The supernatant was recovered and clarified by microcentrifugation for 20 min at 4°C.

Alternatively, yeast lysates were prepared by denaturation with alkaline and reducing agents. Cells were harvested by centrifugation at 2,000 × *g* for 5 min, transferred to a microcentrifuge tube, and resuspended in 240 to 500 µl of 1.85 M NaOH and 7.4% β-mercaptoethanol. The cell suspension was incubated on ice for 5 min and mixed with an equal volume of 50% (w/v) TCA by vortexing. The mixture was further incubated on ice for 5 min and subjected to microcentrifugation at 16,000 × *g* for 10 min at 4°C. The pellet was washed once with water, resuspended first in 50 to 150 µl of Magic A (1 M unbuffered Tris-HCl and 13% SDS) and then in an equal volume of Magic B (30% (v/v) glycerol, 200 mM DTT and 0.25% bromophenol blue). The mixture was boiled for 10 min and then subjected to microcentrifugation at 16,000 × *g* for 1 min. The supernatant was collected.

2.5.2 Precipitation of proteins

Proteins were precipitated from solution by adding TCA to a final concentration of 10% and incubation on ice for 30 min to overnight. Precipitates were collected by microcentrifugation at 16,000 × *g* for 30 min at 4°C. The pellet was washed twice with 1

ml of ice-cold acetone, dried in a rotary vacuum dessicator and dissolved in 2 × sample buffer (Table 2-4).

2.5.3 Determination of protein concentration

The protein concentration of a sample was determined by the method of Bradford (1976). A standard curve was prepared by adding 1 ml of Bio-Rad Protein Assay Dye to 100 µl aliquots of water containing 2 µg, 4 µg, 6 µg, 8 µg, 10 µg, 12 µg, 14 µg, 16 µg, 18 µg and 20 µg of BSA. Samples were incubated for 5 min at room temperature and absorbance was measured at 595 nm using a Beckman DU640 spectrophotometer. Absorbance values were plotted against the BSA concentrations to generate a standard curve. Absorbance of a protein sample was measured in the same way as for BSA standards, and the protein concentration was estimated by comparing the absorbance value with the standard curve.

2.5.4 Separation of proteins by electrophoresis

Proteins were separated by sodium dodecyl sulfate-polyacrylamide gel electrophoresis (SDS-PAGE) as described by Ausubel *et al.* (1989). Protein samples were mixed with an equal volume of 2 × sample buffer (Table 2-4) containing 10 mM DTT, denatured by boiling for 5 min, and separated by electrophoresis on discontinuous slab gels. Stacking gels contained 3% acrylamide (30:0.8 acylamide:*N,N'*-methylene-bis-acrylamide), 60 mM Tris-HCl, pH 6.8, 0.1% SDS, 0.1% (v/v) TEMED, and 0.1% ammonium persulfate. Resolving gels contained 10% acrylamide (30:0.8 acylamide:*N,N'*-methylene-bis-acrylamide), 370 mM Tris-HCl, pH 8.8, 0.1% SDS, 0.1% (v/v) TEMED,

and 0.043% ammonium persulfate. Electrophoresis was conducted in 1 × SDS-PAGE running buffer (Table 2-4) at 50-200 V using a Bio-Rad Mini Protean II vertical gel system.

2.5.5 Detection of proteins by gel staining

Proteins in polyacrylamide gels were visualized by staining with 0.1% Coomassie Brilliant Blue R-250, 10% (v/v) acetic acid, 35% (v/v) methanol for 1 h with gentle agitation. Unbound dye was removed by multiple washes in 10% (v/v) acetic acid, 35% (v/v) methanol. Gels were dried for 1 h at 80°C on a Bio-Rad Model 583 gel drier.

2.5.6 Detection of proteins by immunoblotting

Proteins separated by SDS-PAGE were transferred to nitrocellulose membrane (Bio-Rad) in 1 × transfer buffer (Table 2-4) at 100 mA for 16 h at room temperature using a Trans-Blot tank transfer system with plate electrodes (Bio-Rad). Proteins transferred to nitrocellulose were visualized by staining in Ponceau stain (Table 2-4) for several min and destaining in water. The nitrocellulose was incubated in blocking solution (1% skim milk powder, 1 × TBST (Table 2-4)) with gentle agitation to prevent non-specific binding of antibodies. Specific proteins on nitrocellulose were detected by incubation with primary antibody in blocking solution for 1 h at room temperature with gentle agitation. The nitrocellulose was then incubated with appropriate HRP-labeled secondary antibody in blocking solution for 1 h. After each antibody incubation, unbound antibodies were removed by washing the nitrocellulose three times with 1 × TBST for 10 min each. Antigen-antibody complexes were detected by using an ECL Western Blotting

Detection Kit according to the manufacturer's instructions (Amersham Biosciences) and exposing the nitrocellulose to X-Omat BT film (Kodak).

Used nitrocellulose could be reblotted using a Re-Blot Western Blot Recycling Kit according to the manufacturer's instructions (Chemicon). The nitrocellulose was incubated with 1 × Antibody Stripping Solution at room temperature for 15 to 30 min with gentle agitation, rinsed with 1 × TBST, and blotted as described above.

2.6 Subcellular fractionation of yeast

2.6.1 Peroxisome isolation from *Y. lipolytica*

Peroxisomes were isolated from *Y. lipolytica* cells according to Aitchison (1992). Essentially, cells grown in oleic acid-containing medium were harvested by centrifugation at 800 × *g* in a Beckman JA10 rotor at room temperature and washed twice with water. Cells were then resuspended in spheroplasting solution (0.5 M KCl, 5 mM MOPS, pH 7.2, 10 mM sodium sulphite, 0.25 mg Zymolyase 100T/ml) at a concentration of 4 ml per g of wet cells and incubated at 30°C for 30 min with gentle agitation. Spheroplasts were harvested by centrifugation at 2,200 × *g* in a Beckman JS13.1 rotor for 8 min at 4°C and resuspended in homogenization buffer (5 mM MES, pH 5.5, 1 M sorbitol) containing 1 × PIN (Table 2-4) at a concentration of 3 ml per g of wet cells. Resuspended spheroplasts were transferred to a homogenization mortar and disrupted by 10 strokes of a Teflon pestle driven at 1,000 rpm by a stirrer motor (Model 4376-00, Cole-Parmer). Cell debris, unbroken cells and nuclei were separated from the postnuclear supernatant (PNS) by centrifugation at 1,000 × *g* in a Beckman JS13.1 rotor for 10 min at 4°C. The PNS was fractionated by centrifugation at 20,000 × *g* in a Beckman JS13.1 rotor

for 30 min at 4°C into a pellet (20KgP) enriched for heavy organelles including peroxisomes and mitochondria and a supernatant (20KgS) enriched for cytosol.

The 20KgP was resuspended in homogenization buffer and loaded on the top of a discontinuous sucrose gradient (4.67 ml of 25%, 7 ml of 35%, 14 ml of 42% and 7 ml of 53% (w/w) sucrose in 5 mM MES, pH 5.5). Organelles were separated by centrifugation at 100,000 × *g* for 80 min at 4°C in a Beckman VTi50 rotor. 18 fractions of 2 ml each were collected from the bottom of the gradient.

2.6.2 Peroxisome isolation from *S. cerevisiae*

Isolation of peroxisomes from *S. cerevisiae* cells was performed as described by Smith *et al.* (2002). Cells grown in oleic acid-containing medium were harvested by centrifugation at 800 × *g* in a Beckman JA10 rotor at room temperature and washed twice with water. Cells were resuspended in 10 mM DTT, 100 mM Tris-HCl, pH 9.4, at a concentration of 10 ml per g of wet cells and incubated at 30°C for 35 min with gentle agitation to loosen the outer mannoprotein layer. Cells were collected by centrifugation at 2,500 × *g* in a Beckman JS13.1 rotor for 10 min at 4°C and washed once with Zymolyase buffer (50 mM potassium phosphate, pH 7.5, 1.2 M sorbitol, 1 mM EDTA). Cells were resuspended in Zymolyase buffer containing 0.125 mg of Zymolyase 100T/ml at a concentration of 8 ml per g of wet cells and incubated at 30°C for 45 min to 1 h with gentle agitation to convert cells to spheroplasts. Spheroplasts were harvested by centrifugation at 2,200 × *g* in a Beckman JS13.1 rotor for 8 min at 4°C and washed once with 1.2 M sorbitol, 2.5 mM MES, pH 6.0, 1 mM EDTA. They were then resuspended in buffer H (0.6 M sorbitol, 2.5 mM MES, pH 6.0, 1 mM EDTA, 1 × complete protease

inhibitor cocktail (Roche)) at a concentration of 2 ml per g of wet cells. Resuspended spheroplasts were transferred to a homogenization mortar and disrupted by 10 strokes of a Teflon pestle driven at 1,000 rpm by a stirrer motor (Model 4376-00, Cole-Parmer). Cell debris, unbroken cells and nuclei were pelleted by centrifugation at 1,000 × *g* in a Beckman JS13.1 rotor for 8 min at 4°C. The postnuclear supernatant (PNS) was subjected to four additional centrifugations at 1,000 × *g* in a Beckman JS13.1 rotor for 8 min at 4°C. The PNS was fractionated by centrifugation at 20,000 × *g* in a Beckman JS13.1 rotor for 30 min at 4°C into pellet (20KgP) and supernatant (20KgS) fractions.

The 20KgS fraction can be subfractionated by ultracentrifugation at 250,000 × *g* in a Beckman TLA120.2 rotor for 1 h at 4°C into a pellet (250KgP) fraction enriched for high-speed pelletable organelles and a supernatant (250KgS) fraction enriched for cytosol.

The 20KgP was resuspended in 11% (w/v) Nycodenz in buffer H and loaded onto the top of a discontinuous Nycodenz gradient (6.6 ml of 17%, 16.5 ml of 25%, 4.5 ml of 35% and 3 ml of 50% (w/v) Nycodenz in buffer H). Organelles were separated by ultracentrifugation at 100,000 × *g* for 80 min at 4°C in a Beckman VTi50 rotor. 18 fractions of 2 ml each were collected from the bottom of the gradient.

2.6.3 Extraction and subfractionation of peroxisomes

Extraction and subfractionation of peroxisomes were performed according to Smith (2000) with modifications. Essentially, organelles in the 20KgP fraction (containing ~50 μg of protein) were lysed by incubation in 10 volumes of ice-cold Ti8 buffer (10 mM Tris-HCl, pH 8.0) containing 2 × complete protease inhibitor cocktail

(Roche) on ice for 1 h with occasional vortexing and separated by ultracentrifugation at 200,000 × *g* for 1 h at 4°C in a TLA120.2 rotor into a membrane fraction (Ti8P) and a soluble fraction (Ti8S). The Ti8P fraction was resuspended in ice-cold Ti8 to a final protein concentration of 0.5 mg/ml and mixed with 10 volumes of ice-cold 0.1 M Na_2CO_3, pH 11.3. The mixture was incubated on ice for 45 min with occasional vortexing and subjected to ultracentrifugation at 200,000 × *g* for 1 h at 4°C in a TLA120.2 rotor to yield a fraction enriched for integral membrane proteins (CO_3P) and a fraction enriched for peripheral membrane proteins (CO_3S).

2.7 Assays

2.7.1 Catalase

The *in vitro* measurement of the activity of the peroxisomal enzyme catalase was performed according to Lück (1963) by measuring the consumption of hydrogen peroxide (H_2O_2) by catalase spectrophotometrically. 1 to 50 µl of sample was mixed with 50 mM potassium phosphate, pH 7.5, in a total volume of 950 µl in a quartz cuvette. 50 µl of 0.3% H_2O_2 was added, and the absorbance of the sample at 240 nm was set to zero. The decrease in the absorbance at 240 nm was measured at 10 sec intervals for 2 min. The specific activity of catalase was calculated.

2.7.2 Cytochrome *c* oxidase

The *in vitro* measurement of the activity of the mitochondrial enzyme cytochrome *c* oxidase was performed according to Douma *et al.* (1985) by measuring spectrophotometrically the oxidation of cytochrome *c* by the enzyme. 1 mM cytochrome

c was reduced by the addition of a minute amount of sodium dithionite. Excess sodium dithionite was removed by size exclusion filtration on Sephadex G25 equilibrated with 50 mM potassium phosphate, pH 7.0. The absorbance at 550 nm of 50 µl of 1 mM reduced cytochrome *c* mixed with 900 µl of 50 mM potassium phosphate, pH 7.0, was set to zero. 1 to 50 µl of sample was added, and the decrease in the absorbance at 550 nm was measured at 5 sec intervals for 2 min. The specific activity of cytochrome *c* oxidase was calculated.

2.8 Microscopy

2.8.1 Immunofluorescence microscopy

Indirect immunofluorescence microscopy of yeast cells was performed according to Pringle *et al.* (1991) with modifications. Cells grown in oleic acid-containing medium were fixed in 3.7% (v/v) formaldehyde for 30 min at room temperature with occasional agitation. Cells were then collected by centrifugation at 2,000 × *g* for 5 min, washed with 4 ml of solution B (Table 2-4), and resuspended in solution B at a concentration of 1 ml per 100 µl of wet cells. The cell suspension was mixed with 40 µg of Zymolyase 100T/ml and 38 mM β-mercaptoethanol and incubated for 15 to 60 min at 30°C with gentle rotation. Spheroplasts were spotted onto slides precoated with poly *L*-lysine and allowed to dry at room temperature. Spheroplasts were permeabilized by immersion of the slides in -20°C methanol for 6 min and -20°C acetone for 30 sec, and allowed to dry. Slides were put in a dark humid box at room temperature for the following procedures. Spheroplasts were covered with 50 µl of blocking solution (Section 2.6.6) for 1 h. They were incubated with primary antibody diluted in blocking solution for 1 h, washed 10 to

20 times with 1 × TBST, and then incubated with secondary antibody conjugated to fluorescein or rhodamine diluted in blocking solution for 1 h. Spheroplasts were washed again 10 to 20 times with 1 × TBST and covered with 1 drop of mounting medium (0.4% *N*-propyl gallate, 74.8% (w/v) glycerol in 1 × PBS, pH 7.4). Coverslips were placed on top of slides, and the edges were sealed with nail polish. Images were captured on a LSM510 META (Carl Zeiss) laser scanning microscope or on an Olympus BX50 microscope equipped with a digital fluorescence camera (Spot Diagnostic Instruments).

2.8.2 Staining of yeast mitochondria with MitoTracker Red

Mitochondria of live yeast cells were stained with MitoTracker Red CMXRos according to the manufacturer's instructions (Molecular Probes). Essentially, cells grown in 10 ml of YPBO (Table 2-9) were harvested, washed once with water and resuspended in 10 ml of pre-warmed YPBO. The cell suspension was mixed with 2 µl of 1 mM MitoTracker Red CMXRos and incubated at 30°C for 10 to 15 min in a rotary shaker at 150 rpm. 1.5 ml of culture was pelleted, washed twice with water, and viewed on an Olympus BX50 microscope equipped with a digital fluorescence camera (Spot Diagnostic Instruments).

2.8.3 Confocal video microscopy

Cells grown in YEPR medium (Table 2-9) and then incubated in RIM medium (Table 2-9) for 16 h were prepared for 4D *in vivo* video microscopy. Slides were prepared according to Adames *et al.* (2001) with modifications. Essentially, 850 µl of hot 1% agarose in non-fluorescent medium (Table 2-9) was mixed with 150 µl of 20% (w/v)

galactose, 4 µl of oleic acid and 4 µl of 1,000 × non-fluorescent vitamins (2 mg biotin, 200 mg calcium pantothenate, 2 g inositol, 400 mg pyridoxine-HCl, 400 mg thiamine-HCl per liter), and 200 µl of this agarose mixture was used to prepare a thin agarose pad on a slide with two 18 mm square wells (Cel-line Brand). 1 to 2 µl of culture was placed onto the slide, covered with a cover slip and sealed with Valap (1:1:1 mixture of vaseline, lanolin and paraffin). Cells were incubated at room temperature for image capture. Images were captured according to Hammond and Glick (2000) using a modified LSM 510 META confocal microscope equipped with a 63× 1.4 NA Plan-Apo objective (Carl Zeiss). A piezoelectric actuator was used to drive continuous objective movement, allowing for rapid collection of *z*-stacks. A side of each pixel represented 0.085 µm of sample. Stacks of 8 optical sections spaced 0.45 µm apart were captured every 60 sec. GFP was excited using a 488-nm laser, and its emission was collected using a 505-530-nm band-pass filter. mRFP was excited using a 543-nm laser, and its emission was collected using a 600-nm long-pass filter. Images were filtered three times using a 3×3 hybrid median filter to reduce shot noise. Fluorescence images from each stack were projected using an average intensity algorithm that involved multiplication of each pixel value by an appropriate enhancement factor for better contrast. Correction for exponential photobleaching of GFP and mRFP was performed by exponentially increasing the enhancement factor with each projection. The transmitted light images from each stack were projected using a maximum intensity algorithm. These operations were performed using NIH Image (http://rsb.info.nih.gov/nih-image/). Adobe Photoshop was used to merge fluorescent and transmitted light projections.

2.8.4 Electron microscopy

Cells were processed for electron microscopy as described by Goodman *et al.* (1990). All microcentrifugations were performed at 16,000 × *g* for 1 min and all incubations were done in 1.5 ml microcentrifuge tube at room temperature with agitation, unless indicated otherwise. Cells were harvested and washed twice with water. Approximately 100 µl of cell pellet was fixed in 1 ml of 3% $KMnO_4$ for 15 min, washed twice with water, and incubated in 1 ml of 1% sodium periodate for 10 min. Cells were pelleted, washed once with water, and incubated with 1 ml of 1% NH_4Cl for 10 min. Cells were again pelleted, washed once with water, and subjected to serial dehydration procedures in 60%, 80%, 95%, and 100% ethanol and in propylene oxide. Each incubation was for 5 min. Incubation in propylene oxide was repeated three times. Cells were collected and incubated in 1 ml of a 1:1 mixture of propylene oxide and resin (a mixture of TAAB 812 resin, specially distilled DDSA, methyl nadic anhydride and 2,4,6,-tri-(dimethylaminomethyl) phenol in proportions suggested by the manufacturer Marivac) for 1 h. Cells were next pelleted and resuspended in 1 ml of resin. Incubation in resin was carried out for 1 h with agitation and 3 h in a fume hood with caps opened. Finally, cells were harvested by microcentrifugation for 8 min, and small portions of cells were transferred to embedding capsules (EMS) containing resin. Embedding capsules were placed in an oven at 60°C to allow the resin to polymerize. Ultra-thin sections were cut by Honey Chan, Department of Cell Biology, University of Alberta, using an Ultra-Cut E Microtome (Reichert-Jung) and examined on a Phillips 410 electron microscope. Images were captured with a digital camera (Soft Imaging System). Occasionally, cells were prefixed in 1 ml of 3% glutaldehyde prepared in 0.1 M cacodylate buffer, pH 7.2,

for 20 min at 4°C with agitation. Cells could be stored at 4°C until needed and processed for electron microscopy as described above.

2.8.5 Morphometric analysis of peroxisomes

For each strain analyzed, electron images of 100 randomly selected cells were processed for measurements of peroxisome area and number, and cell area. The areas of individual cells and of individual peroxisomes were determined by the program analySIS 3.1 (Soft Imaging System). To determine the average area of a peroxisome, the total peroxisome area was calculated and divided by the total number of peroxisomes counted. To quantify peroxisome number, the numerical density of peroxisomes (number of peroxisomes per μm^3 of cell volume) was calculated by the method described previously for spherical organelles (Weibel and Bolender 1973). Briefly, the total number of peroxisome profiles was counted and reported as the number of peroxisomes per cell area assayed (N_A). The peroxisome volume density (V_V) was then calculated as (total peroxisome area/total cell area assayed). Using the values of N_A and V_V, the numerical density of peroxisomes was determined.

2.9 Construction of plasmids

2.9.1 Plasmids for gene expression in yeast

2.9.1.1 pUB4-PEX24

DNA sequence containing the *PEX24* gene flanked by 939 bp of sequence upstream and 846 bp of sequence downstream of the *PEX24* ORF was amplified by PCR using primers AA0975 and AA0978 containing the *Eco*RI recognition sequence. The

PCR product was digested by *Eco*RI and ligated into the corresponding site of pUB4 (Kerscher *et al.*, 2001) to produce the plasmid pUB4-PEX24.

2.9.1.2 YEp-PEX27 and YEp-PEX25

DNA sequence containing the *PEX27* gene flanked by 770 bp of sequence upstream and the 309 bp of sequence downstream of the *PEX27* ORF was amplified by PCR using primers 0082SG and 0083SG containing the *Xho*I recognition sequence. The fragment was cleaved with *Xho*I and cloned into the corresponding site of the vector YEp13 (Broach *et al.*, 1979) to generate YEp-PEX27. To construct YEp13-PEX25, a DNA fragment consisting of the *PEX25* gene flanked by 753 bp of sequence upstream and 319 bp of sequence downstream of the *PEX25* ORF was amplified by PCR using primers 0084SG and 0085SG containing the *Bgl*II recognition sequence and ligated into the *Bam*HI site of YEp13.

2.9.1.3 p20aa-GFP, p46aa-GFP and pFull_length-GFP

A DNA fragment containing 503 bp of sequence downstream of the *PEX3* gene was amplified by PCR using primers 0473QC and 0474QC, digested with *Bam*HI and *Xho*I, and ligated into the corresponding sites of pRS315 (Sikorski and Hieter, 1989) to make the plasmid pRS315-T. The plasmids p20aa-GFP, p46aa-GFP and pFull_length-GFP were constructed by amplifying DNA fragments containing 497 bp of sequence upstream of the *PEX3* gene and sequence encoding the amino-terminal 20 amino acids (using primers 0383SG and 0463QC) or the amino-terminal 46 amino acids of Pex3p (using primers 0383SG and 0464QC) or full-length Pex3p (using primers 0383SG and

0465QC), respectively, cleaved with *Xba*I and *Bam*HI, and ligated into the corresponding sites of pRS315-T, followed by insertion of the sequence encoding GFP$^+$ (Scholz *et al.*, 2000) into the *Bam*HI site. Sequence encoding GFP$^+$ was amplified by PCR using primers 0467QC and 0395SG.

2.9.1.4 pmRFP-SKL

pmRFP-SKL was constructed by replacing the gene for red fluorescent protein (RFP) in the pRS316-based plasmid pDsRed-PTS1 (Smith et al., 2002) with the gene encoding monomeric RFP (mRFP) (Campbell *et al.*, 2002). A cassette containing the DsRed-PTS1 ORF flanked by the *FAA2* (acyl-CoA synthetase) promoter and terminator sequences was released from pDsRed-PTS1 by digestion with *Xba*I and *Xho*I. The cassette was ligated between the *Xba*I/*Xho*I sites of pBluescript II SK(-) to form pBSSK-DsRed-PTS1. The DsRed-PTS1 ORF was released from pBSSK-DsRed-PTS1 by digestion with *Bst*BI and *Bam*HI to form pBSSK. A DNA fragment encoding the ORF of mRFP was amplified by PCR using forward primer 0324QC and reverse primer 0356SG containing the reverse complement sequence encoding PTS1 (SKL), cleaved with *Bst*BI and *Bam*HI and ligated into the corresponding sites of pBSSK to produce the plasmid pmRFP-SKL.

2.9.1.5 pTC3-mRFP$^{1.5}$SKL and pTC3-THIGFP$^+$

The *Y. lipolytica* expression plasmids pTC3-mRFP$^{1.5}$SKL and pTC3-THIGFP$^+$ were constructed as follows. A DNA fragment containing the ORF of mRFP$^{1.5}$ (Campbell et al., 2002) was amplified by PCR using forward primer 0501QC and reverse primer

0502QC containing the reverse complement sequence encoding SKL, digested with *Eco*RI, and ligated into the corresponding site of pTC3 (Smith, 2000) to produce the plasmid pTC3-mRFP$^{1.5}$SKL. DNA sequences encoding the ORFs of *Y. lipolytica* thiolase and GFP^{+} were amplified by PCR using primers 0503QC and 0504QC, and 0505QC and 0506QC, respectively. These two fragments were linked together by PCR using primers 0503QC and 0506QC. The linked product was cleaved with *Eco*RI and ligated into the corresponding site of pTC3 to produce pTC3-THIGFP^{+}.

2.9.2 Plasmids for carboxyl-terminal tagging of specific genes

The plasmids that follow were all constructed in essentially the same manner. pGFP(HIS5) (Dilworth *et al.*, 2001) was digested with *Eco*RI to release the fragment coding for GFP and produce the plasmid pHIS5. Genes encoding fluorescent proteins with or without targeting signal were cloned into the *Eco*RI site of pHIS5 to generate the following plasmids:

2.9.2.1 pmRFP$^{1.3}$(HIS5)

DNA sequence encoding mRFP$^{1.3}$ (Campbell et al., 2002) was amplified by PCR using forward primer 0456QC containing the 3WebA sequence and reverse primer 0457QC. The PCR product was cleaved with *Eco*RI and ligated into the corresponding site of pHIS5 to produce pmRFP$^{1.3}$(HIS5).

2.9.2.2 pmRFP$^{1.5}$HDEL(HIS5) and pGFP^{+}HDEL(HIS5)

To amplify the ORFs of mRFP$^{1.5}$ and GFP^{+} by PCR, forward primers containing the 3WebA sequence and reverse primers containing the reverse complement sequence encoding HDEL were used. mRFP$^{1.5}$ was amplified using primers 0456QC and 0740SG. GFP^{+} was amplified using primers s*Eco*RIGFP^{+} and 0732SG. The PCR products were cleaved with *Eco*RI and ligated into the corresponding site of pHIS5 to produce pmRFP$^{1.5}$HDEL(HIS5) and pGFP^{+}HDEL(HIS5), respectively.

2.9.2.3 pmRFP$^{1.5}$SKL(HIS5) and pGFP^{+}SKL(HIS5)

To amplify the ORFs of mRFP$^{1.5}$ and GFP^{+} by PCR, forward primers containing the 3WebA sequence and reverse primers containing the reverse complement sequence encoding SKL were used. mRFP$^{1.5}$ was amplified using primers 0456QC and 0502QC. GFP^{+} was amplified using primers s*Eco*RIGFP^{+} and 0588SG. The PCR products were cleaved with *Eco*RI and ligated into the corresponding site of pHIS5 to produce pmRFP$^{1.5}$SKL(HIS5) and pGFP^{+}SKL(HIS5), respectively.

2.10 Construction of yeast mutant strains

2.10.1 Integrative disruption of *Y. lipolytica PEX24*

The *URA3* gene of *Y. lipolytica* was used for targeted integrative disruption of the *PEX24* gene. The plasmid pΔPEX24 was constructed by Dr. Richard Rachubinski, Department of Cell Biology, University of Alberta. Essentially, 939 bp of DNA immediately upstream of the *PEX24* ORF was amplified by PCR using the primers AA0975 and AA0976 containing *Eco*RI and *Sal*I recognition sequences, respectively.

The PCR product was cleaved with *Eco*RI and *Sal*I and inserted into the corresponding sites of the vector pGEM4Zf (Promega) to generate the plasmid pUP. 846 bp of DNA immediately downstream of the *PEX24* ORF was amplified by PCR using the primers AA0977 and AA0984 containing *Sal*I and *Hin*dIII recognition sequences, respectively. The fragment was cleaved with *Sal*I and *Hin*dIII and inserted into pUP to produce the plasmid pUP-D*S*. A 1.7-kbp fragment containing the *Y. lipolytica URA3* gene obtained from digestion of the plasmid pSU with *Sal*I was ligated into the *Sal*I site of pUP-DS to produce the plasmid pΔPEX24. A fragment containing the *URA3* gene flanked by the 939 bp of sequence upstream and the 846 bp of sequence downstream of the *PEX24* ORF was amplified by PCR using primers AA0975 and AA0984. This fragment was used to transform *Y. lipolytica* wild-type strain *E122* to uracil prototrophy (Section 2.3.4). Ura^+ transformants were selected and screened for their inability to grow on oleic acid-containing medium. Approximately 350 transformants obtained from the same transformation were screened. Integration of the *URA3* gene into the correct locus was confirmed by PCR.

2.10.2 Construction of double deletion mutants of *S. cerevisiae*

Construction of *pex27Δ/pex25Δ*, *pex27Δ/pex11Δ* and *pex25Δ/pex11Δ* mutants was performed by mating, sporulation and tetrad dissection of various mutant strains according to Section 2.2.3. Essentially, the homozygous deletion diploid strains *pex27Δ-HD* and *pex25Δ-HD* (Table 2-8) were sporulated, and tetrads were dissected to select for the haploid *MATa* strains *pex27Δ-A* and *pex25Δ-A* (Table 2-8). These strains were mated to the haploid *MATα* strains *pex25Δ* and *pex11Δ* (Table 2-8) by replica plating to obtain

three heterozygous diploid strains harboring deletions for *PEX27* and *PEX25*, *PEX27* and *PEX11*, and *PEX25* and *PEX11*. The heterozygous diploid strains were sporulated, and tetrads from 16 heterozygous diploids were dissected for each gene deletion pair. All spores were grown in YPD, and DNA was extracted. Haploid strains harboring deletions in the *PEX27* and *PEX25* genes, the *PEX27* and *PEX11* genes, and the *PEX25* and *PEX11* genes were confirmed by PCR.

2.10.3 Construction of the *pex27Δ/pex25Δ/pex11Δ* mutant

Construction of the *pex27Δ/pex25Δ/pex11Δ* mutant was performed by mating, sporulation and tetrad dissection of various mutant strains according to Section 2.2.3. The haploid strains *pex27Δ/pex11Δ* containing the plasmid pDsRed-PTS1 and *pex27Δ/pex25Δ* were mated. The resulting diploid cells were sporulated, and tetrads from 8 diploids were dissected. DNA was extracted from all spores. The haploid strain deleted for *PEX27*, *PEX25* and *PEX11* was confirmed by PCR.

2.10.4 Integrative disruption of *S. cerevisiae PEX14* and *PEX19*

PEX14 was deleted by PCR-based integrative transformation of yeast. Essentially, a DNA fragment encoding the *URA3* gene of *S. cerevisiae* was amplified by PCR using the plasmid pRS406 (Brachmann *et al.*, 1998) as template, forward primer 0863SG containing 50 bp of sequence immediately upstream of the start codon of *PEX14*, and reverse primer 0864SG containing 50 bp of sequence immediately downstream of the stop codon of *PEX14*. The PCR product was used to transform *S. cerevisiae* strains *46aa-GFP*, *GAL1PEX3/POT1-mRFP* and *GAL1PEX3-mRFP* to uracil prototrophy (Section

2.3.4). Ura^+ transformants were selected, and integration of the *URA3* gene into the correct locus was confirmed by PCR. The deletion of the *PEX19* gene was performed as described above except that primers 0865SC and 0866SC were used.

2.10.5 Introduction of the *GAL1* promoter upstream of the *PEX3* gene

The *GAL1* promoter was introduced upstream of the *PEX3* gene by PCR-based integrative transformation of yeast. A DNA fragment comprising the *GAL1* promoter was amplified by PCR using the plasmid pFA6a-kanMX6-PGAL1 (Longtine *et al.*, 1998) as template, forward primer 0198SG containing 50 bp of sequence 50 bp upstream of the start codon of *PEX3*, and reverse primer 0199SG containing 50 bp of sequence immediately downstream of the start codon of *PEX3*. The fragment was transformed into *S. cerevisiae* strain *BY4742*. Transformants were selected by growth on medium containing geneticin (Invitrogen). Integration of the *GAL1* promoter into the correct locus was confirmed by PCR.

2.10.6 Construction of strains expressing Pex27-pA, Pex3p-GFP, 46aa-GFP, Fox2p-mRFP-SKL, Kar2p-mRFP-HDEL and Pot1p-mRFP

Genes were tagged with sequences encoding protein A or fluorescent proteins by PCR-based integrative transformation of haploid yeast. DNA sequences encoding tags of interest were amplified by PCR using plasmid templates and primers listed in Table 2-10. PCR products were transformed into *S. cerevisiae* strains to confer histidine prototrophy. Integration of tags into correct loci was confirmed by PCR. Certain haploid strains were

made by mating of parental strains listed in Table 2-10 and sporulation of the resulting diploids. Spores expressing the correct fluorescent proteins were confirmed by PCR.

Table 2-10. Construction of strains expressing tagged proteins

Final strain	Parental strain(s)	Method	Template[a]
PEX27-pA	*BY4742*	PCR using primers YOR193w-PTAF and AA1543	pProtA(HIS5)
46aa-GFP	*BY4741*	PCR using primers 0560SG and YDR329c-3WebB	pGFP^{+}(HIS5)
PEX3-GFP	*BY4741*	PCR using primers YDR329c-3WebA and YDR329c-3WebB	pGFP^{+}(HIS5)
GAL1PEX3-mRFP	*GAL1PEX3*	PCR using primers YDR329c-3WebA and YDR329c-3WebB	pmRFP$^{1.3}$(HIS5)
GAL1PEX3/FOX2-mRFP-SKL	*GAL1PEX3*	PCR using primers 0614SG and 0615SG	pmRFP$^{1.5}$SKL(HIS5)
KAR2-mRFP-HDEL	*BY4742*	PCR using primers 0751SG and 0752SG	pmRFP$^{1.5}$HDEL(HIS5)
POT1-mRFP	*BY4741*	PCR using primers YIL160c-3WebA and YIL160c-3WebB	pmRFP$^{1.3}$(HIS5)
46aa-GFP/KAR2-mRFP-HDEL	*46aa-GFP* and *KAR2-mRFP-HDEL*	Mating and sporulation	Not applicable
GAL1PEX3/POT1-mRFP	*GAL1PEX3* and *POT1-mRFP*	Mating and sporulation	Not applicable

[a]pGFP^{+}(HIS5) was a gift of Dr. Richard Wozniak, Department of Cell Biology, University of Alberta. pProtA(HIS5) was a gift of Dr. John Aitchison, Institute for Systems Biology, Seattle, Washington.

2.11 Polyclonal antibody production

Antibodies were raised in rabbit and guinea pig against protein fusions to maltose-binding protein (MBP) as described below.

Production and purification of fusion proteins were performed using the pMAL Protein Fusion and Purification System according to the manufacturer's instructions (NEB). This method is based on the induction of fusion protein synthesis by IPTG and affinity chromatography of the fusion proteins on amylose resin. DNA fragments were cloned into the vector pMAL-c2 (NEB) in-frame and downstream of the ORF encoding MBP. The plasmids were transformed into *DH5α* or *BLR-DE3* cells (Table 2-5). Synthesis of fusion proteins was induced by adding IPTG to a final concentration of 1 mM to the growing cells (OD_{600}~0.5). Cells were incubated in the presence of IPTG for 2 to 3 h at 37°C, harvested by centrifugation, and resuspended in new column buffer (200 mM Tris-HCl, pH 7.4, 2 M NaCl, 10 mM EDTA, 1 × PIN) containing 1 mM DTT at a concentration of 10 ml per g of wet cells. Cells were lysed by sonication in 30 sec bursts using a Branson Sonifier 250 (duty 30%, output control 3). Cell debris was pelleted by centrifugation. The supernatant was diluted with two volumes of new column buffer (200 mM Tris-HCl, pH 7.4, 2 M NaCl, 10 mM EDTA, 1 × PIN) and passed through an amylose resin column. MBP fusion proteins were eluted by addition of 10 mM maltose. Protein concentration was determined as described in Section 2.6.3.

Proteins were further purified by gel electrophoresis according to Harlow and Lane (1988). Proteins were separated on 10% SDS-PAGE gels. Gels were stained in 0.05% Coomassie Brilliant Blue R-250 in water for 10 to 15 min and destained in water. Gel fragments containing a protein of interest were excised and placed in dialysis tubing.

Elution buffer (0.2 M Tris-acetate, pH 7.4, 1% SDS, 10 mM DTT) was added to the tubing at a concentration of 10 ml per g of wet gel. Proteins were eluted from the gel by electrophoresis at 50 V overnight at 4°C in 50 mM Tris-HCl, pH 7.4, 0.1% SDS. The eluate was placed in 2 to 3 new dialysis tubings and dialyzed against 4 L of 50 mM ammonium bicarbonate once at room temperature and three times at 4°C. The protein solution was then frozen at -80°C and dried by lyophilization overnight. Lyophilized protein was resuspended in a minimal volume of water, and the protein concentration was measured as described in Section 2.6.3.

Animals were immunized according to Harlow and Lane (1988). Proteins were adjusted to a concentration of 500 μg/ml and mixed with an equal volume of Freund's complete or incomplete adjuvant for primary and subsequent injections, respectively. Rabbits and guinea pigs were injected with 1 ml (containing 200 μg of protein) and 0.4 ml (containing 80 μg of protein), respectively, at several subcutaneous sites every six weeks. Bleeds were taken 10 days after each injection. Serum was separated from red blood cells in clotted blood by centrifugation at 2,000 × *g* for 15 min at room temperature. Serum was stored at -20°C in aliquots. The presence of specific antibodies in serum was analyzed by immunoblotting (Section 2.6.6).

2.11.1 Production of antisera directed against *Y. lipolytica* Pex24p

The plasmid pMAL-PEX24 was constructed by Dr. Richard Rachubinski, Department of Cell Biology, University of Alberta, and used to derive the plasmid pMAL-PEX24C. The ORF of *PEX24* was amplified by PCR using primers AA0972 and AA0973 containing *Eco*RI and *Xba*I recognition sequences, respectively. The fragment

was digested with *Eco*RI and *Xba*I and ligated into the corresponding site of pMAL-c2 to produce the plasmid pMAL-PEX24. This plasmid was digested with *Hin*dIII to release a fragment encoding the carboxyl-terminal 227 amino residues of Pex24p. The fragment was ligated into the corresponding site of pMAL-c2 to produce the plasmid pMAL-PEX24C. Antibodies to MBP-Pex24p were raised in rabbits (L257, L258) and guinea pigs (A174, A175) as described in Section 2.12, and affinity-purified as described (Crane *et al.*, 1994).

2.11.2 Production of antisera directed against *S. cerevisiae* Pex3p

The plasmid pMAL-PEX3C was constructed as described below. DNA sequence encoding the carboxyl-terminal 301 amino residues of Pex3p was amplified by PCR using primers 0636SG and 0420SG containing the *Bam*HI recognition sequence. The PCR fragment was digested with *Bam*HI and cloned into the corresponding site of pMAL-c2 to produce the plasmid pMAL-PEX3C. Production and purification of MBP-Pex3p was performed by Elena Savidov, Department of Cell Biology, University of Alberta, as described in Section 2.12. MBP-Pex3p was cleaved with Factor Xa (NEB) to release Pex3p. Antibodies to Pex3p were raised in rabbits (P84, P86) and guinea pigs (Q12, Q13) as described in Section 2.12.

2.12 Yeast two-hybrid analysis

Yeast two-hybrid analysis was performed using the Matchmaker Two-Hybrid System according to the manufacturer's instructions (Clontech) with modifications.

2.12.1 Construction of chimeric genes

Chimeric genes were made by amplifying the ORFs of *PEX27*, *PEX25* and *PEX11* by PCR and ligating then in-frame and downstream of sequences encoding the activation domain (AD) and DNA-binding domain (DB) of the GAL4 transcriptional activator in plasmids pGAD424 and pGBT9, respectively. To construct pGAD424-PEX27 and pGBT9-PEX27, the *PEX27* ORF was amplified by PCR using primers 0041SG and 0042SG. To construct pGAD424-PEX25 and pGBT9-PEX25, the *PEX25* ORF was amplified by PCR using primers 0043SG and 0044SG. To construct pGAD424-PEX11 and pGBT9-PEX11, the *PEX11* ORF was amplified by PCR using primers 0045SG and 0046SG. All primers contained the *Eco*RI recognition sequence. All PCR products were digested with *Eco*RI and ligated into pGAD424 and pGBT9.

2.12.2 Assays for two-hybrid interactions

Plasmid pairs encoding AD and DB fusion proteins were transformed into *S. cerevisiae* strain *SFY526* as described in Section 2.3.3. Transformants were grown in SM medium (Table 2-9). Possible interaction between AD and DB fusion proteins were detected by testing for activation of the integrated *lacZ* construct using β-galactosidase filter and liquid assays according to the instructions of Clontech, with modifications. For filter assays, cells were streaked directly onto filter paper placed on solid media and broken by 4 freeze-thaw cycles at -80°C. For liquid assays, yeast from 1 ml of culture was used instead of from 1.5 ml of culture.

2.13 Computer-aided DNA and protein sequence analyses

Protein sequences were compared to other sequences using the BLAST algorithms (http://www.ncbi.nlm.nih.gov/BLAST/) (National Center for Biotechnology Information) and aligned using the ClustalW program (http://www.edi.ac.uk/clustalw/) (EMBL-EBI). Protein sequences were analyzed using the Yeast Proteome Database (http://www.proteome.com/) (BIOBASE), the *Saccharomyces* Genome Database (http://www.yeastgenome.org/) (Stanford University), and the CBS Prediction Servers (http://www.cbs.dtu.dk/services/TMHMM/) (Center for Biological Sequence Analysis). DNA sequences were analyzed using Visual Cloning 3 (Redasoft).

CHAPTER 3

PEX24P IS A PEROXISOMAL MEMBRANE PROTEIN AND IS REQUIRED FOR PEROXISOME ASSEMBLY IN *YARROWIA LIPOLYTICA*

A version of this chapter has previously been published as "*Yarrowia lipolytica* cells mutant for the *PEX24* gene encoding a peroxisomal membrane peroxin mislocalize peroxisomal proteins and accumulate membrane structures containing both peroxisomal matrix and membrane proteins" (Yuen Yi C. Tam and Richard A. Rachubinski. 2002. *Mol. Biol. Cell* 13: 2681-2691). Reprinted with permission.

3.1 Overview

This chapter describes the identification and characterization of a novel peroxin, Pex24p, of the yeast *Y. lipolytica*. A genetic screen was used to identify mutants of peroxisome biogenesis of *Y. lipolytica*. The mutant *mut1-1* was isolated on the basis of its inability to grow on medium containing oleic acid as the sole carbon source, the metabolism of which requires intact peroxisomes. Functional complementation of the *mut1-1* strain has identified the novel gene, *PEX24*. *PEX24* encodes Pex24p, a protein of 550 amino acids, with a predicted molecular mass of 61,100 Da. Pex24p is an integral membrane protein of peroxisomes that exhibits high sequence homology to two proteins encoded by the ORFs *YHR150w* and *YDR479c* of the *S. cerevisiae* genome. These two genes were later renamed *PEX28* and *PEX29*, respectively. Pex24p is detectable in wild-type cells grown in glucose-containing medium, and its levels are significantly increased by incubation of cells in oleic acid-containing medium.

Cells of the *mut1-1* and *pex24KOA* (a *PEX24* gene disruption strain) strains are compromised in the targeting of both matrix and membrane proteins to peroxisomes. Although they fail to assemble functional peroxisomes, they do harbor membrane structures that contain subsets of peroxisomal proteins. These results suggest a role for Pex24p in the import of peroxisomal matrix and membrane proteins.

3.2 Identification of the *mut1-1* mutant strain

A previously developed screen was used to identify mutants of peroxisome biogenesis of the yeast *Y. lipolytica* (Brown, 2000). The *mut1-1* mutant strain (Table 2-7) was isolated from randomly mutagenized wild-type *E122* cells by its inability to grow on

medium containing oleic acid as the sole carbon source (the ole phenotype, see Figure 3-1). Morphological and biochemical analyses determined that the *mut1-1* mutant strain was defective in the targeting and import of peroxisomal proteins (a detailed discussion follows), which corresponds to the classical *pex* mutant phenotype.

3.3 Isolation and characterization of the *PEX24* gene

Isolation of the *PEX24* gene was performed by Dr. Melchior Evers, Department of Cell Biology, University of Alberta, as described below. The *PEX24* gene was isolated from a *Y. lipolytica* genomic DNA library by functional complementation, *i.e.*, restoration of growth on oleic acid-containing medium (the OLE phenotype), of the *mut1-1* strain. DNA was isolated from the complemented strain, and the complementing plasmid was recovered by transformation of *E. coli*. The complementing fragment, CS-01, was mapped by restriction endonuclease digestion (Figure 3-2 A). Various restriction fragments were subcloned and introduced by transformation into the *mut1-1* strain to delineate the region of complementation (Figure 3-2 A). Sequencing of the complementing fragment CS-SS revealed an ORF, termed *PEX24*, of 1650 nucleotides encoding a protein of 550 amino acids, termed Pex24p, with a predicted molecular weight of 61,100 (Figure 3-2 B). Based on algorithms predicting membrane-associated regions in proteins (Eisenberg *et al.*, 1984; Rao and Argos, 1986), Pex24p is predicted to contain two membrane-spanning domains at amino acids 216-249 and 335-361.

A search of protein databases with the use of the GENINFO(R) BLAST Network Service of the National Center for Biotechnology Information revealed two proteins encoded by the ORFs *YHR150w* and *YDR479c* of the *S. cerevisiae* genome (Figure 3-3)

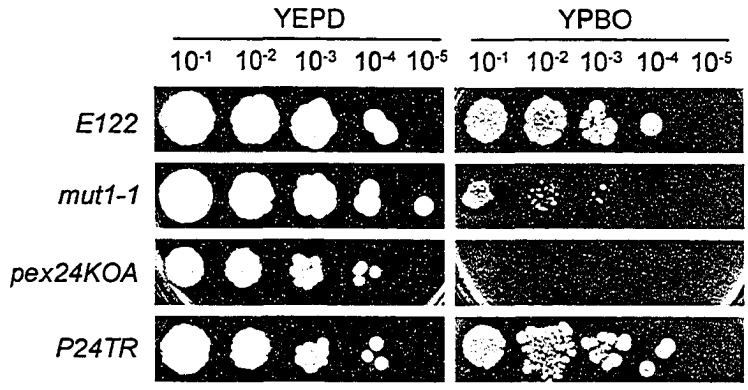

Figure 3-1. Growth of various *Y. lipolytica* strains on glucose-containing (YEPD) and oleic acid-containing (YPBO) media. The strains listed in Table 2-7 were grown to mid log phase in liquid YEPD medium, spotted at dilutions of 10^{-1} to 10^{-5} on both YEPD and YPBO agar, and grown for 5 days at 30°C.

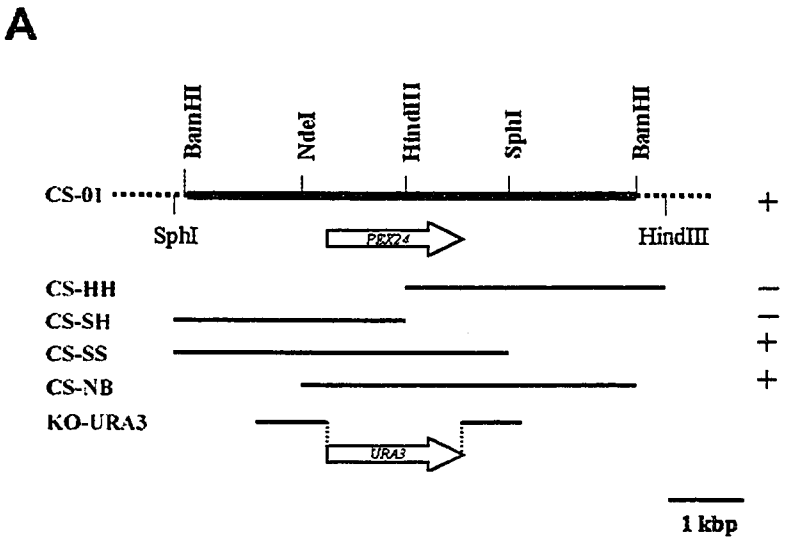

Figure 3-2. Cloning and analysis of the *PEX24* gene. (A) Complementing activity of inserts, restriction map analysis, and targeted gene disruption strategy for the *PEX24* gene. The thick black line represents the original complementing insert DNA. (Solid lines) *Y. lipolytica* genomic DNA; (dotted lines) vector DNA. The ORFs of the *PEX24* and *URA3* genes and their directionality are denoted by the wide arrows. (+) Ability and (−) inability of an insert to confer growth on oleic acid to strain *mut1-1*. (B) (page 79) Nucleotide sequence of the *PEX24* gene and deduced amino acid sequence of Pex24p. Black lines delineate putative transmembrane sequences. These sequence data have been deposited in the DDBJ/EMBL/GenBank databases under accession number AF480881.

B

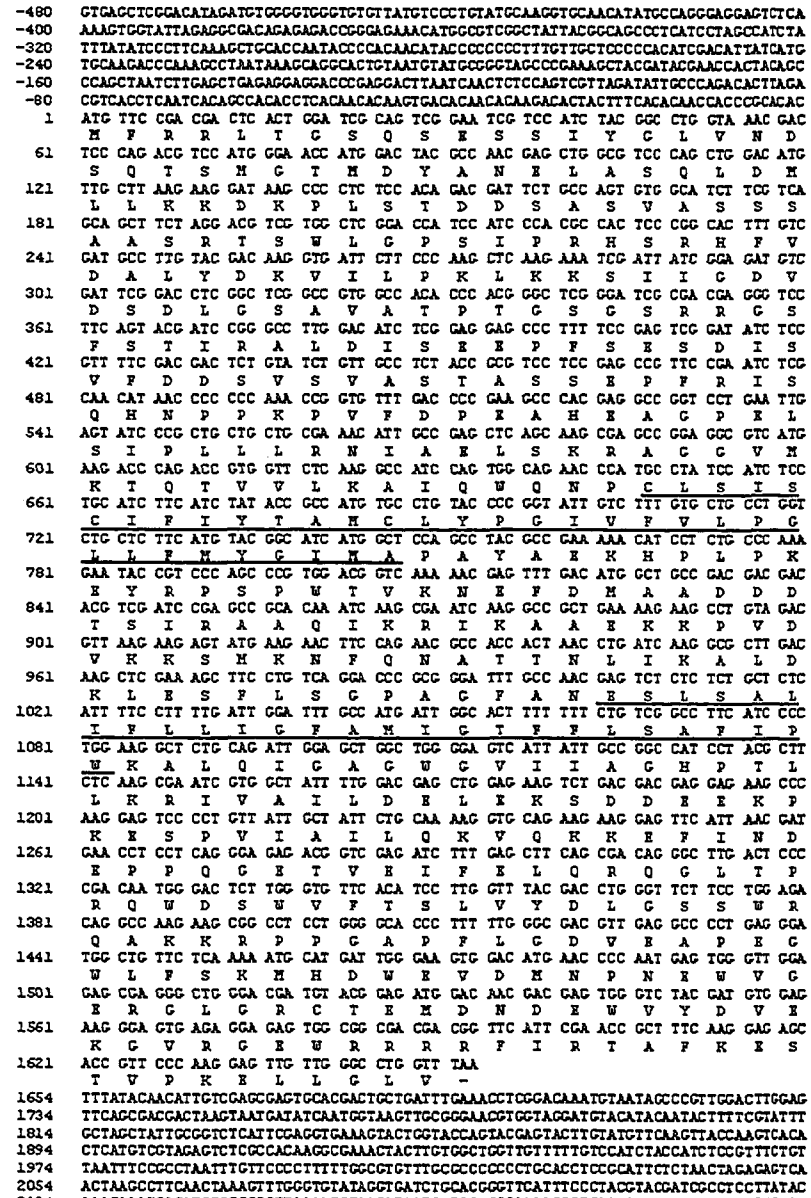

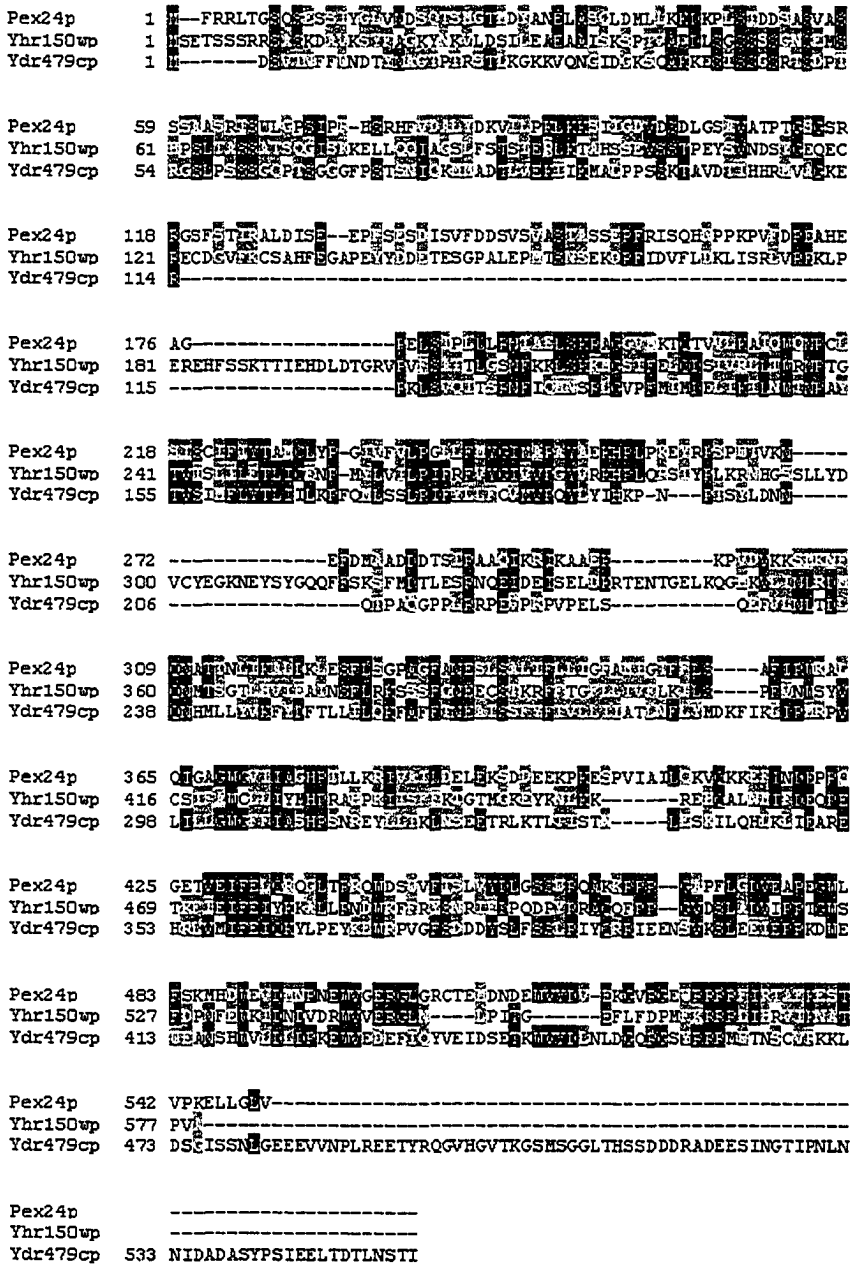

Figure 3-3. Sequence alignment of Pex24p with the proteins Yhr150p and Ydr479p encoded by the ORFs *YHR150w* and *YDR479c*, respectively, of the *S. cerevisiae* genome. Amino acid sequences were aligned with the use of the ClustalW program (EMBL, Heidelberg, Germany). Identical residues (black) and similar residues (gray) in at least two of the proteins are shaded. Similarity rules: G = A = S; A = V; V = I = L = M; I = L = M = F = Y = W; K = R = H; D = E = Q = N; and S = T = Q = N. Dashes represent gaps.

that share extensive sequence homology with Pex24p. Pex24p and Yhr150p exhibit 21.1% amino acid identity and 44.4% amino acid similarity, while Pex24p and Ydr479p exhibit 20.8% amino acid identity and 42.1% amino acid similarity (Figure 3-3). The characterization of Yhrp150p and Ydr479p was performed by Franco Vizeacoumar, Department of Cell Biology, University of Alberta (Vizeacoumar *et al.*, 2003). Yhr150p and Ydr479p were renamed Pex28p and Pex29p, respectively, and were shown to be involved in controlling peroxisome number, size and distribution in *S. cerevisiae*.

The *PEX24* gene was deleted by targeted integration of the *Y. lipolytica URA3* gene (Figure 3-2 A) to generate the strain *pex24KOA* (Table 2-7). This strain was unable to grow on oleic acid-containing medium (Figure 3-1) and showed morphological and biochemical defects similar to those of the original *mut1-1* strain (described below).

3.4 *pex24* cells lack normal peroxisomes and mislocalize peroxisomal proteins to the cytosol

In electron micrographs, normal peroxisomes of *Y. lipolytica* grown in oleic acid-containing medium appear as round vesicular structures, 0.2-0.5 μm in diameter, surrounded by a single unit membrane and containing an homogenous granular matrix (Figure 3-4 A). The original mutant strain *mut1-1* (Figure 3-4 B) contained small vesicular structures and some larger vesicles resembling peroxisomes and accumulated membranous sheets around the nucleus that were rarely seen in wild-type cells. The deletion strain *pex24KOA* showed no morphologically recognizable peroxisomes but again showed an accumulation of extended membranes (Figure 3-4 C). Strain *P24TR* (Table 2-7) transformed with the *PEX24* gene had the appearance of the wild-type strain,

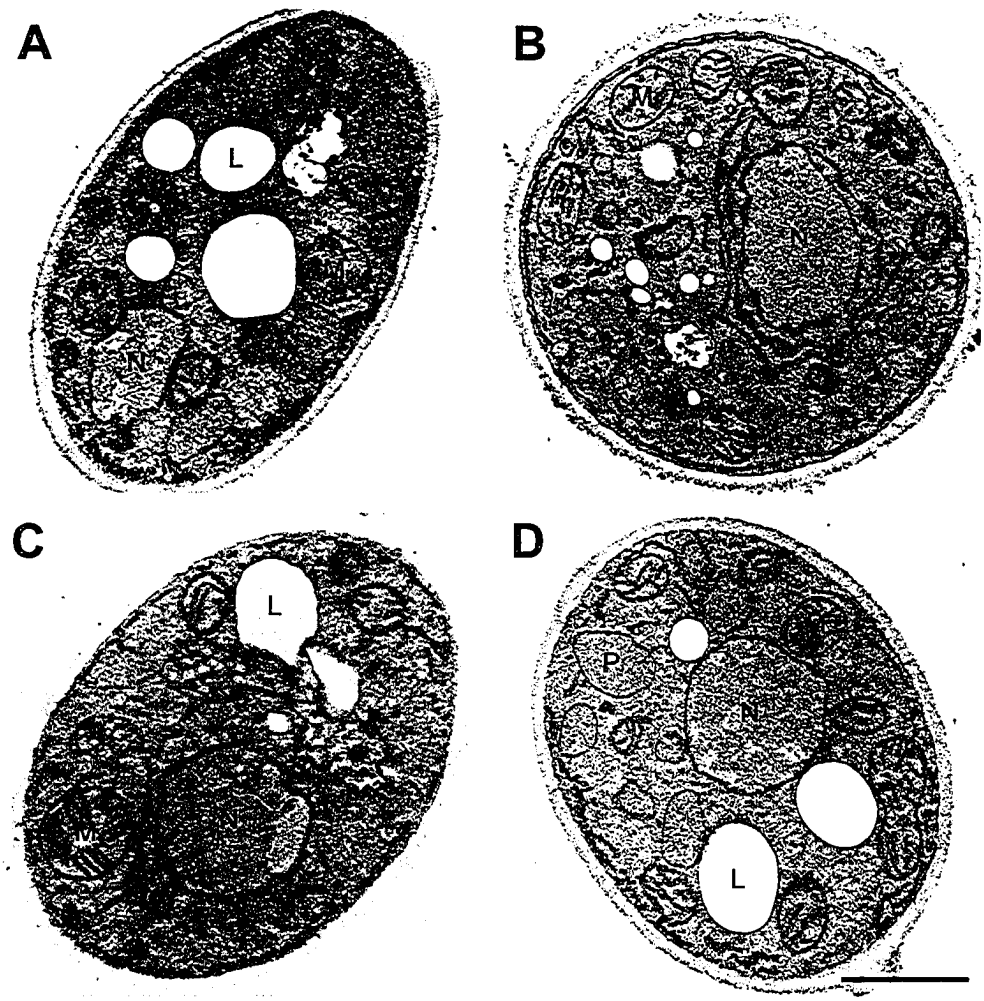

Figure 3-4. Ultrastructure of wild-type, *pex24* mutant, and *PEX24*-transformed strains. The *E122* (A), *mut1-1* (B), *pex24KOA* (C), and *P24TR* (D) strains were grown in glucose-containing YEPD medium for 16 h, shifted to oleic acid-containing YPBO medium and incubated for an additional 9 h. Cells were fixed in 1.5% $KMnO_4$ and processed for electron microscopy. L, lipid droplet; M, mitochondrion; N, nucleus; P, peroxisome. Bar, 1 μm.

as it grew on oleic acid-containing medium at a rate very similar to that of wild-type cells (Figure 3-1) and showed normal peroxisome morphology (Figure 3-4 D).

Immunofluorescence analysis of oleic acid-incubated wild-type *E122* cells with anti-SKL antibodies and antibodies to the matrix proteins acyl-CoA oxidase (AOX), isocitrate lyase (ICL), and thiolase (THI) and to the peroxisomal integral membrane protein Pex2p showed a punctate pattern of staining characteristic of peroxisomes (Figure 3-5). In contrast, *mut1-1* and *pex24KOA* cells stained with the same antibodies showed a more diffuse pattern of fluorescence characteristic of a cytosolic localization (Figure 3-5). Strain *P24TR* transformed with the *PEX24* gene showed the characteristic peroxisomal staining pattern observed in wild-type cells, indicating the ability of this gene to rescue the import of these peroxisomal proteins.

Subcellular fractionation was performed to further investigate the localization of peroxisomal proteins in *pex24* cells. Cells of the wild-type strain *E122* and of the mutant strains *mut1-1* and *pex24KOA* were grown for 16 h in glucose-containing medium, shifted to oleic acid-containing medium for an additional 9 h, and then fractionated into a 20,000 × *g* pellet (20KgP) fraction enriched for peroxisomes and mitochondria and a 20,000 × *g* supernatant (20KgS) fraction enriched for cytosol. In agreement with data from immunofluorescence microscopy, peroxisomal matrix proteins, SKL-containing proteins, AOX, ICL and THI, were preferentially localized to the 20KgP fraction of wild-type cells (Figure 3-6); however, they were localized primarily to the 20KgS fraction of both mutant strains. It is noteworthy that AOX was found equally distributed between the 20KgS and 20KgP fractions of the original mutant strain *mut1-1*. Because in *pex24* mutant strains all matrix proteins investigated mislocalized preferentially to the 20KgS

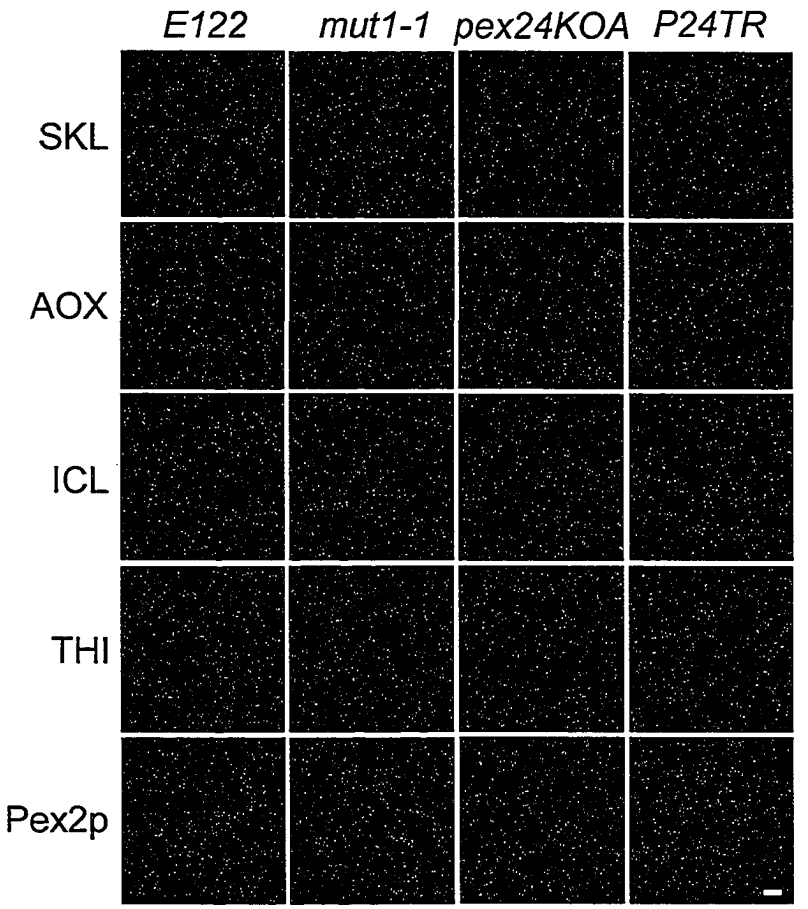

Figure 3-5. Peroxisomal matrix and membrane proteins are mislocalized in *pex24* mutant strains. Wild-type strain *E122*, mutant strains *mut1-1* and *pex24KOA*, and transformed strain *P24TR* were grown in YEPD medium for 16 h, transferred to YPBO medium, and incubated for an additional 9 h. Cells were processed for immunofluorescence microscopy with antibodies to the PTS1 tripeptide SKL (SKL), acyl-CoA oxidase (AOX), isocitrate lyase (ICL), thiolase (THI), and the integral peroxisomal membrane protein Pex2p. Rabbit primary antibodies (SKL, AOX, and ICL) were detected with fluorescein-conjugated secondary antibodies. Guinea pig primary antibodies (THI and Pex2p) were detected with rhodamine-conjugated secondary antibodies. Bar, 1 μm.

fraction enriched for cytosol and exhibited a generalized pattern of fluorescence characteristic of the cytosol in immunofluorescence microscopy, *pex24* mutants are compromised in the import of PTS1 (ICL and SKL-containing proteins), PTS2 (THI), and non-PTS1, non-PTS2 proteins (AOX; Wang *et al.*, 1999). The peroxisomal peroxin Pex19p (Lambkin and Rachubinski, 2001), the peripheral peroxisomal membrane peroxin Pex16p (Eitzen *et al.*, 1997) and the integral peroxisomal membrane peroxin Pex2p (Eitzen *et al.*, 1996) were all localized primarily to the 20KgP of *E122* cells (Figure 3-6). In contrast, these peroxins were localized almost exclusively to the 20KgS of both *mut1-1* and *pex24KOA* cells, demonstrating a preferential mislocalization of these peroxisomal membrane peroxins to the cytosol in these strains.

3.5 *pex24* cells contain membrane structures containing both peroxisomal matrix and membrane proteins

To determine if there is any peroxisomal membrane structure in *pex24* cells, the 20KgP fractions of the wild-type strain *E122* and of the *mut1-1* and *pex24KO* mutant strains incubated in oleic acid-containing medium were subjected to isopycnic sucrose gradient density centrifugation, and fractions were analyzed. The distributions of the mitochondrial marker cytochrome *c* oxidase and the peroxisomal marker catalase were determined by analyzing their enzymatic activities in fractions obtained from *E122*, *mut1-1* and *pex24KO* cells (Figure 3-7 A). The fractions were also analyzed by immunoblotting with antibodies to peroxisomal matrix proteins (SKL-containing proteins, ICL, AOX, and THI), to the peroxins Pex16p, Pex19p, and Pex2p, and to the endoplasmic reticulum-resident protein, Kar2p (Figure 3-7 B). The mitochondrial marker

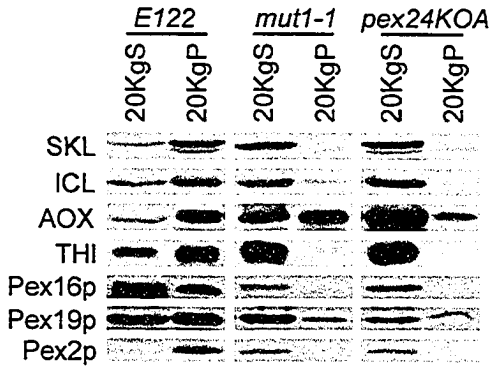

Figure 3-6. Peroxisomal matrix proteins and peroxisomal peroxins show mislocalization in *pex24* mutant strains. The wild-type strain *E122*, the original mutant strain *mut1-1*, and the deletion strain *pex24KOA* were grown in glucose-containing YEPD medium for 16 h, transferred to oleic acid-containing YPBO medium, and incubated for an additional 9 h. Cells were subjected to subcellular fractionation to yield a 20KgP fraction enriched for peroxisomes and mitochondria and a 20KgS fraction enriched for cytosol. Equal portions of the 20KgS and 20KgP were analyzed by immunoblotting to peroxisomal matrix proteins (SKL, ICL, AOX, and THI) and to peroxisomal peroxins.

A

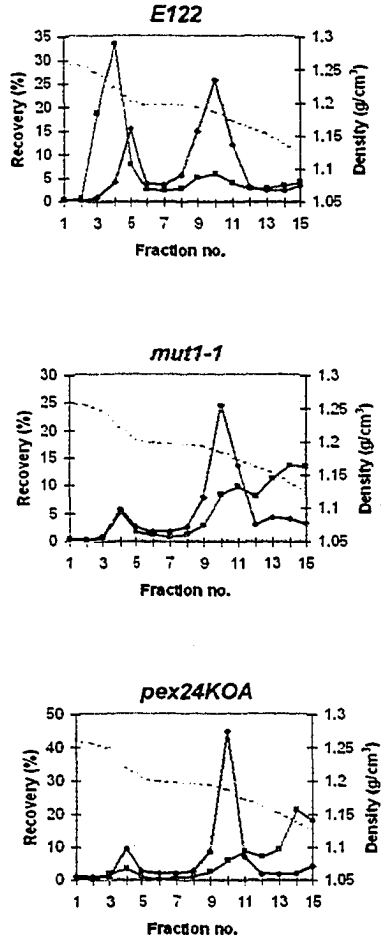

Figure 3-7. Peroxisomal proteins of *pex24* cells localize in part to membrane structures that are of the same density as wild-type peroxisomes. The 20KgP fractions of the wild-type strain *E122*, the original mutant strain *mut1-1* and the deletion strain *pex24KOA* incubated in oleic acid-containing medium for 9 h were subjected to isopycnic centrifugation on discontinuous sucrose gradients. Fifteen 2-ml fractions were collected from the bottom of each tube. Equal volumes of each fraction were analyzed. (A) The enzymatic activities of the mitochondrial enzyme cytochrome *c* oxidase (blue line) and the peroxisomal maker enzyme catalase (pink line) were measured. Green dotted line represents the density of each fraction. (B) (page 88) Immunoblot analysis using antibodies to the indicated proteins was performed. The volume of fractions of the *mut1-1* and *pex24KOA* strains analyzed by SDS-PAGE was 10 times that of fractions of the wild-type strain *E122*.

B

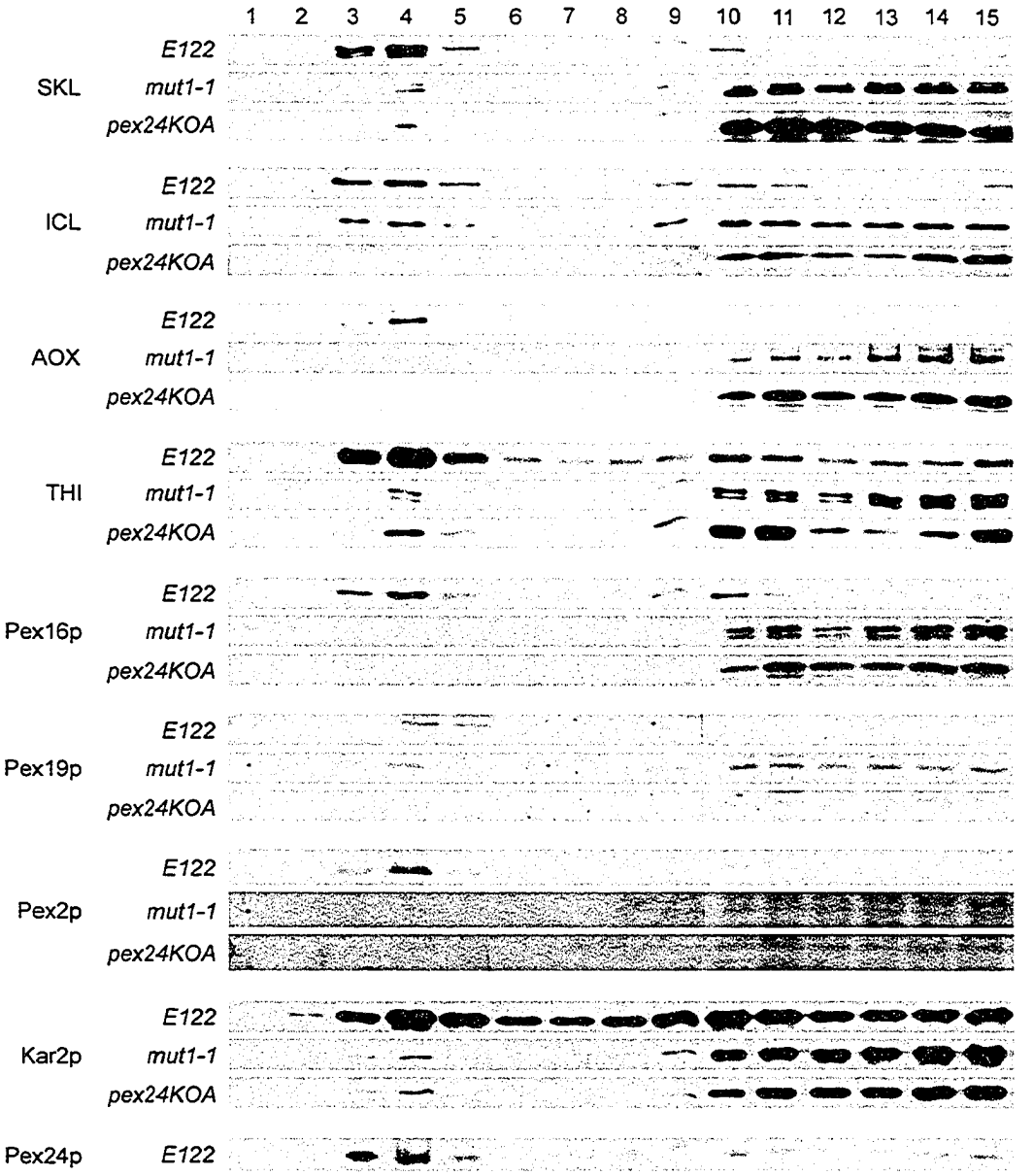

cytochrome *c* oxidase localized primarily to fractions 9-11 in all strains, peaking in fraction 10 at a density of 1.17 g/cm^3, well separated from fraction 4 containing the peak immunodetection of peroxisomal proteins for the wild-type strain (described below). In *E122* cells, all peroxisomal proteins investigated were found primarily in fractions 3-5 (Figures 3-7 A and B), peaking in fraction 4 at a density of 1.21 g/cm^3, which has previously been reported as the density of peroxisomes of *Y. lipolytica* in sucrose (Szilard *et al.*, 1995; Titorenko *et al.*, 1996; Brown *et al.*, 2000), whereas Kar2p exhibited an almost even distribution across all gradient fractions (Figure 3-7 B). In *mut1-1* and *pex24KOA* cells, evidence of membrane structures having a density similar to that of wild-type peroxisomes was observed; however, these structures contained a complement of proteins different from that of wild-type peroxisomes. SKL-containing proteins, ICL, THI, and Pex19p, but not the peripheral membrane protein Pex16p or the integral membrane protein Pex2p, were detected in structures found in fraction 4 of the *mut1-1* strain. Only SKL-containing proteins, ICL and THI, were detected in structures found in fraction 4 of the deletion strain *pex24KOA*. Membrane structures of density less than that of wild-type peroxisomes but containing peroxisomal proteins were also observed for both wild-type cells and, to a much greater extent, for *mut1-1* and *pex24KOA* cells. The origin of these membrane structures is unknown, but it should be noted that Kar2p is readily seen to cofractionate with them in gradients of the *mut1-1* and *pex24KOA* strains. It is noteworthy that both the 47-kDa precursor form and the 45-kDa mature form of thiolase were detected in the *mut1-1* strain, whereas only the precursor form was detected in the *pex24KOA* deletion strain.

3.6 Pex24p is an integral membrane protein of peroxisomes

To analyze Pex24p, antibodies against Pex24p were raised in rabbit and guinea pig. Double-labeling indirect immunofluorescence microscopy and subcellular fractionation of wild-type cells incubated in oleic acid-containing medium were performed to examine the subcellular localization of Pex24p. Cells labeled with antibodies to thiolase and to Pex24p showed colocalization of these proteins to punctate structures (Figure 3-8 A). Furthermore, Pex24p was localized exclusively to the 20KgP fraction enriched for peroxisomes and mitochondria from wild-type cells (Figure 3-8 B) and fractionated with peroxisomes in isopycnic density gradient centrifugation (Figure 3-7). Together these data suggest that Pex24p is a peroxisomal protein. To determine the subperoxisomal localization of Pex24p, peroxisomes were chemically treated as described below. Lysis of peroxisomes with alkali Na_2CO_3, followed by high-speed centrifugation, showed that Pex24p cofractionated with Pex2p to the pellet fraction enriched for integral membrane proteins (Figure 3-8 C). Therefore, Pex24p is an integral membrane protein of peroxisomes.

3.7 Synthesis of Pex24p is induced by incubation of cells in oleic acid-containing medium

The synthesis of many peroxisomal proteins is induced by incubating yeast cells in medium containing oleic acid. Wild-type *E122* cells grown in glucose-containing medium were transferred to oleic acid-containing YPBO and incubated for 8 h in this medium. Aliquots of cells were removed at various times during the incubation in YPBO, and their lysates were subjected to SDS-PAGE and immunoblotting. Pex24p was barely

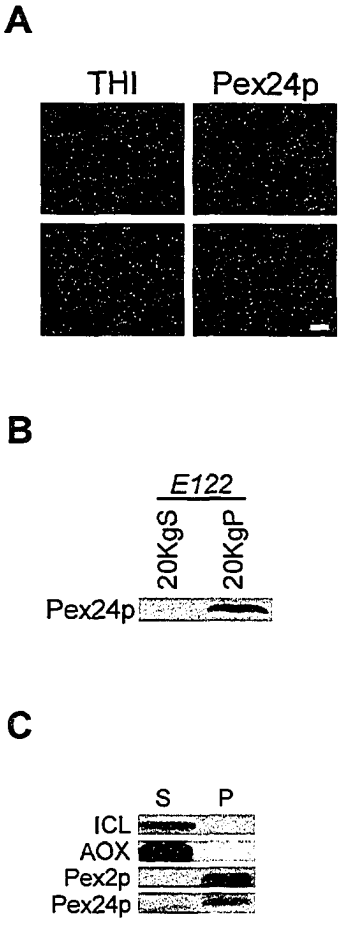

Figure 3-8. Pex24p is an integral peroxisomal membrane protein. (A) Double-labelling, indirect immunofluorescence microscopy of wild-type cells with antibodies to thiolase (THI) and to Pex24p. Bar, 1 μm. (B) Immunoblot analysis of 20KgS and 20KgP subcellular fractions from wild-type cells incubated in oleic acid-containing medium with anti-Pex24p antibodies. Equivalent portions of each fraction were analyzed. (C) Immunoblot analysis of wild-type peroxisomes treated with alkali Na_2CO_3 and separated by centrifugation into supernatant (S) and pellet (P) fractions. The top and second blots were probed with antibodies to THI and acyl-CoA oxidase (AOX), respectively, to detect peroxisomal matrix proteins. The third blot was probed with antibodies to the peroxisomal integral membrane protein Pex2p. The bottom blot was probed with antibodies to Pex24p. Equivalent portions of the supernatant and pellet fractions were analyzed.

detectable at the time of transfer to YPBO, but its synthesis increased with time after the transfer (Figure 3-9). Under the same conditions, the level of the peroxisomal matrix enzyme thiolase (THI) increased dramatically, whereas the level of the cytosolic enzyme glucose-6-phosphate dehydrogenase (G6PDH) remained unchanged.

3.8 Analysis of the *mut1-1* mutant allele of the *PEX24* gene

To further characterize the *mut1-1* mutant strain, the *mut1-1* mutant allele of the *PEX24* gene was amplified by PCR using genomic DNA isolated from the *mut1-1* mutant as template and subcloned into a plasmid vector for DNA sequencing. Sequencing of the *mut1-1* mutant allele of the *PEX24* gene revealed a nonsense mutation at codon 118, suggesting that *mut1-1* mutant cells express a mutant form of Pex24p that lacks most of its carboxyl-terminal amino acids.

3.9 Discussion

3.9.1 Pex24p of *Y. lipolytica*

Pex24p is a novel peroxin of the yeast *Y. lipolytica*. It is composed of 550 amino acids and predicted to have a molecular mass of 61,100 Da. Pex24p was shown to be peroxisomal by both double-label, indirect immunofluorescence microscopy and subcellular fractionation. Pex24p is predicted to contain two membrane-spanning domains and displays the characteristics of an integral membrane protein during extraction of a subcellular fraction enriched for peroxisomes with alkali sodium carbonate. Pex24p shows strong sequence similarity to two putative proteins encoded by the ORFs *YHR150w* and *YDR479c* of the *S. cerevisiae* genome. These proteins have been

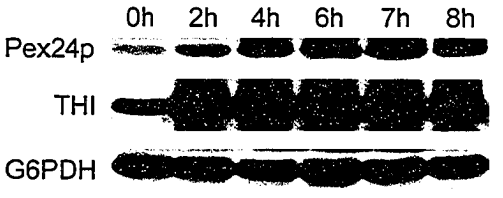

Figure 3-9. Synthesis of Pex24p is induced by incubation of *Y. lipolytica* in oleic acid-containing medium. Wild-type *E122* cells grown for 16 h in glucose-containing YEPD medium were transferred to, and incubated in, oleic acid-containing YPBO medium. Aliquots of cells were removed from the YPBO medium at the times indicated, and total cell lysates were prepared. Equal amounts of protein from the total cell lysates were analyzed by SDS-PAGE and immunoblotting with antibodies to Pex24p, thiolase (THI), and glucose-6-phosphate dehydrogenase (G6PDH).

shown to be involved in the regulation of peroxisome size, number and distribution in *S. cerevisiae* (Vizeacoumar *et al.*, 2003) Possible functional redundancy between these two proteins may have prevented their ready identification as *PEX* genes in *S. cerevisiae* by selection procedures involving random mutagenesis.

3.9.2 Reduced functionality of the mutant form of Pex24p

The ability to use oleic acid as a sole carbon source was greatly reduced in the original mutant strain *mut1-1*, whereas it was completely abolished in the deletion strain *pex24KOA*. DNA sequencing revealed a nonsense mutation at codon 118 of the *PEX24* gene of the *mut1-1* strain. Judging from the reduced growth of the *mut1-1* strain on oleic acid-containing medium and the presence of small vesicular structures resembling peroxisomes in *mut1-1* cells seen by electron microscopy, it can be speculated that the shortened form of Pex24p synthesized in the *mut1-1* strain retains some, but not all, of its function(s). The carboxyl-terminal part of Pex24p, which is missing in the mutant form of Pex24p of the *mut1-1* strain, contains two predicted transmembrane domains. The mutant Pex24p may therefore be unable to exhibit its entire range of functions due to an inability to associate tightly with the peroxisomal membrane.

3.9.3 Possible roles of Pex24p in peroxisome biogenesis

Isopycnic density gradient centrifugation analysis showed that both the original mutant strain *mut1-1* and the deletion strain *pex24KOA* contain membrane structures having densities both like and less than that of normal peroxisomes. These membrane structures are not "peroxisome ghosts", which are found in cells of Zellweger syndrome

patients and were defined originally as membranous structures containing peroxisomal membrane proteins but not peroxisomal matrix proteins (Santos *et al.*, 1988), because they contain both peroxisomal matrix and membrane proteins. Similar membrane structures have been reported for other *Y. lipolytica pex* strains (Brown *et al.*, 2000; Lambkin and Rachubinski, 2001). Whether these structures are precursors to mature peroxisomes (South and Gould, 1999; Titorenko *et al.*, 2000) or simply types of peroxisomes lacking their full complement of peroxisomal proteins is unknown at present. It is possible that Pex24p assists the maturation of peroxisomes by facilitating import of peroxisomal proteins.

Pex5p and Pex7p act as cytosolic receptors for PTS1- and PTS2-containing proteins, respectively. Although there is distinct separation in these two pathways of matrix protein import at this initial stage, convergence of the two pathways is believed to occur at the level of the peroxisome and to involve the peroxins Pex13p and Pex14p. Pex13p and Pex14p are integral proteins of the peroxisomal membrane that recognize both Pex5p and Pex7p and form a complex with each other (for reviews, see Subramani, 1998; Hettema *et al.*, 1999; Purdue and Lazarow, 2001; Titorenko and Rachubinski, 2001). Because the import of all peroxisomal matrix proteins investigated in this study is compromised in the *pex24* mutant strains regardless of their type of PTS, Pex24p may act downstream of the point of convergence of the PTS1 and PTS2 pathways, thereby affecting the import of all peroxisomal matrix proteins. It should be noted that the targeting of peroxisomal membrane proteins is also compromised in *pex24* mutant strains. Since the targeting of peroxisomal matrix and membrane proteins apparently occurs by independent pathways and mechanisms (for reviews, see Subramani, 1998; Hettema *et*

al., 1999; Purdue and Lazarow, 2001; Titorenko and Rachubinski, 2001), the primary role of Pex24p may actually be in the targeting and/or assembly of peroxisomal membrane proteins. The effects of mutation of Pex24p on peroxisomal matrix protein import would therefore be secondary to the primary defect in peroxisomal membrane protein targeting/assembly. Dysfunction and/or absence of Pex24p could also be proposed to lead to major structural alterations in the peroxisomal membrane that would prevent or hinder the correct assembly of the translocation machineries required for the import of matrix and membrane proteins. How exactly Pex24p is involved in the peroxisome assembly process is not known and requires further investigation.

CHAPTER 4

A ROLE FOR PEX27P IN CONTROLLING PEROXISOME SIZE AND NUMBER IN *SACCHAROMYCES CEREVISIAE*

A version of this chapter has previously been published as "Pex11-related proteins in peroxisome dynamics: a role for the novel peroxin Pex27p in controlling peroxisome size and number in *Saccharomyces cerevisiae*" (Yuen Yi C. Tam, Juan C. Torres-Guzman, Franco J. Vizeacoumar, Jennifer J. Smith, Marcello Marelli, John D. Aitchison, and Richard A. Rachubinski. 2003. *Mol. Biol. Cell* 14: 4089-4102). Reprinted with permission.

4.1 Overview

This chapter reports the identification and characterization of a novel *PEX* gene, *PEX27*, in the yeast *S. cerevisiae*. Transcriptome profiling identified the gene *PEX25* encoding Pex25p, a peroxisomal membrane peroxin required for the regulation of peroxisome size and maintenance in *S. cerevisiae*. Pex25p is related to a protein of unknown function encoded by the ORF, *YOR193w*, of the *S. cerevisiae* genome. Yor193p, renamed Pex27p, is a peripheral peroxisomal membrane protein that exhibits high sequence similarity not only to Pex25p but also to the peroxisomal membrane peroxin Pex11p. Unlike Pex25p and Pex11p, Pex27p is constitutively expressed in wild-type cells grown in oleic acid-containing medium, the metabolism of which requires intact peroxisomes.

Cells deleted for the *PEX27* gene show a few enlarged peroxisomes. Peroxisomes are greatly enlarged in cells harboring double deletions of the *PEX27* and *PEX25* genes, the *PEX27* and *PEX11* genes, and the *PEX25* and *PEX11* genes. Interestingly, cells deleted for *PEX27*, *PEX25* and *PEX11* are defective in the import of peroxisomal matrix proteins and contain peroxisomes that are smaller than those observed in cells of the double deletion strains. Yeast two-hybrid analyses showed that Pex27p interacts with Pex25p and itself, Pex25p interacts with Pex27p and itself, and Pex11p interacts only with itself. Overexpression of *PEX27*, *PEX25*, or *PEX11* led to peroxisome proliferation and the formation of small peroxisomes. These results suggest a role for Pex27p in controlling peroxisome size and number in *S. cerevisiae*.

4.2 Identification of Pex27p in *S. cerevisiae*

Pex25p, a novel peripheral peroxisomal membrane protein identified by transcriptome profiling, has been shown to be required for the regulation of peroxisome size and number in *S. cerevisiae* (Smith *et al.*, 2002). A search of the Yeast Proteome Database (http://www.proteome.com/) showed that a protein of unknown function encoded by the hypothetical ORF, *YOR193w*, of the *S. cerevisiae* genome shares extensive sequence similarity with Pex25p (19.5% identical amino acids, 25.9% similar amino acids; Figure 4-1). Pex25p has been reported to show similarity also to Pex11p (Smith *et al.*, 2002) (10.9% identical amino acids, 19.0% similar amino acids; Figure 4-1), and likewise Yor193p, renamed Pex27p, shows similarity to Pex11p (9.3% identical amino acids, 18.4% similar amino acids; Figure 4-1). Pex27p is predicted to be a protein 376 amino acids in length with a molecular weight of 44,149. Pex27p has no predicted transmembrane domain (http://www.cbs.dtu.dk/services/TMHMM/) (Krogh *et al.*, 2001).

4.3 Cells deleted for one or two of the *PEX27*, *PEX25* and *PEX11* genes contain enlarged peroxisomes

Since Pex27p, Pex25p and Pex11p share extensive sequence homology, phenotypes of cells deleted for one or two of the *PEX27*, *PEX25* and *PEX11* genes were examined. Yeast strains harboring individual deletions of the *PEX27*, *PEX25* and *PEX11* genes, or double deletions of the *PEX27* and *PEX25*, *PEX27* and *PEX11*, and *PEX25* and *PEX11* genes (Table 2-8) were assayed for growth in the presence of glucose or oleic acid as the sole carbon source. As expected, cells deleted for the *PEX3* gene, which lack functional peroxisomes (Höhfeld *et al.*, 1991; Hettema *et al.*, 2000), failed to grow on

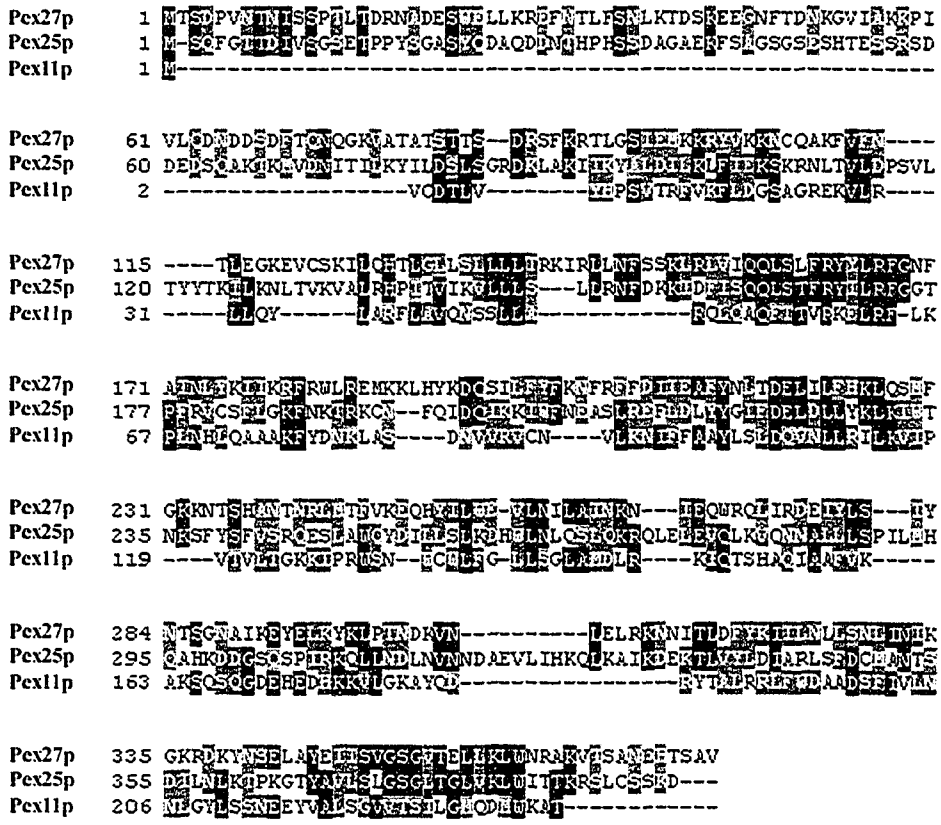

Figure 4-1. Sequence alignment of Pex27p, Pex25p and Pex11p. Amino acid sequences were aligned with the use of the ClustalW program (EMBL-EBI, Cambridge, United Kingdom) (http://www.ebi.ac.uk/clustalw/). Identical residues (black) and similar residues (gray) in at least two of the proteins are shaded. Similarity rules: G = A = S; A = V; V = I = L = M; I = L = M = F = Y = W; K = R = H; D = E = Q = N; and S = T = Q = N. Dashes represent gaps.

oleic acid-containing YPBO medium. Although cells deleted for *PEX27* or *PEX25* grew on YPBO medium at a rate like or very similar to that of wild-type *BY4742* cells, cells deleted for both the *PEX27* and *PEX25* genes displayed a growth defect on YPBO, suggesting that Pex27p and Pex25p together influence the rate of growth on oleic acid-containing medium (Figure 4-2). Cells deleted for the *PEX27* and *PEX11* genes or the *PEX25* and *PEX11* genes showed a similar growth defect on YPBO as did cells deleted for *PEX11* alone, suggesting that Pex11p plays the dominant role among these three proteins in growth on oleic acid medium (Figure 4-2).

Immunofluorescence analysis of oleic acid-incubated wild-type *BY4742* cells with antibodies to the carboxyl-terminal PTS1 tripeptide Ser-Lys-Leu (SKL) or to the PTS2-containing enzyme thiolase (THI) showed a pattern of numerous small punctate structures characteristic of peroxisomes (Figure 4-3). In contrast, the majority of cells of the *pex27Δ*, *pex25Δ*, *pex11Δ*, *pex27Δ/pex25Δ*, *pex27Δ/pex11Δ*, and *pex25Δ/pex11Δ* strains stained with the same antibodies showed one or two large peroxisomes per cell (Figure 4-3). In electron micrographs, wild-type cells grown in oleic acid-containing medium contained characteristic peroxisomes 0.2 to 0.4 μm in diameter (Figure 4-4 A). In contrast, cells of the *pex27Δ*, *pex25Δ* and *pex11Δ* strains contained enlarged peroxisomes (Figures 4-4 B-D). The peroxisomes were even larger in *pex27Δ/pex25Δ*, *pex27Δ/pex11Δ*, and *pex25Δ/pex11Δ* cells (Figures 4-4 E-G). Morphometric analysis showed that cells harboring double gene deletions contained less peroxisomes than did wild-type cells or cells deleted for one of the *PEX27, PEX25* and *PEX11* genes and that, on average, these peroxisomes were much larger (Table 4-1). Cells of all deletion strains contained much greater numbers of peroxisomes with areas of 0.15 μm^2 or larger than did wild-type cells

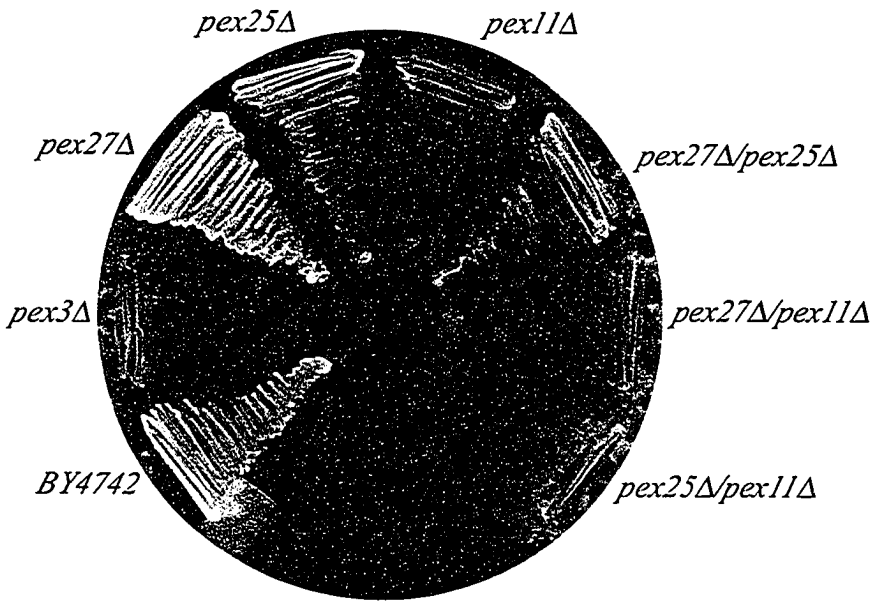

Figure 4-2. Growth of various strains on oleic acid-containing (YPBO) medium. All strains were grown on YPBO agar for 4 days at 30°C.

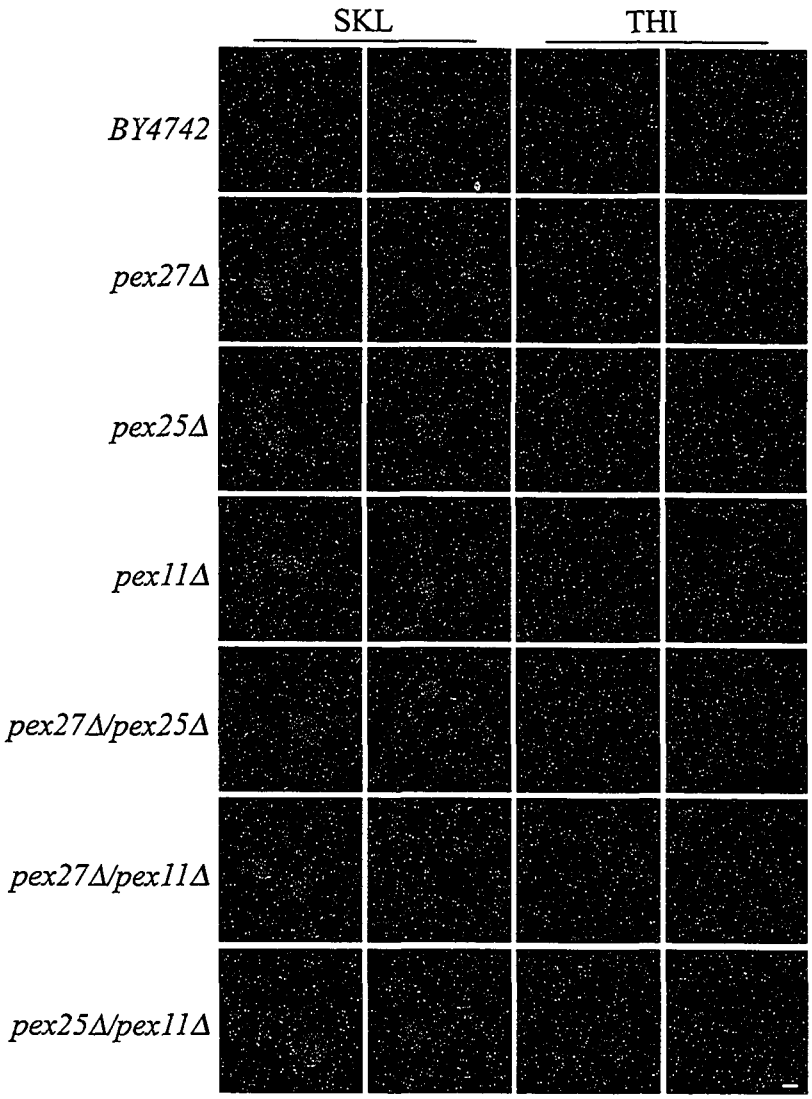

Figure 4-3. Peroxisomes are enlarged in cells deleted for one or two of the *PEX27*, *PEX25* and *PEX11* genes. Wild-type *BY4742* cells and cells of the *pex27Δ*, *pex25Δ*, *pex11Δ*, *pex27Δ/pex25Δ*, *pex27Δ/pex11Δ*, and *pex25Δ/pex11Δ* deletion strains were grown in YEPD medium for 16 h, transferred to YPBO medium, and incubated for 8 h in YPBO medium. Cells were processed for immunofluorescence microscopy with antibodies to the PTS1 tripeptide SKL or to the PTS2-containing protein THI. Rabbit primary antibodies (SKL) were detected with fluorescein-conjugated secondary antibodies. Guinea pig primary antibodies (THI) were detected with rhodamine-conjugated secondary antibodies. Bar, 1 μm.

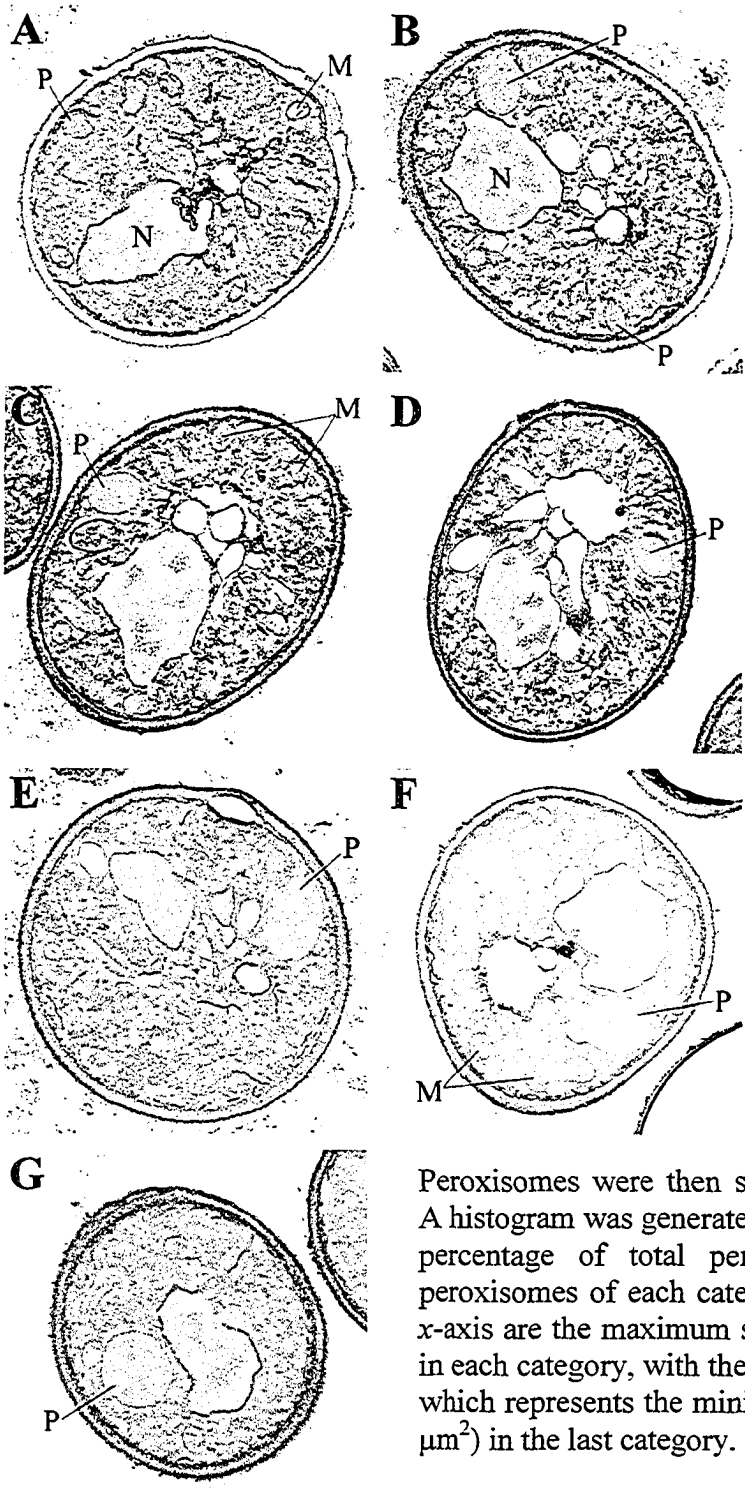

Figure 4-4. Cells harboring double deletions of *PEX27/PEX25*, *PEX27/PEX11*, and *PEX25/PEX11* contain greatly enlarged peroxisomes. Ultrastructure of wild-type *BY4742* (A), *pex27Δ* (B), *pex25Δ* (C), *pex11Δ* (D), *pex27Δ/pex25Δ* (E), *pex27Δ/pex11Δ* (F), and *pex25Δ/pex11Δ* (G) cells. Cells were grown in YEPD medium for 16 h, shifted to YPBO medium, and incubated in YPBO medium for an additional 8 h. Cells were fixed in 3% $KMnO_4$ and proceed for electron microscopy. P, peroxisome; M, mitochondrion; N, nucleus. Bar, 1 μm. (H) (page 105) Morphometric analysis of peroxisomes. For each strain analyzed, the areas of individual peroxisomes of 100 randomly selected cells were determined using the program analySIS 3.1. Peroxisomes were then separated into size categories. A histogram was generated for each strain depicting the percentage of total peroxisomes occupied by the peroxisomes of each category. The numbers along the *x*-axis are the maximum sizes of peroxisomes (in μm^2) in each category, with the exception of the last number, which represents the minimum size of peroxisomes (in μm^2) in the last category.

H

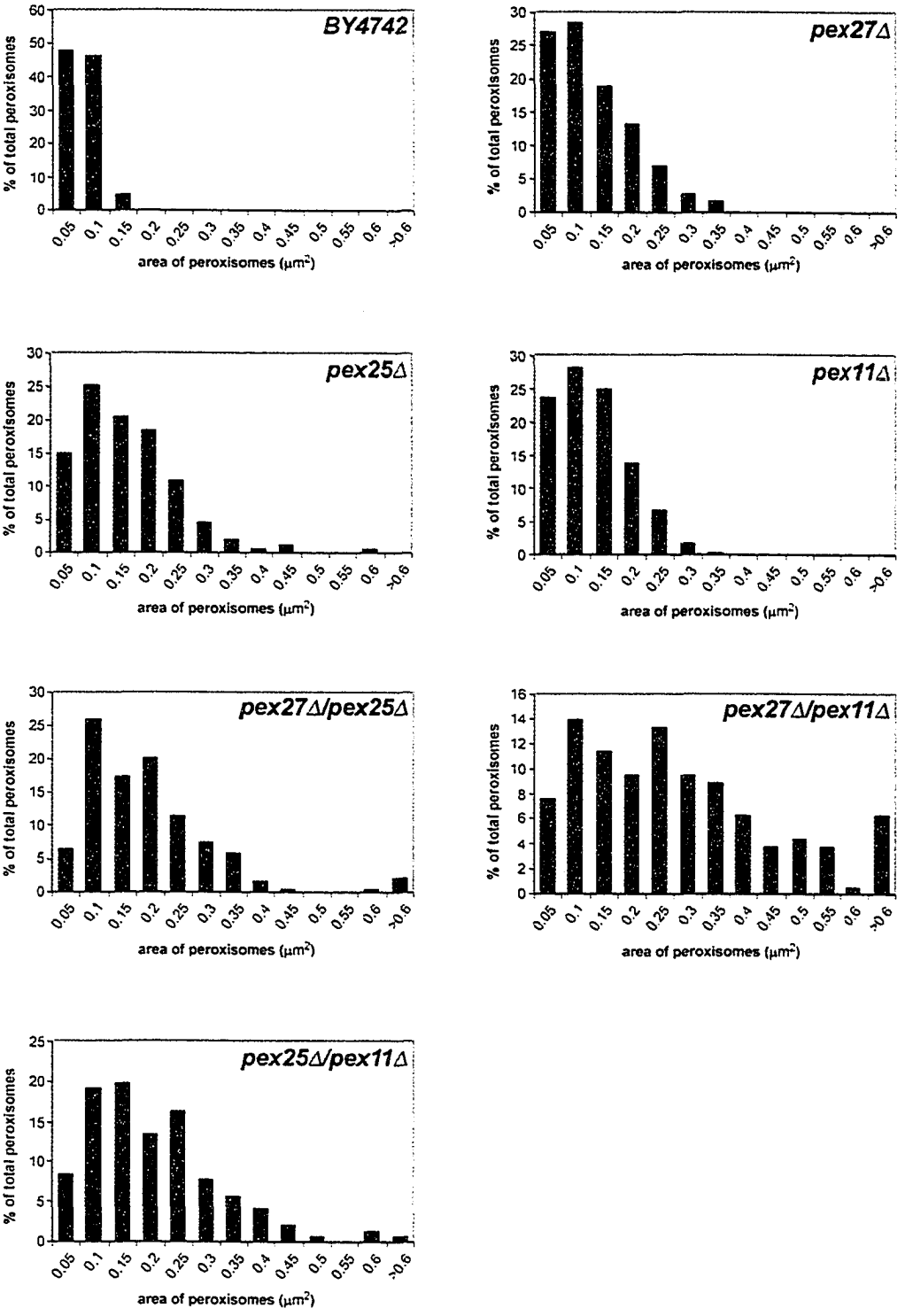

Table 4-1. Average area and numerical density of peroxisomes in cells of wild-type and deletion strains

Strain	Cell area assayed (μm^2)	Peroxisome count[a]	Numerical density of peroxisomes[b]	Average area of peroxisomes[c] (μm^2)
BY4742	853	0.21	0.98	0.051
pex27Δ	909	0.23	0.77	0.088
pex25Δ	892	0.16	0.48	0.113
pex11Δ	918	0.24	0.81	0.097
pex27Δ/pex25Δ	1114	0.16	0.30	0.152
pex27Δ/pex11Δ	999	0.16	0.33	0.224
pex25Δ/pex11Δ	914	0.15	0.39	0.158

[a]Number of peroxisomes counted per μm^2 of cell area on micrographs.
[b]Number of peroxisomes per μm^3 of cell volume (Weibel and Bolender, 1973).
[c]Average area on micrographs.

(Figure 4-4 H). Cells harboring double deletions of the *PEX27* and *PEX25*, the *PEX27* and *PEX11*, and the *PEX25* and *PEX11* genes contained greatly enlarged peroxisomes with areas of $\geq 0.6\ \mu m^2$. Peroxisomes of these sizes were not observed in wild-type cells or cells deleted for any one of the *PEX27*, *PEX25*, and *PEX11* genes.

Nycodenz density gradient centrifugation analysis showed that peroxisomes isolated from all deletion strains have peak densities (fraction 4, 1.2328 g/cm^3, in *pex11Δ* and *pex25Δ/pex11Δ* cells; fraction 5, 1.221 g/cm^3, in *pex27Δ* and *pex27Δ/pex11Δ* cells; fraction 6, 1.2106 g/cm^3, in *pex25Δ* and *pex27Δ/pex25Δ* cells) greater than that of peroxisomes isolated from wild-type cells (fraction 7, 1.2077 g/cm^3) (Figure 4-5).

4.4 Pex27p is a peripheral membrane protein of peroxisomes

To detect Pex27p, a genomically encoded protein A chimera of Pex27p (Pex27-pA) was constructed. A plasmid encoding a fluorescent chimera between *Discosoma* sp. red fluorescent protein (DsRed) and the PTS1 Ser-Lys-Leu was transformed into cells to fluorescently label peroxisomes of *S. cerevisiae* (Smith *et al.*, 2002). Pex27-pA and the peroxisomal protein, Pex17-pA (Huhse *et al.*, 1998; Vizeacoumar *et al.*, 2003), colocalized with DsRed-PTS1 to punctuate structures characteristic of peroxisomes by confocal microscopy (Figure 4-6 A). Subcellular fractionation was also used to establish whether Pex27p is associated with peroxisomes. Pex27-pA, like the peroxisomal matrix protein thiolase, localized preferentially to the 20KgP fraction enriched for peroxisomes and mitochondria (Figure 4-6 B). Isopycnic density gradient centrifugation of the 20KgP fraction showed that Pex27p cofractionated with thiolase but not with the mitochondrial

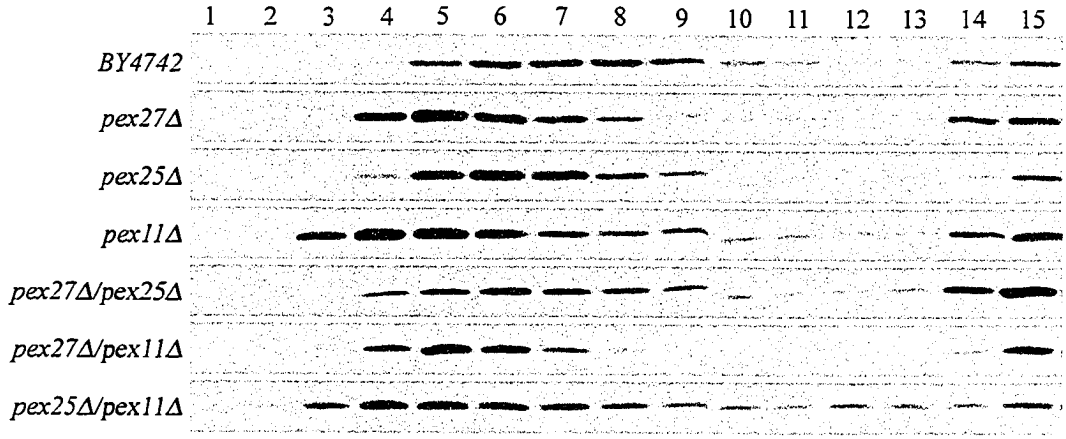

Figure 4-5. Peroxisomes isolated from cells deleted for one or two of the *PEX27*, *PEX25* and *PEX11* genes are more dense than isolated wild-type peroxisomes. The wild-type strain *BY4742* and the deletion strains *pex27Δ*, *pex25Δ*, *pex11Δ*, *pex27Δ/pex25Δ*, *pex27Δ/pex11Δ*, and *pex25Δ/pex11Δ* were grown overnight in YEPD medium, transferred to YPBO medium, and incubated in YPBO medium for 8 h. A PNS fraction was prepared from cells of each strain and divided by centrifugation into 20KgS and 20KgP fractions. Organelles in the 20KgP fraction were separated by isopycnic centrifugation on a continuous 30–60% Nycodenz gradient. Fifteen 2-ml fractions were collected from the bottom of each gradient. Equal volumes of each fraction were analyzed by immunoblotting with antibodies to the peroxisomal matrix enzyme thiolase to detect peroxisomes.

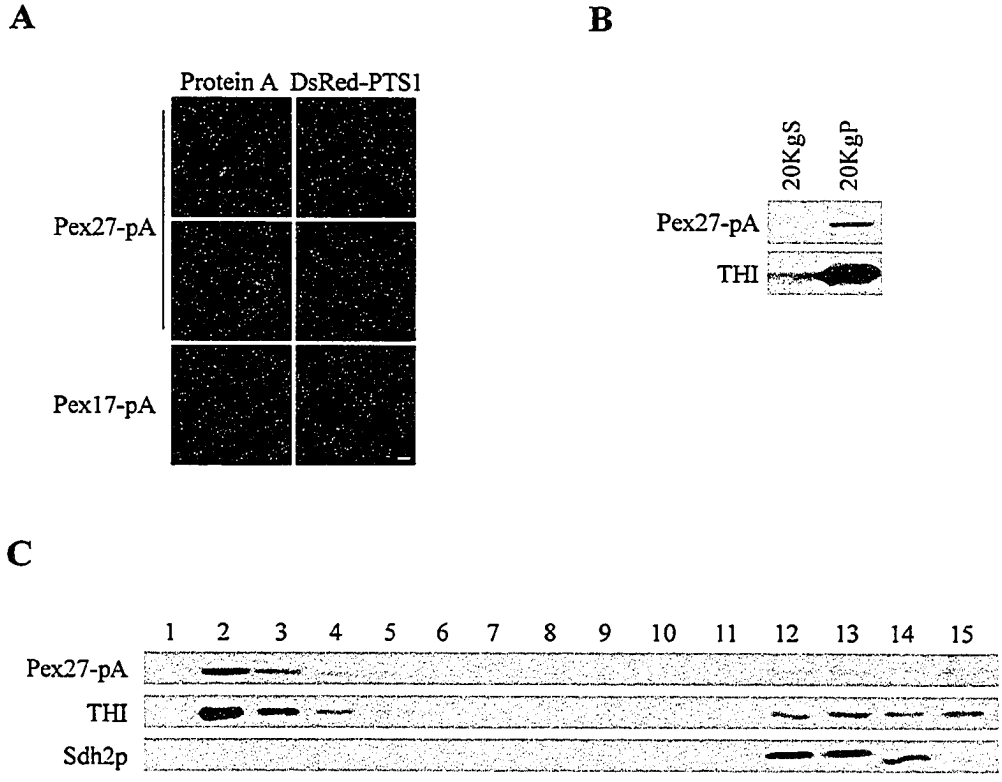

Figure 4-6. Pex27-pA is a peripheral peroxisomal membrane protein. (A) Pex27-pA colocalizes with DsRed-PTS1 in punctate structures characteristic of peroxisomes by double labeling, indirect immunofluorescence microscopy. Bar, 1 μm. (B) Pex27-pA localizes to the 20KgP subcellular fraction enriched for peroxisomes. Immunoblot analysis of the 20KgS and 20KgP subcellular fractions from cells expressing Pex27-pA was performed with antibodies to THI. (C) Pex27-pA cofractionates with peroxisomes. Organelles in the 20KgP fraction were separated by isopycnic centrifugation on a discontinuous Nycodenz gradient. Fractions were collected from the bottom of the gradient, and equal portions of each fraction were analyzed by immunoblotting. Fractions enriched for peroxisomes and mitochondria were identified by immunodetection of thiolase and Sdh2p, respectively. (D) The 20KgP fraction from cells expressing Pex27-pA, Pex17-pA, or Pxa1-pA was treated with 10 mM Tris-HCl, pH 8.0, to lyse peroxisomes and then subjected to centrifugation to yield a supernatant (Ti8S) fraction enriched for matrix proteins and a pellet (Ti8P) fraction enriched for membrane proteins. The Ti8P fractions were further treated with 0.1 M Na_2CO_3, pH 11.3, and separated by centrifugation into a supernatant (CO_3S) fraction enriched for peripherally associated membrane proteins and a pellet (CO_3P) fraction enriched for integral membrane proteins. Equal portions of each fraction were analyzed by immunoblotting.

protein, Sdh2p (Figure 4-6 C). Therefore, both confocal microscopy and subcellular fractionation showed Pex27p to be a peroxisomal protein.

Organelle extraction was used to determine the suborganellar location of Pex27p. Peroxisomes were hypotonically lysed in dilute alkali Tris buffer and subjected to ultracentrifugation to yield a supernatant (Ti8S) fraction enriched for matrix proteins and a pellet (Ti8P) fraction enriched for membrane proteins (Figure 4-6 D). Pex27-pA cofractionated with the protein A chimeras of the peripheral peroxisomal membrane protein Pex17p (Huhse *et al.*, 1998; Vizeacoumar *et al.*, 2003) and the integral peroxisomal membrane protein Pxa1p (Swartzman *et al.*, 1996) to the Ti8P fraction. The soluble peroxisomal matrix protein thiolase was found almost exclusively in the Ti8S fraction. The Ti8P fractions were then extracted with alkali Na_2CO_3 and subjected to ultracentrifugation. This treatment releases proteins associated with, but not integral to, membranes (Fujiki *et al.*, 1982). Pex27-pA cofractionated with Pex17-pA to the supernatant (CO_3S) fraction enriched for peripheral membrane proteins (Figure 4-6 D). In contrast, Pxa1-pA fractionated to the pellet (CO_3P) fraction enriched for integral membrane proteins. Therefore, these data suggest that Pex27p is a peripheral membrane protein of peroxisomes, as has been shown for Pex25p (Smith *et al.*, 2002) and Pex11p (Marshall *et al.*, 1995).

4.5 Synthesis of Pex27p remains constant during incubation of cells in oleic acid-containing medium

The levels of Pex25p and Pex11p increase in yeast cells incubated in medium containing oleic acid (Smith *et al.*, 2002, Marshall *et al.*, 1995). Genomically encoded

Pex27-pA was analyzed to monitor the expression of *PEX27* under the control of its endogenous promoter. Cells synthesizing Pex27-pA were grown in glucose-containing YEPD medium and transferred to oleic acid-containing YPBO medium. Aliquots of cells were removed at various times after the transfer to YPBO medium, and their lysates were subjected to SDS-PAGE and immunoblotting (Figure 4-7). Pex27-pA was detected in YEPD medium at the time of transfer, and its level remained unchanged during incubation in YPBO. Under the same conditions, the level of the peroxisomal matrix enzyme THI increased dramatically from undetectable levels with time of incubation in YPBO, whereas the level of the cytosolic enzyme G6PDH remained constant and acted as a control for protein loading.

4.6 Physical interactions between Pex27p, Pex25p, and Pex11p

To identify any physical interactions between Pex27p, Pex25p, and Pex11p, a limited yeast two-hybrid screen was performed. Others have used this methodology to detect interactions between peroxins (for examples, see Girzalsky *et al.*, 1999; Smith and Rachubinski, 2001; Sichting *et al.*, 2003). Chimeric genes were made by ligating the ORFs of *PEX27*, *PEX25* and *PEX11* in-frame and downstream of sequences encoding one of the two functional domains (AD or DB) of the GAL4 transcriptional activator. All possible combinations of plasmid pairs encoding AD and DB fusion proteins were transformed into *S. cerevisiae* strain *SYF526*, and initially β-galactosidase filter detection assays were performed. An interaction was detected between Pex27p and Pex25p (Figure 4-8 A). An interaction was also detected between Pex11p and itself (Figure 4-8 A), which

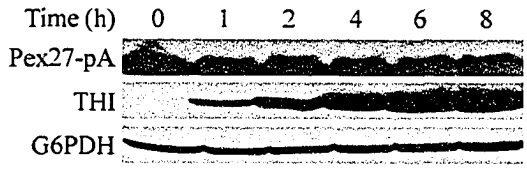

Figure 4-7. Synthesis of Pex27-pA remains constant during incubation of *S. cerevisiae* in oleic acid-containing medium. Cells grown for 16 h in YEPD medium were shifted to, and incubated in, YPBO medium. Aliquots of cells were removed from the YPBO medium at the times indicated, and total cell lysates were prepared. Equal amounts of protein from the total cell lysates were separated by SDS-PAGE and analyzed by immunoblotting with antibodies to thiolase to visualize the protein A fusion and thiolase. Antibodies directed against G6PDH were used to confirm the loading of equal amount of proteins in each lane.

A

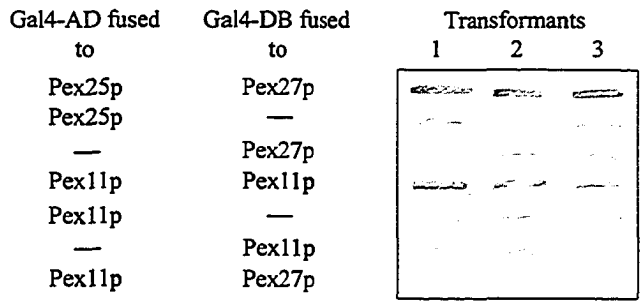

B

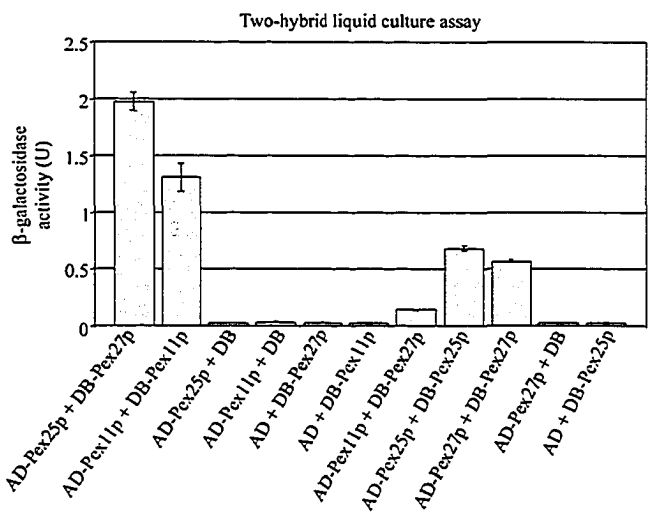

Figure 4-8. Analysis of interactions between Pex27p, Pex11p and Pex25p by the yeast two-hybrid system. (A) β-Galactosidase filter detection assay. *SFY526* cells synthesizing both Gal4-AD (left) and Gal4-DB (right) fusion proteins were tested for β-galactosidase activity. The color intensities of three independent transformants for each strain are shown. (B) β-Galactosidase liquid culture assay. A comparison of β-galactosidase activities of strains doubly transformed with plasmids encoding the designated fusion or fusions (*x*-axis). β-Galactosidase activity is measured in arbitrary units (AU) as defined by the manufacturer (BD Biosciences Clontech). Each bar reports the average β-galactosidase activity of three individual transformants ± SD.

was expected because Pex11p has been shown previously to form homodimers (Marshall *et al.*, 1996).

To confirm the results of the filter detection assay, a more sensitive liquid β-galactosidase assay was performed (Figure 4-8 B). Cell lysates of strains synthesizing both Pex27p and Pex25p, Pex11p and Pex11p, Pex25p and Pex25p, and Pex27p and Pex27p fusion proteins showed greater β-galactosidase activity than lysates of control strains synthesizing either one or the other of the fusion proteins. These results suggest that Pex27p and Pex25p interact physically and that Pex11p, Pex25p and Pex27p interact with themselves. Further experimentation is required to determine whether these interactions are direct or bridged by other proteins.

4.7 Overexpression of *PEX27*, *PEX25*, or *PEX11* promotes peroxisome division

Electron microscopy and immunofluorescence microscopy of oleic acid-grown cells deleted for one or two of the genes *PEX27*, *PEX25* and *PEX11* showed enlarged peroxisomes (Figures 4-3 and 4-4). To examine the effects of oversynthesis of Pex27p, Pex25p and Pex11p, the wild-type strain *BY4742* and strains deleted for one or two of the genes *PEX27*, *PEX25* and *PEX11* were transformed with multicopy plasmids for overexpression of the *PEX27*, *PEX25* and *PEX11* genes. Transformants grown in oleic acid-containing medium were analyzed by indirect immunofluorescence microscopy with antibodies to the PTS1 SKL and to the PTS2-containing protein thiolase (Figure 4-9 A) and by electron microscopy (Figures 4-9 B-D) (Table 4-2). It had been reported previously that overexpression of Pex11p promotes peroxisome proliferation (Marshall *et al.*, 1995; Li and Gould, 2002; Li *et al.*, 2002). Overexpression of *PEX11* in all deletion

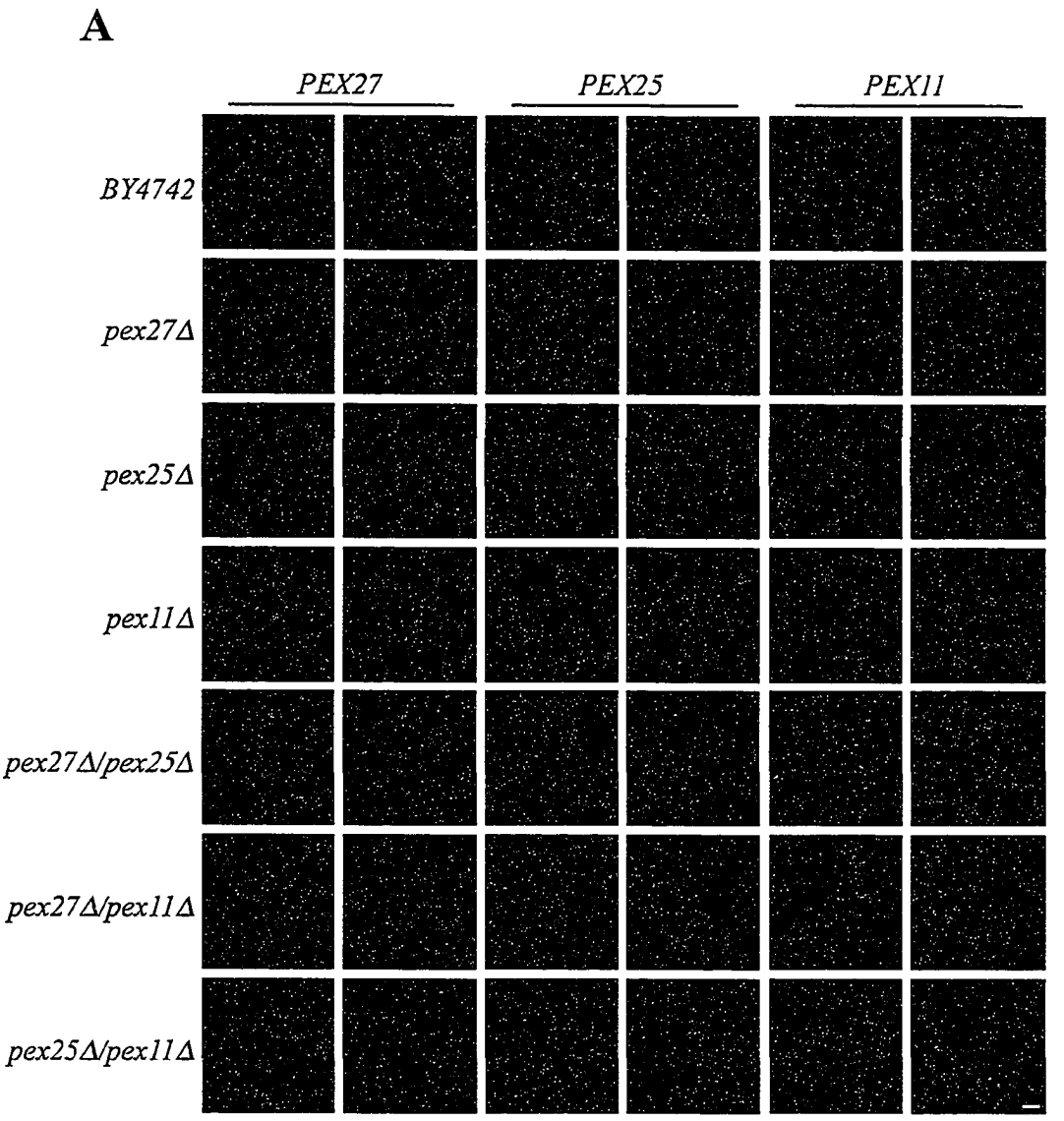

Figure 4-9. Overexpression of *PEX27*, *PEX25* and *PEX11* induces peroxisome division. Cells were grown for 16 h in SM medium, transferred to YPBO medium, and incubated in YPBO medium for 8 h. (A) The gene being overexpressed is given at the top of the figure, and the strains in which overexpression is being done are given at the left or right of the figure. Analysis of overexpression of the *PEX27*, *PEX25* and *PEX11* genes by immunofluorescence microscopy using rabbit anti-SKL antibodies and guinea pig anti-thiolase antibodies, followed by fluorescein-conjugated anti-rabbit IgG secondary antibodies and rhodamine-conjugated anti-guinea pig IgG secondary antibodies (A), and by electron microscopy (B – D) (pages 116-118). Bar, 1 μm.

B

Overexpression of *PEX27*

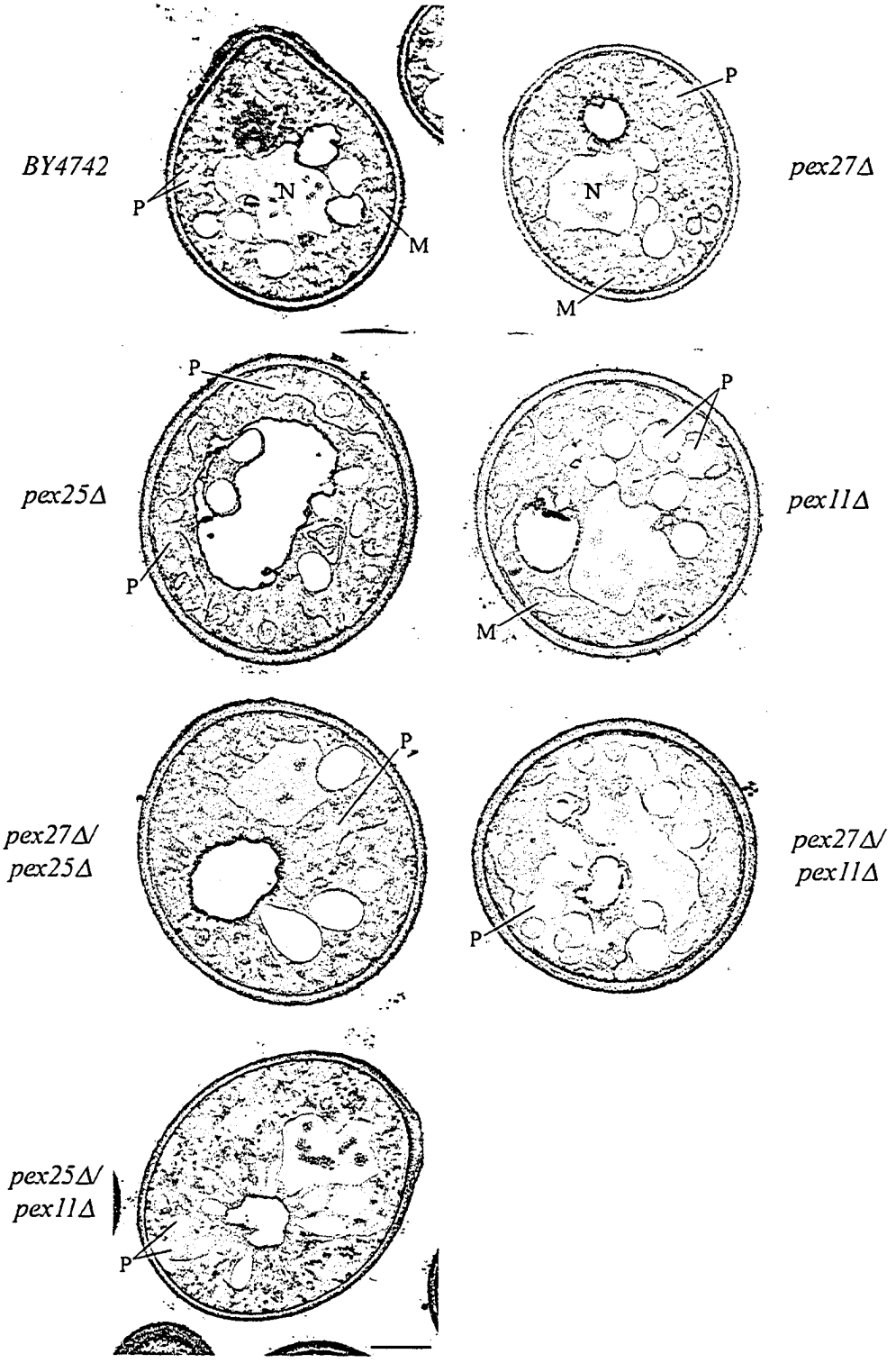

C

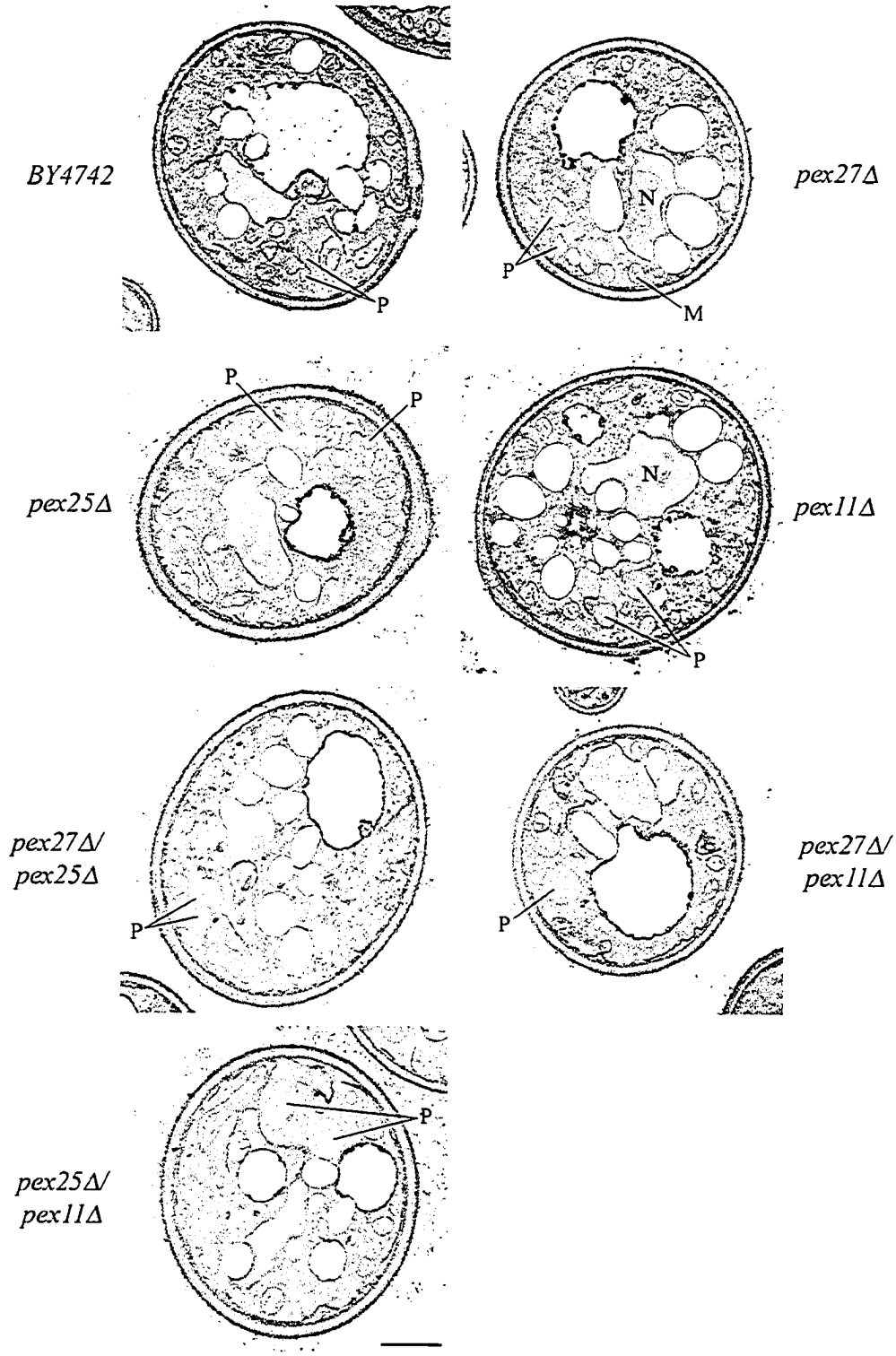

D

Overexpression of *PEX11*

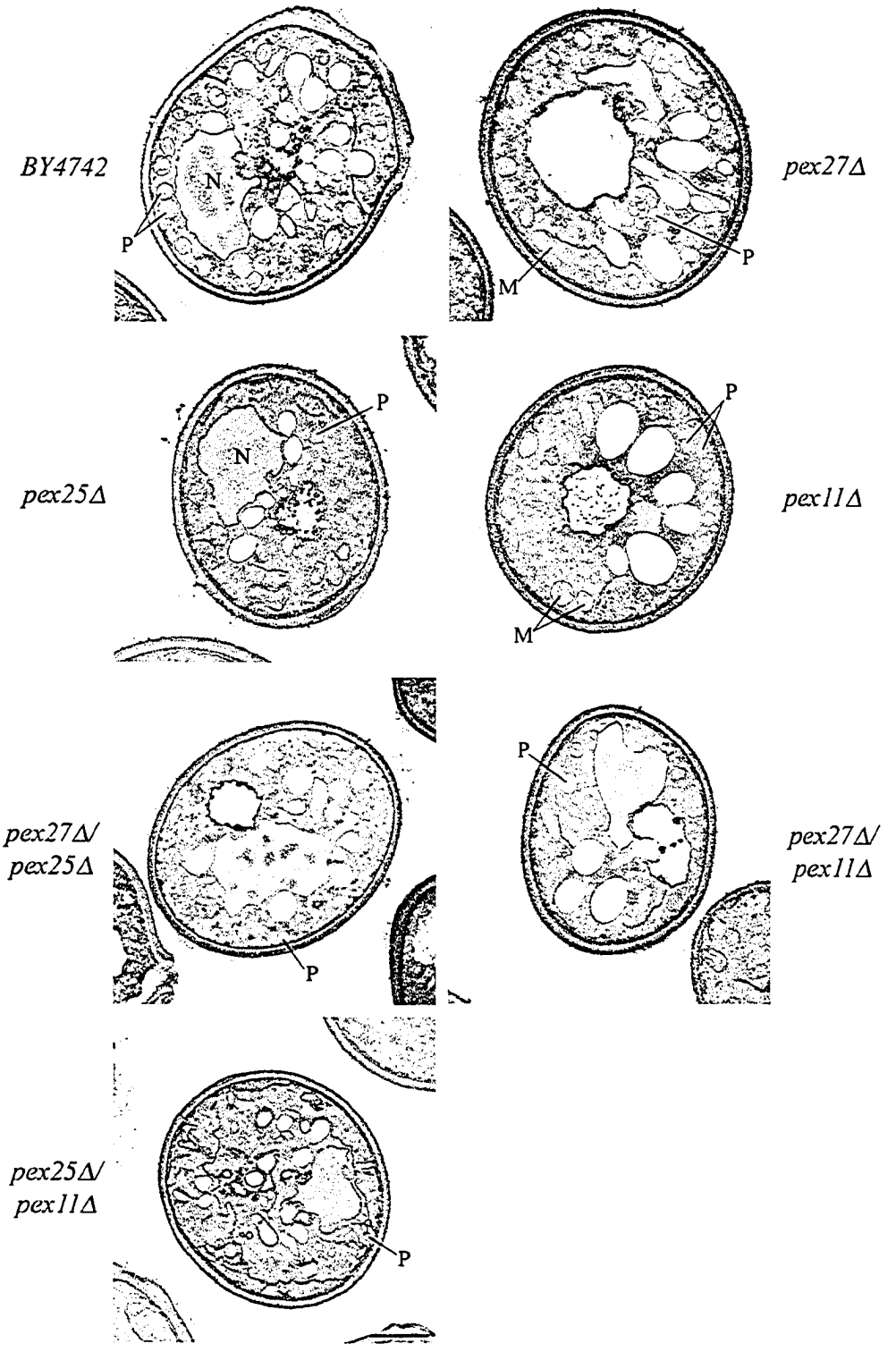

Table 4-2. Summary of phenotypes observed in cells overexpressing *PEX27*, *PEX25* or *PEX11*

Strain	Overexpressed gene	Normal peroxisomes	Large peroxisomes	Small peroxisomes	Clustered peroxisomes
pex27Δ	–	++[a]	+++		
pex27Δ	*PEX27*	++++		+	
pex27Δ	*PEX25*	++++	+		
pex27Δ	*PEX11*			++++	+
pex25Δ	–	++	+++		
pex25Δ	*PEX27*	+	+	+++	
pex25Δ	*PEX25*	++++	+		
pex25Δ	*PEX11*		+	+++	+
pex11Δ	–	+	++++		
pex11Δ	*PEX27*		+		++++
pex11Δ	*PEX25*		++		+++
pex11Δ	*PEX11*		+	+	+++
pex27Δ/pex25Δ	–	+	++++		
pex27Δ/pex25Δ	*PEX27*	++	+	+	+
pex27Δ/pex25Δ	*PEX25*	++	++		+
pex27Δ/pex25Δ	*PEX11*			+++	++
pex27Δ/pex11Δ	–		+++++		
pex27Δ/pex11Δ	*PEX27*		+++++		
pex27Δ/pex11Δ	*PEX25*		+++++		
pex27Δ/pex11Δ	*PEX11*		+	++	++
pex25Δ/pex11Δ	–		+++++		
pex25Δ/pex11Δ	*PEX27*	+	++++		
pex25Δ/pex11Δ	*PEX25*		+++++		
pex25Δ/pex11Δ	*PEX11*			+++	++
BY4742	–	+++++			
BY4742	*PEX27*	+++			++
BY4742	*PEX25*	++	+		++
BY4742	*PEX11*	+++			++

[a]The (+) symbol denotes the presence of a particular peroxisomal phenotype. Increased numbers of (+) symbols denote increased prevalence of a particular peroxisomal morphological phenotype. The absence of a (+) symbol denotes the absence of a particular peroxisomal morphological phenotype.

strains led to the formation of small peroxisomes, some of which seemed to cluster, and to the almost total disappearance of the enlarged peroxisomes that were observed in the original deletion strains (Figures 4-9 A, D and Table 4-2). Overexpression of *PEX27* in *pex27Δ* cells restored the wild-type phenotype and led to the production of a small number of small peroxisomes (Figures 4-9 A, B and Table 4-2). Formation of both normal and small peroxisomes was observed in *pex25Δ* and *pex27Δ/pex25Δ* cells overexpressing *PEX27* (Figures 4-9 A, B and Table 4-2). In contrast, overexpression of *PEX27* had little or no effect on peroxisome size in *pex11Δ*, *pex27Δ/pex11Δ*, and *pex25Δ/pex11Δ* cells (Figures 4-9 A, B and Table 4-2). Normal peroxisomes were observed in *pex27Δ*, *pex25Δ*, and *pex27Δ/pex25Δ* cells overexpressing *PEX25* (Figures 4-9 A, C and Table 4-2); however, these cells also contained some large peroxisomes and clusters of peroxisomes (Table 4-2). No reduction in peroxisome size was observed in *pex11Δ*, *pex27Δ/pex11Δ*, and *pex25Δ/pex11Δ* cells overexpressing *PEX25* (Figures 4-9 A, C and Table 4-2). It should be noted that overexpression of *PEX27* or *PEX25* caused extensive clustering of peroxisomes in cells deleted for the *PEX11* gene (Figures 4-9 B, C and Table 4-2). Last, minor clustering of peroxisomes was observed in wild-type cells overexpressing *PEX27*, *PEX25*, or *PEX11* (Table 4-2).

4.8 Cells deleted for *PEX27*, *PEX25* and *PEX11* are compromised in the import of peroxisomal matrix proteins

To investigate the effects of the absence of the *PEX27*, *PEX25* and *PEX11* genes, cells deleted for all three genes were incubated in oleic acid-containing medium and analyzed by immunofluorescence and electron microscopy. Wild-type *BY4742* cells

showed characteristic punctate structures labeled with anti-SKL and anti-thiolase antibodies (Figure 4-10), while cells of the *pex27Δ/pex25Δ/pex11Δ* strain showed mostly cytosolic staining of SKL-containing proteins and thiolase (Figure 4-10). It is noteworthy that punctate structures containing SKL-containing proteins and thiolase were observed occasionally in *pex27Δ/pex25Δ/pex11Δ* cells (Figure 4-10). In electron micrographs, *BY4742* cells contained characteristic peroxisomes (Figure 4-11 A). In contrast, large numbers of *pex27Δ/pex25Δ/pex11Δ* cells lacked identifiable peroxisomes (Figure 4-11 B), while the remaining cells contained peroxisomes smaller in size (Figure 4-11 C) than those observed in cells of a double deletion strain (Figures 4-11 D).

4.9 Discussion

4.9.1 The use of global transcriptional profiling and database mining to identify novel *PEX* genes

Completion of the sequencing of the *S. cerevisiae* genome has permitted the use of transcriptome profiling of cells incubated in oleic acid-containing medium versus cells incubated in glucose-containing medium to predict gene involvement in peroxisome biogenesis or function (Smith *et al.*, 2002). This method led to the successful identification of a novel *PEX* gene, *PEX25*, involved in the regulation of peroxisome size and maintenance (Smith *et al.*, 2002). A search of the Yeast Proteome Database revealed that Pex25p shares extensive amino acid identity and similarity to a protein of unknown function encoded by the ORF *YOR193w* of the *S. cerevisiae* genome. Yor193p, renamed Pex27p, also shows a great degree of amino acid identity and similarity to another previously characterized peroxisomal protein, Pex11p. A genomically encoded protein A

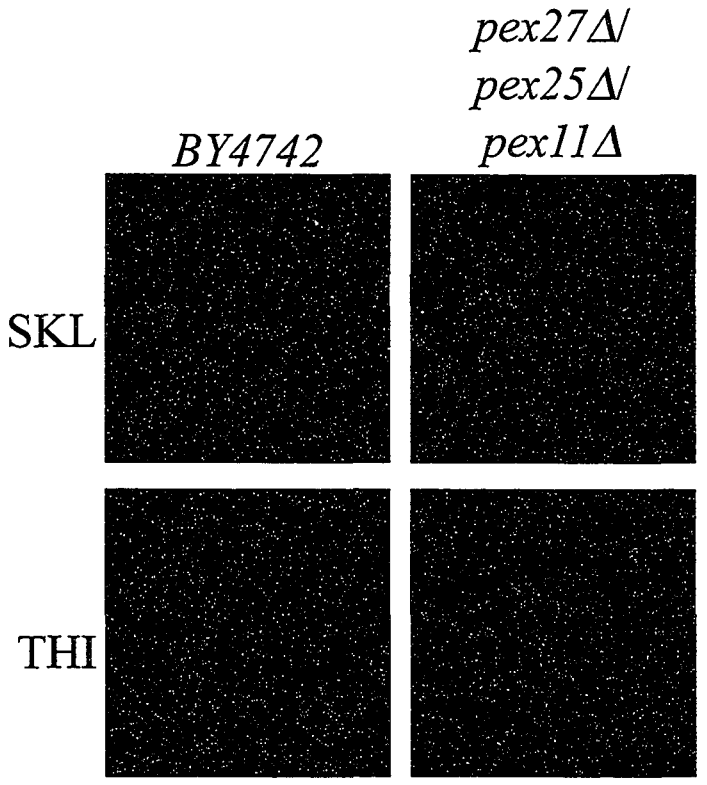

Figure 4-10. Import of peroxisomal matrix proteins is compromised in cells deleted for *PEX27*, *PEX25* and *PEX11*. Wild-type *BY4742* cells and cells of the *pex27Δ/pex25Δ/pex11Δ* deletion strain were grown in YEPD medium for 16 h, transferred to YPBO medium, and incubated for 8 h in YPBO medium. Cells were processed for immunofluorescence microscopy with antibodies to the PTS1 tripeptide SKL or to the PTS2-containing protein thiolase (THI). Rabbit primary antibodies (SKL) were detected with fluorescein-conjugated secondary antibodies. Guinea pig primary antibodies (THI) were detected with rhodamine-conjugated secondary antibodies.

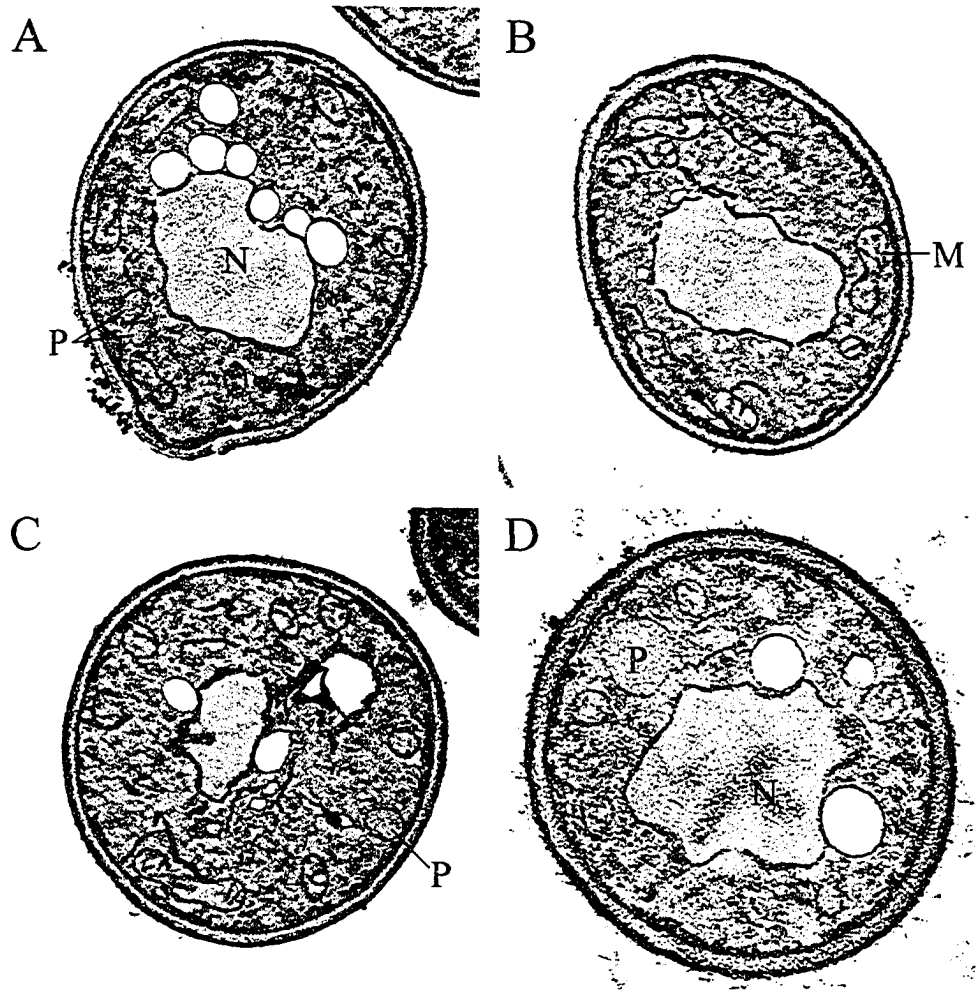

Figure 4-11. Cells of *pex27Δ/pex25Δ/pex11Δ* strain either lack peroxisomes or contain peroxisomes that are smaller than those in cells of a double deletion mutant. Ultrastructure of wild-type *BY4742* (A), *pex27Δ/pex25Δ/pex11Δ* (B, C) and *pex27Δ/pex25Δ* cells (D). Cells were grown in YEPD medium for 16 h, shifted to YPBO medium, and incubated in YPBO medium for an additional 8 h. Cells were fixed in 3% $KMnO_4$ and proceed for electron microscopy. P, peroxisome; M, mitochondrion; N, nucleus.

chimera of Pex27p localizes to peroxisomes and displays the characteristics of a peripheral membrane protein, as do both Pex25p and Pex11p (Marshall *et al.*, 1996; Smith *et al.*, 2002). Based on the conservation of amino acid sequence and function (discussed below) among Pex27p, Pex25p and Pex11p, they are classified as members of the Pex11p protein family.

Pex27p is not required for growth of cells on oleic acid-containing medium, because *pex27Δ* cells showed a growth rate comparable with that of wild-type cells on this medium. This finding might explain why *PEX27* was not identified as a gene required for peroxisome assembly by classical negative selection procedures involving the isolation of mutant yeast strains that fail to grow in the presence of oleic acid as sole carbon source. Also, synthesis of Pex27p remains constant during growth of cells in oleic acid-containing medium, providing an explanation for why *PEX27* was not identified by transcriptome profiling as a gene potentially involved in peroxisome assembly (Smith *et al.*, 2002).

4.9.2 Pex27p is involved in controlling peroxisome division

Pex27p, as well as Pex25p and Pex11p, are not required for peroxisome assembly *per se*, because cells lacking the *PEX27*, *PEX25*, or *PEX11* gene still contain peroxisomes. These peroxisomes are partially functional, as the cells harboring individual gene deletions could still grow on oleic acid-containing medium, although at rates slower than that of wild-type cells. However, these peroxisomes are not normal, because they are larger than wild-type peroxisomes. Peroxisomes of cells containing deletions of two of the *PEX27*, *PEX25* and *PEX11* genes are even larger than those of cells deleted for the

individual genes. These abnormally large peroxisomes could result from a disruption of components of the peroxisome division machinery in cells of the gene deletion strains, which is consistent with a role for *PEX27* in the control of peroxisome size, as has been proposed for *PEX25* and *PEX11* (Marshall *et al.*, 1995; Erdmann and Blobel, 1995; Smith *et al.*, 2002). Although the majority of the *pex27Δ*, *pex25Δ* and *pex11Δ* cells contain enlarged peroxisomes, significant numbers of cells of these deletion strains still contain peroxisomes that are wild-type in appearance. This heterogeneity in the population of peroxisomes in cells harboring single gene deletions implies the existence of more than one checkpoint for peroxisome division. Moreover, the fact that peroxisomes are even larger in cells harboring two gene deletions suggests that Pex27p, Pex25p and Pex11p function additively to control peroxisome division.

4.9.3 How might Pex27p, Pex25p and Pex11p act and interact to regulate the size and number of peroxisomes?

Previous studies have implicated Pex11p as an effector of peroxisome division in different organisms (Marshall *et al.*, 1995; Erdmann and Blobel, 1995; Sakai *et al.*, 1995; Abe and Fujiki, 1998; Lorenz *et al.*, 1998; Passreiter *et al.*, 1998; Schrader *et al.*, 1998; Li and Gould, 2002; Li *et al.*, 2002). Pex25p has also been implicated in the control of peroxisome size and number in *S. cerevisiae* (Smith *et al.*, 2002). So how might Pex27p, Pex25p and Pex11p act and interact to regulate the size and number of peroxisomes in *S. cerevisiae*? To address this question, we performed a limited yeast two-hybrid screen to identify physical interactions among Pex27p, Pex25p and Pex11p and overexpressed the genes for these proteins in cells of the wild-type strain and of the various gene deletion

mutant strains to determine the effects of protein overproduction on peroxisome morphology.

Overexpression of *PEX11* in *S. cerevisiae* cells deleted for this gene has been reported to induce the formation of large numbers of small peroxisomes (Marshall *et al.*, 1995). In contrast, overexpression of *PEX27* and *PEX25* in their respective gene deletion backgrounds did not induce the production of large numbers of small peroxisomes but resulted essentially in the recovery of the wild-type peroxisomal phenotype. However, overexpression of *PEX27* in both *pex27Δ* and *pex25Δ* cells promoted the formation of a limited amount of small peroxisomes, whereas some large peroxisomes could still be observed in cells overexpressing *PEX25*. Small peroxisomes are produced in all deletion strains overexpressing the *PEX11* gene. Therefore, Pex11p is likely to play the dominant effector role in peroxisome division, whereas Pex27p and Pex25p are secondary effectors of peroxisome division, with Pex27p being stronger than Pex25p. Interestingly, in all strains overexpressing *PEX11*, the small peroxisomes that are formed remain largely adherent. Considering peroxisome proliferation as a two-step process, namely, peroxisome division and peroxisome separation, Pex11p may be involved primarily in division with limited or no significant contribution to separation. Overexpression of *PEX27* or *PEX25* in wild-type, *pex11Δ* or *pex27Δ/pex25Δ* cells led to the formation of some adherent peroxisomes, suggesting that Pex27p and Pex25p have some, but limited, effects on peroxisome separation. Other proteins are expected to influence this separation step. Indeed, the identification of two peroxisomal membrane proteins, Pex28p and Pex29p, required for peroxisomal separation in *S. cerevisiae* has recently been reported

(Vizeacoumar *et al.*, 2003). Cells lacking Pex28p and Pex29p contain clusters of peroxisomes that often exhibit thickened membranes between adjacent peroxisomes.

Using the yeast two-hybrid system, interactions were observed between Pex27p and Pex25p and self-interactions were observed with Pex27p, Pex25p and Pex11p. Results from liquid β-galactosidase assays suggest that the interaction between Pex27p and Pex25p is the strongest among all detected interactions. It should be noted, however, that because the two-hybrid analysis was performed within an homologous system, *i.e.*, within *S. cerevisiae* cells containing wild-type copies of the *PEX27*, *PEX11* and *PEX25* genes, the interactions observed may represent only a subset of all possible interactions because of competition from endogenous Pex27p, Pex11p and Pex25p. No interaction was detected between Pex27p and Pex11p or between Pex25p and Pex11p, suggesting that Pex11p might act in a pathway independent from that of Pex27p and Pex25p, which might act together in the same pathway. Pex11p has been proposed to initiate peroxisome proliferation in its monomeric form and to terminate peroxisome division when it forms homodimers (Marshall *et al.*, 1996). Given that Pex27p and Pex25p are similar to Pex11p in amino acid sequence and in their roles in peroxisome division, Pex27p and Pex25p might act in a manner similar to that of Pex11p in controlling divisional events. Because Pex25p seems to be the least efficient effector of peroxisome division, it is possible that interaction between Pex27p and Pex25p could act as an additional molecular switch to initiate peroxisome division in this second pathway of divisional control.

The dynamin-like proteins Vps1p of *S. cerevisiae* (Hoepfner *et al.*, 2001) and mammalian DLP1 (Koch *et al.*, 2003) have been implicated in peroxisomal fission. It has been suggested that Pex11p recruits DLP1 to peroxisomes for peroxisomal fission events

in mammalian cells. Whether yeast Pex11p, Pex25p or Pex27p recruits dynamin-like proteins in *S. cerevisiae* awaits further investigation.

4.9.4 A possible role for Pex11p family in early events of peroxisome biogenesis

If Pex27p, Pex25p and Pex11p only play role in promoting the division of existing peroxisomes, the phenotype of cells lacking all three proteins would be predicted to be an exaggeration of that of cells lacking any two of the proteins. However, cells lacking Pex27p, Pex25p and Pex11p are compromised in the import of both PTS1 and PTS2 matrix proteins. Also, a large number of these cells do not appear to have peroxisomes by electron microscopy. These observations suggest a possible role for the Pex11p family in early events of peroxisome biogenesis. Pex3p has been suggested to initiate peroxisome formation from the ER (see Chapter 5). How peroxisome precursors bud from the ER is still unknown. Given that Pex11p has the potential to recruit dynamin-like proteins for peroxisome division, Pex11p family members might interact with some unidentified protein(s) that promote the budding of peroxisome precursors from the ER membrane. Further experimentation is required to test this possibility.

4.9.5 Mammalian PEX11 genes

Interestingly, a third PEX11 gene, PEX11γ, has recently been reported for mammalian cells (Li *et al.*, 2002; Tanaka *et al.*, 2003). Like PEX11β, PEX11γ is constitutively expressed. PEX11γ differs from PEX11α and PEX11β in that its overexpression does not promote peroxisome proliferation. How exactly Pex11α, β and γ interplay in peroxisome proliferation in mammals remains unknown. The yeast *PEX11*,

PEX25 and *PEX27* genes may be the yeast functional equivalents of the mammalian PEX11α, PEX11β and PEX11γ genes. But which yeast gene corresponds to which mammalian gene or if they correspond to each other at all remains to be determined.

4.9.6 Role of medium chain oxidation in peroxisome division

Pex11p has been proposed to act in transporting medium-chain fatty acids across the peroxisomal membrane in *S. cerevisiae* and to control peroxisome proliferation indirectly through the generation of a signaling molecule resulting from medium-chain fatty acid oxidation (van Roermund *et al.*, 2000). However, this indirect control of peroxisome proliferation by Pex11p has recently been challenged by Li and Gould (2002) who showed that Pex11 proteins could promote peroxisome division in both yeast and mammalian cells in the absence of peroxisomal metabolic activity. They concluded that Pex11 proteins act directly in peroxisome division and that the block of medium-chain fatty acid oxidation observed by van Roermund and colleagues in *S. cerevisiae pex11Δ* cells was the indirect consequence of altered peroxisomal membrane structure or dynamics. Therefore, whether Pex11 proteins, including their relations Pex27p and Pex25p, control peroxisome proliferation directly or indirectly by modulating peroxisomal metabolism remains a debated question.

In conclusion, the maintenance of the size and number of peroxisomes is a tightly controlled process involving separation and division steps. The present results point to Pex11p as the primary regulator of peroxisome division in *S. cerevisiae*, whereas Pex27p and Pex25p act as secondary regulators of this process and have some role in peroxisome separation.

CHAPTER 5

PEX3P INITIATES THE FORMATION OF A PREPEROXISOMAL COMPARTMENT FROM A SUBDOMAIN OF THE ER IN *SACCHAROMYCES CEREVISIAE*

5.1 Overview

This chapter describes the initiation of peroxisome formation from a subdomain of the ER in the yeast *S. cerevisiae*. Peroxisomes are dynamic organelles that often proliferate in response to compounds they metabolize. Peroxisomes can proliferate by two apparent mechanisms – division of pre-existing peroxisomes and the *de novo* synthesis of peroxisomes. Evidence for *de novo* peroxisome synthesis comes from studies of cells lacking the peroxisomal integral membrane peroxin Pex3p. These cells lack peroxisomes, but peroxisomes can assemble upon reintroduction of Pex3p. The source of these peroxisomes has been the subject of debate. In this chapter, we show that the amino-terminal 46 amino acids of Pex3p of *S. cerevisiae* targets to a subdomain of the ER and initiates the formation of a preperoxisomal compartment for *de novo* peroxisome synthesis. Confocal video microscopy showed that this preperoxisomal compartment can import both peroxisomal matrix and membrane proteins leading to the formation of *bona fide* peroxisomes through the continued activity of full-length Pex3p. Peroxisome formation from the preperoxisomal compartment depends on the activity of the genes *PEX14* and *PEX19*, which are required for the targeting of peroxisomal matrix and membrane proteins, respectively. These findings demonstrate a direct role for the ER in *de novo* peroxisome formation.

5.2 Truncated Pex3p proteins reveal regions of Pex3p required for targeting to peroxisomes and the presence of a hitherto unknown cellular compartment

Pex3p and Pex19p act early in the biogenesis of peroxisomes in *S. cerevisiae*, as cells lacking either peroxin do not contain peroxisomes and peroxisomes can be observed

to form upon their reintroduction. Pex3p is reported to be the docking factor for Pex19p on the peroxisomal membrane (Fang *et al.*, 2004). This observation places the function of Pex3p in peroxisome biogenesis ahead of that of Pex19p, and therefore, Pex3p serves as the best candidate protein to study the early events of peroxisome biogenesis.

Genes encoding GFP fused to the amino-terminal 20 (20aa-GFP) or 46 amino acids (40aa-GFP) of Pex3p, or to full-length Pex3p (Pex3p-GFP), were expressed under the control of the native *PEX3* promoter from plasmid in the parental haploid strain *BY4741* and in the peroxisome-deficient strains *pex3Δ* and *pex19Δ*. pmRFP-PTS1 was cotransformed into the various strains to fluorescently label peroxisomes, and cells were grown in oleic acid medium and analyzed by confocal microscopy (Figure 5-1 A). Pex3p-GFP was able to target to peroxisomes in *BY4741* and *pex3Δ* cells, as shown by the colocalization of GFP and mRFP signals in punctate structures; however, in *pex19Δ* cells, Pex3p-GFP was targeted to punctate structures that did not fluorescently label with mRFP-PTS1, which labeled the cytosol, and therefore do not correspond to peroxisomes, confirming that the formation of peroxisomes requires a copy of *PEX19*. The 20aa-GFP chimera localized to the cytosol of cells of all strains despite the fact that *BY4741* cells contain peroxisomes. *pex3Δ* cells expressing 20aa-GFP were unable to form peroxisomes, suggesting that the information for the formation of peroxisomes is not encompassed by the first 20 amino acids of Pex3p. 46aa-GFP was targeted to peroxisomes in *BY4741* cells. Since 20aa-GFP was unable to target to peroxisomes, the peroxisome targeting signal (PTS) of Pex3p must extend to between amino acids 21 to 46. Interestingly, in *pex3Δ* and *pex19Δ* cells, 46aa-GFP localized to an unknown

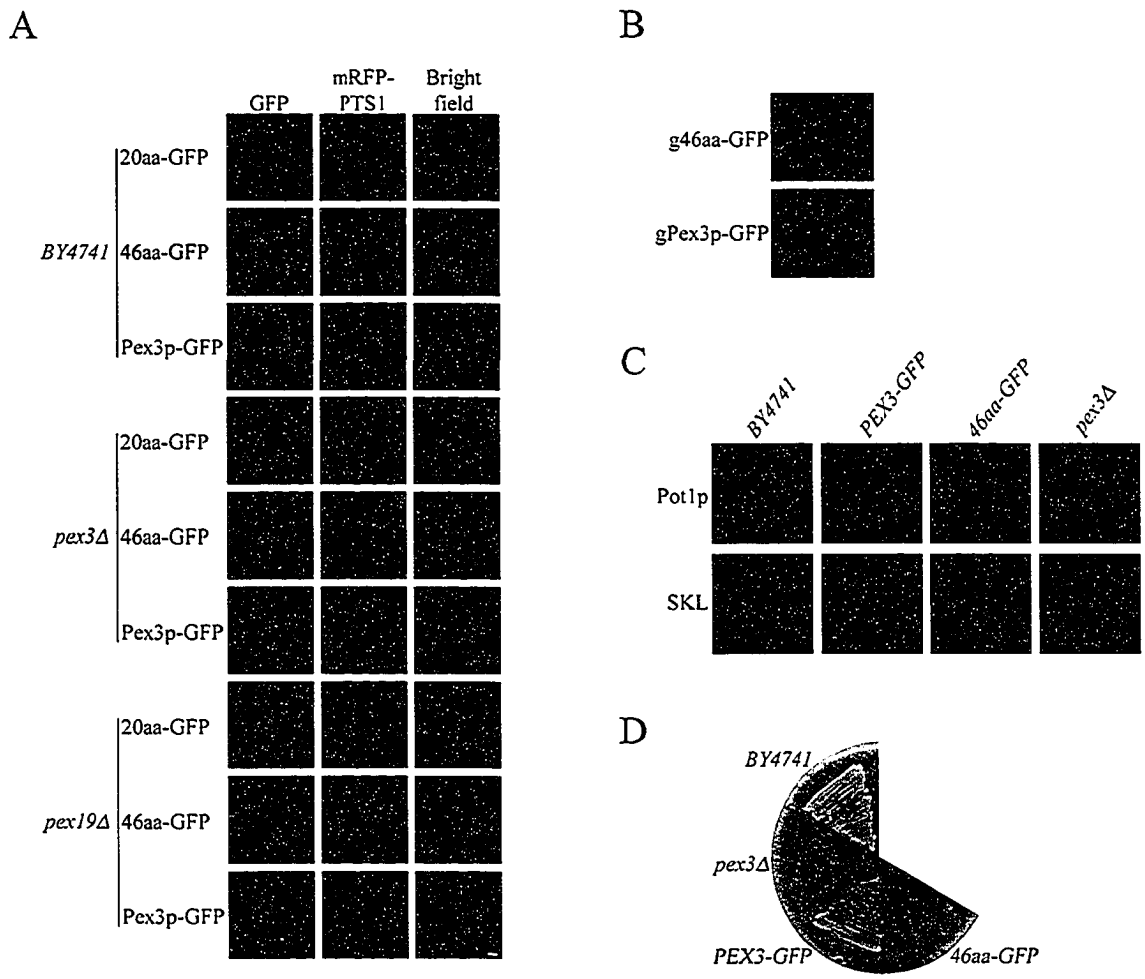

Figure 5-1. Peroxisome formation requires Pex3p. Cells were incubated in oleic acid-containing YNO medium. (A) Confocal images of *BY4741*, *pex3Δ* and *pex19Δ* cells containing pmRFP-PTS1 and a plasmid encoding one of 20aa-GFP, 46aa-GFP and Pex3p-GFP. (B) Epifluorescence microscopy of genomically encoded GFP chimeras of the amino-terminal 46amino acids of GFP and full-length Pex3p. (C) Immunofluorescence microscopy of *BY4741*, *PEX3-GFP*, *46aa-GFP* and *pex3Δ* cells using antibodies to Pot1p or to the PTS1 tripeptide Ser-Lys-Leu (SKL). (D) Growth of various strains on YPBO agar for 5 days. (E) (page 134) Electron micrographs of *BY4741*, *pex3Δ* and *46aa-GFP* cells. P, peroxisome; M, mitochondrion; N, nucleus; V, vacuole. Bar, 1 μm.

E

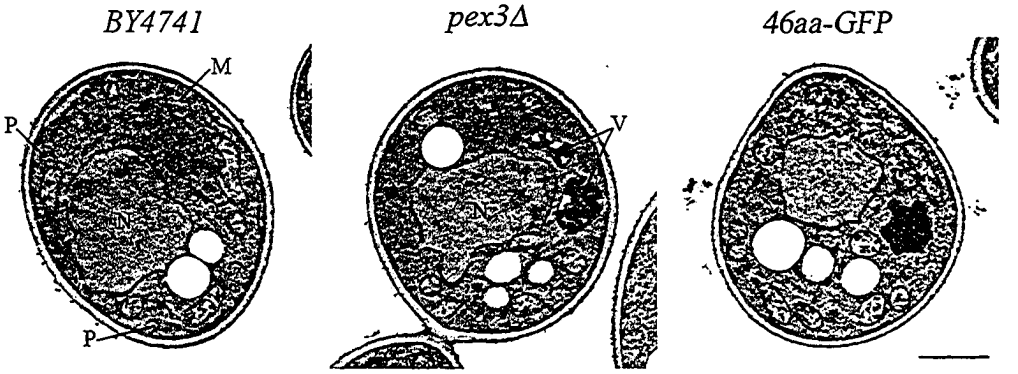

compartment represented by one or two small punctate fluorescent structures. These structures were not peroxisomes, as they did not label with mRFP-PTS1, which mislocalized to the cytosol. The capacity of 46aa-GFP to be targeted to peroxisomes in *BY4741* cells that contain peroxisomes and to an unknown compartment in *pex3Δ* and *pex19Δ* cells that lack peroxisomes suggested that this unknown compartment might serve as a preperoxisomal compartment from which peroxisomes could form upon provision of cells with full-length Pex3p. Targeting of 46aa-GFP to the unknown compartment is independent of Pex19p, consistent with a previous report that Pex19p is not required to target Pex3p to peroxisomes (Fang *et al.*, 2004).

To avoid possible artefacts of gene overexpression from multicopy plasmids, genomically encoded GFP chimeras of Pex3p (gPex3p-GFP) and the amino-terminal 46 amino acids of Pex3p (g46aa-GFP) were constructed. As observed with construct expression from plasmid (Figure 5-1 A), epifluorescence analysis of oleic acid-incubated cells showed that gPex3p-GFP localized to punctate structures with the characteristics of peroxisomes, while g46aa-GFP localized to an unknown compartment that presented usually as one or two fluorescent dots (Figure 5-1 B). Immunofluorescence analysis of oleic acid-incubated cells with antibodies to the carboxyl-terminal PTS1 tripeptide Ser-Lys-Leu (SKL) or to the PTS2-containing enzyme Pot1p (thiolase) showed that cells expressing gPex3p-GFP contained peroxisomes having both Pot1p and PTS1-containing proteins, as observed for parental *BY4741* cells (Figure 5-1 C). In contrast, cells expressing g46aa-GFP showed a cytosolic location for both Pot1p and PTS1-containing proteins, as in *pex3Δ* cells, consistent with the absence of peroxisomes in both cell types (Figure 5-1 C). The functionality of the GFP chimeras was determined by growing cells

on agar medium containing oleic acid as the sole carbon source, the metabolism of which requires functional peroxisomes. Cells expressing Pex3p-GFP grew at a rate like or similar to that of *BY4741* cells (Figure 5-1 D), suggesting that gPex3p-GFP functions like wild-type Pex3p. As expected, *pex3Δ* cells failed to grow. Cells expressing g46aa-GFP grew poorly or not at all, indicating that peroxisomal function is compromised in these cells. In electron micrographs, *BY4741* cells incubated in oleic acid medium contained characteristic peroxisomes (Figure 5-1 E). In contrast, *pex3Δ* cells and cells expressing g46aa-GFP lacked identifiable peroxisomes.

5.3 The amino terminus of Pex3p targets a subdomain of the ER

Since cells expressing g46aa-GFP do not contain peroxisomes (Figure 5-1 C), we attempted to define the subcellular compartment containing the chimera by performing colocalization analyses of g46aa-GFP with known organellar markers. g46aa-GFP did not colocalize with mitochondria marked with MitoTracker dye but showed an almost absolute colocalization with a genomically encoded fluorescent chimera (gKar2p-mRFP-HDEL) of the ER-resident chaperone, Kar2p (Figure 5-2 A). Subcellular fractionation also supported localization of g46aa-GFP to the ER compartment (Figure 5-2 B). Pex3p in *BY4741* cells localized mainly to the 20KgP fraction enriched for heavy organelles, including peroxisomes. Kar2p also localized preferentially to the 20KgP fraction, but a substantial fraction of Kar2p was also detected in the 20KgS fraction enriched for cytosol and lighter organelles. g46aa-GFP localized almost exclusively to the 20KgS fraction. Upon ultracentrifugation of the 20KgS fraction, g46aa-GFP cofractionated to both the 250KgS and 250KgP fractions in a manner almost identical to that of Kar2p, consistent

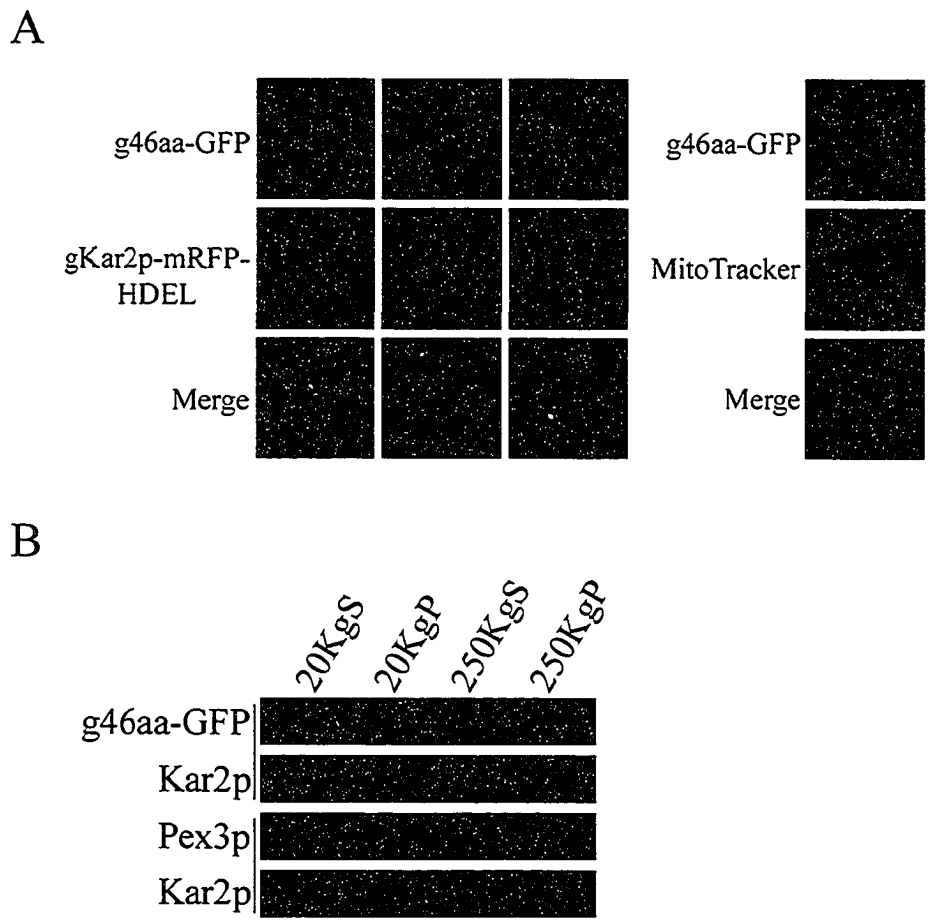

Figure 5-2. g46aa-GFP targets to a subdomain of the ER. (A) Confocal microscopy of YPBO-incubated cells expressing g46aa-GFP and gKar2p-mRFP-HDEL and epifluorescence microscopy of YPBO-incubated cells expressing g46aa-GFP and treated with MitoTracker to visualize mitochondria. Bar, 1 μm. (B) Immunoblot analysis of 20KgS, 20KgP, 250KgS and 250KgP subcellular fractions from *46aa-GFP* and *BY4741* cells incubated in YPBO with antibodies to GFP, Kar2p and Pex3p. Equivalent portions of each fraction were analyzed.

with a colocalization of g46aa-GFP and that portion of Kar2p initially found in the 20KgS fraction. Together these results suggest that the previously unknown compartment to which g46aa-GFP targets is a subdomain of the ER.

5.4 The profile of oleic acid induction for g46aa-GFP is similar to that of Pex3p-GFP

Massive proliferation of peroxisomes occurs when cells are shifted from growth in glucose-containing medium to growth in oleic acid-containing medium. It has been shown previously that cells grown in glucose-containing medium contain readily detectable levels of Pex3p that increase gradually after transfer of cells to oleic acid-containing medium (Erdmann and Blobel, 1995). Cells expressing either g46aa-GFP or Pex3p-GFP were grown in glucose-containing medium and transferred to oleic acid-containing medium. Aliquots of cells were removed at various time points, and their lysates were subjected to SDS-PAGE and immunoblotting (Figure 5-3). The levels of g46aa-GFP and Pex3p-GFP increased gradually and in a similar manner. Under the same conditions, thiolase increased from nondetectible to substantial levels, whereas the levels of the cytosolic enzyme G6PDH remained constant.

5.5 Peroxisomes form from the compartment targeted by the amino terminus of Pex3p

Might the g46aa-GFP-containing compartment be a preperoxisomal compartment? To investigate the dynamics of this compartment upon synthesis of full-length Pex3p, haploid cells expressing g46aa-GFP were mated to haploid cells expressing Pex3p under the control of a genomically integrated galactose inducible promoter

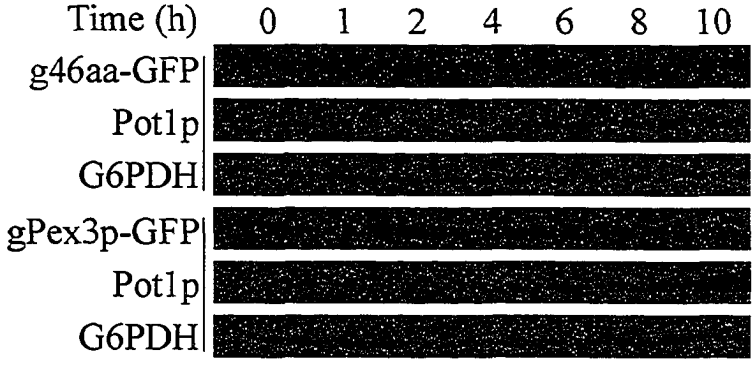

Figure 5-3. Expression profile of g46aa-GFP. Cells grown in YEPD medium were shifted to, and incubated in, YPBO medium. Aliquots of cells were removed from the YPBO medium at the times indicated, and total cell lysates were prepared. Equal amounts of protein from the total cell lysates were separated by SDS-PAGE and analyzed by immunoblotting with antibodies to GFP, thiolase and glucose-6-phosphate dehydrogenase (G6PDH).

(*GAL1*), and the diploid cells were analyzed by epifluorescence microscopy. The diploid strains also expressed one of the fluorescently labeled versions of the peroxisomal matrix enzymes Pot1p (Pot1p-mRFP) and Fox2p (Fox2p-mRFP-SKL) or Pex3p-mRFP (under the *GAL1* promoter). Cells were grown in raffinose/oleic acid medium (RIM) and transferred to galactose/oleic acid medium (GIM). Fluorescence images were taken at various times after transfer to GIM (Figure 5-4 A). At 0 h, both matrix enzymes were localized to the cytosol, and no signal for Pex3p-mRFP was observed. With increased synthesis of Pex3p-mRFP at later times, Pex3p-mRFP appeared in and colocalized with the punctate structures labeled by g46aa-GFP. Upon induction of Pex3p, both Pot1p-mRFP and Fox2p-mRFP-SKL also targeted to the g46aa-GFP-labeled structures. Electron micrographs of the diploid strain *B59P* showed no recognizable peroxisomal structures at 0 h but characteristic peroxisomes at 6 h after transfer to GIM (Figure 5-4 B). It is noteworthy that cells showed peroxisome clustering after being incubated in GIM for more than 4 h (Figures 5-4 A, B) possibly due to high levels of synthesis of Pex3p (Figure 5-4 C). In contrast, during incubation in GIM, the levels of g46aa-GFP decreased over time, suggesting that galactose inhibits the normal induction pattern observed for Pex3p in oleic acid-containing medium.

4D *in vivo* microscopy has proven a valuable tool to study the dynamics of cellular processes. It has recently been used to observe the *de novo* formation of transitional ER sites and Golgi structures (Bevis *et al.*, 2002). We used 4D *in vivo* microscopy to visualize the dynamics of the g46aa-GFP compartment and the formation of peroxisomes. Diploid *B5P3* and *B59P* cells were grown in RIM, transferred to GIM for 1.5 h, and then spotted onto an agarose pad containing SCIM and galactose. Diploid

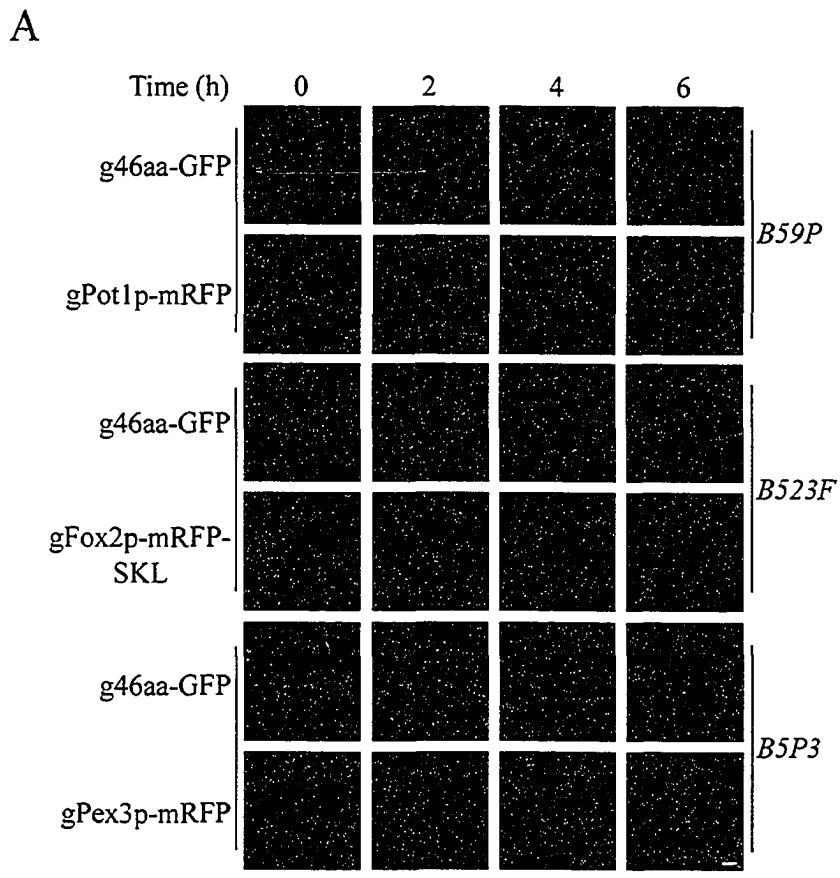

Figure 5-4. Peroxisomes form upon synthesis of full-length Pex3p. (A) Cells of strains *B59P*, *B523F* and *B5P3* incubated in RIM containing raffinose and oleic acid were shifted to, and incubated in, GIM containing galactose and oleic acid. Cells were removed from GIM at the times indicated and analyzed by epifluorescence microscopy. Bar, 1 μm. (B) (page 142) Electron micrographs of *B59P* cells incubated in GIM for 0 h or 6 h. Abbreviations as in the legend to Figure 1 E. Bar, 1 μm. (C) (page 142) Immunoblot analysis of lysates of *B59P*, *BY4741* and *pex3Δ* cells incubated in GIM for different lengths of time, as indicated, with antibodies to Pex3p, GFP and G6PDH.

B

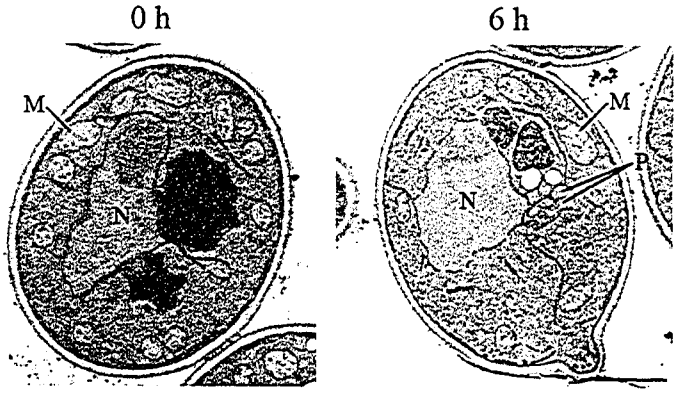

C

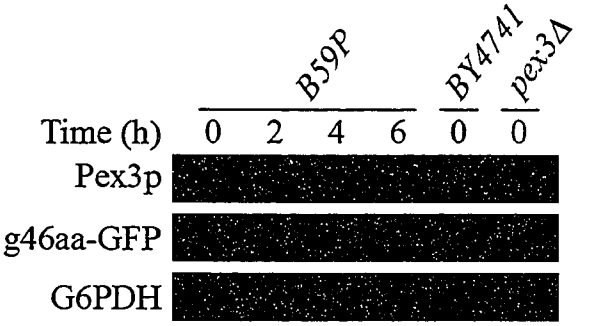

B5P3 cells (Figure 5-4 A), which express the gene for Pex3p-mRFP from one *PEX3* locus under the control of the *GAL1* promoter, showed the synthesis and import of Pex3p-mRFP into g46aa-GFP-labeled structures (Figure 5-5 A). In contrast, diploid *B59P* cells, which express wild-type Pex3p from one *PEX3* locus under the control of the *GAL1* promoter, showed the import of gPot1p-mRFP from the cytosol into the g46aa-GFP-labeled compartment (Figure 5-5 B). These results suggest that the amino-terminal 46 amino acids of Pex3p contain information to target to a preperoxisome compartment but insufficient information to drive the formation of peroxisomes. Only in the presence of full-length Pex3p, which is initially targeted to the same compartment as the g46aa-GFP, can peroxisomes form. Transit of Pex3p through the ER en route to peroxisomes has not been observed in wild-type cells, perhaps due to the predominance of peroxisome division over peroxisome *de novo* formation or because the transit of Pex3p through the ER is so rapid that microscopy is unable to capture the event. Expression of the g46aa-GFP construct might delay the exit of the peroxisomal precursor from the ER compartment, as it lacks those sequences of Pex3p downstream of the first amino-terminal amino acids responsible for this process. As we have observed, expression of full-length Pex3p together with g46aa-GFP led to the formation of *bona fide* peroxisomes capable of peroxisomal matrix and membrane protein import from the cytosol (Figures 5-4 A and 5-5), consistent with information for the exit of the peroxisomal precursor from the ER being provided by sequences of Pex3p carboxyl-terminal to its first 46 amino acids. It should be noted that some mother cells expressing g46aa-GFP and full-length Pex3p appeared to be devoid of peroxisomes (Figure 5-5). However, peroxisomes capable of importing matrix (gPot1p-mRFP) and membrane (gPex3p-mRFP) proteins

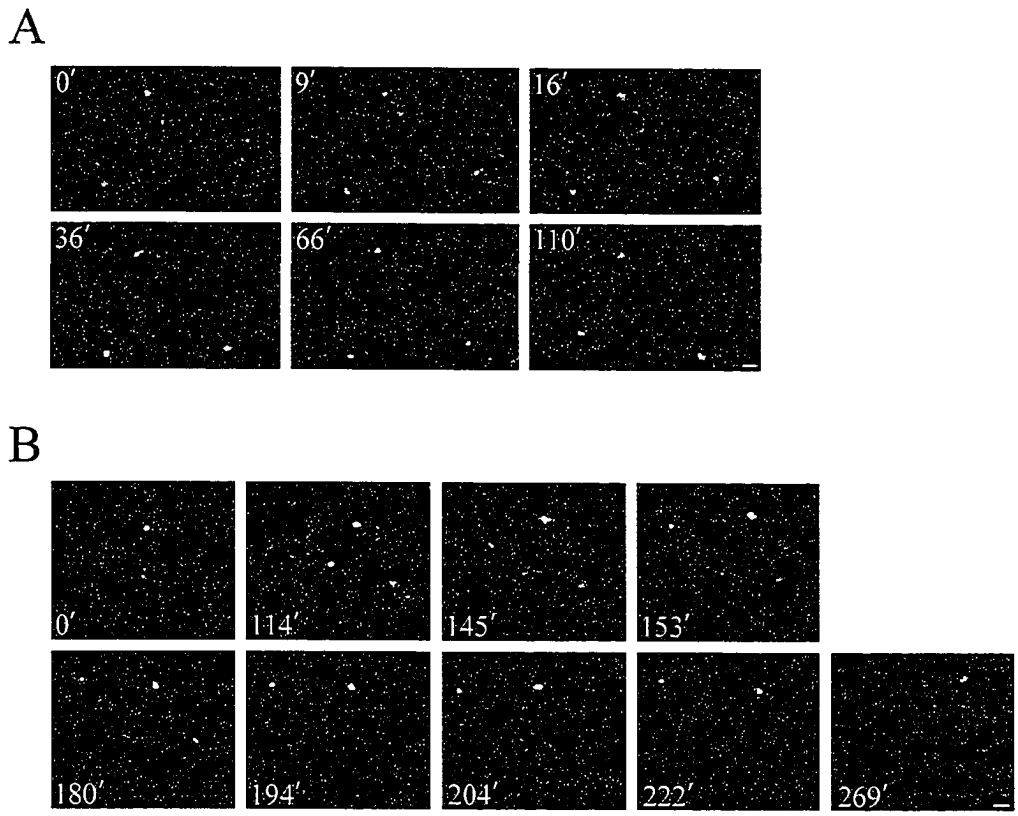

Figure 5-5. Peroxisome formation visualized by 4D *in vivo* video microscopy. Cells grown in RIM for 16 h were transferred to GIM for 1.5 h and placed onto a slide covered with a thin agarose pad containing SCIM and galactose. Cells were visualized at room temperature on a LSM 510 META confocal microscope specially modified for 4D *in vivo* video microscopy. Representative frames from videos show the import of gPex3p-mRFP and gPot1p-mRFP into the g46aa-GFP-labeled compartment. Numbers indicate the time in minutes. (A) Continuous targeting of gPex3p-mRFP into the g46aa-GFP-labeled structures in *B5P3* cells. (B) Progressive import of gPot1p-mRFP from the cytosol into g46aa-GFP-labeled structures in *B59P* cells. Partitioning of peroxisomes from mother cells to buds occurs between 180 min and 269 min.

were observed in mother cells after prolonged periods of incubation. We did not observe the reappearance of typical g46aa-GFP-labeled structures in these cells, possibly because of rapid photobleaching of newly synthesized GFP.

5.6 Peroxisome formation from the preperoxisomal compartment requires Pex14p and Pex19p

Both Pex14p and Pex19p are required for peroxisome assembly. Pex14p is the point of convergence of the PTS1 and PTS2 matrix protein import pathways (Albertini *et al.*, 1997). Pex19p is required for the stability in and/or targeting to the peroxisomal membrane of most peroxisomal membrane proteins (Sacksteder *et al.*, 2000; Hettema *et al.*, 2000). We therefore investigated what roles Pex14p and Pex19p might have in regulating the dynamics of the g46aa-GFP-labeled compartment. Cells lacking Pex14p or Pex19p were grown in RIM and then transferred to GIM, and aliquots of cells were taken at various times after transfer. The fluorescence signals for g46aa-GFP, Pot1p-mRFP and Pex3p-mRFP were analyzed (Figure 5-6). Cells deleted for either *PEX14* or *PEX19* showed colocalization of g46aa-GFP with Pex3p-mRFP when shifted to GIM, and the synthesis of Pex3p-mRFP was turned on. However, Pot1p-mRFP remained mostly cytosolic and was not targeted to g46aa-GFP-labeled structures. Therefore, both *PEX14* and *PEX19* are required for the development of g46aa-GFP-labeled structures into peroxisomes.

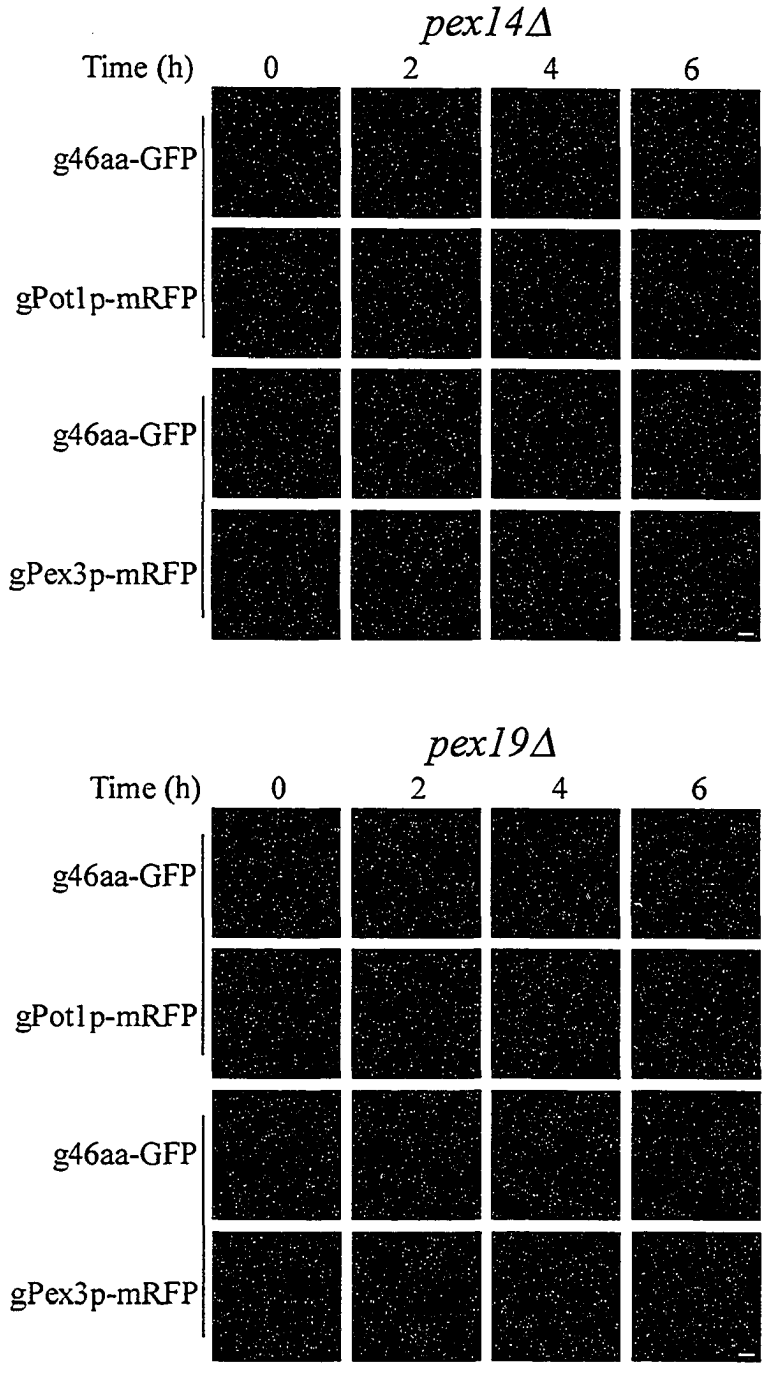

Figure 5-6. Formation of peroxisomes, but not targeting of Pex3p, depends on *PEX14* and *PEX19*. *B59P* and *B5P3* cells deleted for *PEX14* and *PEX19* were shifted from RIM containing raffinose and oleic acid to GIM containing galactose and oleic acid. Cells were removed from GIM at the times indicated and analyzed by epifluorescence microscopy. Bar, 1 μm.

5.7 Discussion

5.7.1 *De novo* peroxisome biogenesis initiates at the ER

This study shows that the amino terminus of Pex3p targets to peroxisomes in wild-type cells and a subdomain of the ER in cells lacking peroxisomes. This subdomain of the ER can be developed into functional peroxisomes through the activity of full-length Pex3p. Further analysis of this region has to be made to determine if other proteins are localized to the same region and participate in the formation of peroxisome.

Immunoelectron microscopy of mouse dendritic cells has shown that the peroxisomal membrane protein Pex13p can be found in a specialized ER subdomain (Geuze *et al.*, 2003). 3D image reconstruction demonstrated continuity between this specialized ER subdomain and a reticular structure resembling peroxisomes. These results suggest a peroxisome maturation pathway initiating at the ER. However, a peroxisomal reticulum has not been observed in yeasts. We were unable to observe any unique membranous structure in electron micrographs that might correspond to the punctate structure targeted by g46aa-GFP. This is not surprising given that that the preperoxisomal vesicles of *Y. lipolytica* have a rather routine appearance that does not distinguish them from the overall population of vesicles in the cell (Titorenko *et al.*, 2000).

5.7.2 Seeing is believing

To support a model for peroxisome maturation that initiates at the level of the ER, it is important to show the development of peroxisomes in relation to the ER in terms of the import of both peroxisomal membrane and matrix proteins. Using 4D *in vivo*

microscopy, we showed the targeting of the peroxisomal membrane chimeric protein Pex3p-mRFP to punctate structures (Figure 5-4 A) that exhibited both the morphological (Figure 5-2 A) and biochemical (Figure 5-2 B) characteristics of a subdomain of the ER. The formation of this compartment was initiated by the expression of g46aa-GFP (Figure 5-2 A), and this compartment was also able to import fluorescently labeled derivatives of the PTS1-containing matrix protein Fox2p (gFox2p-mRFP-SKL) and the PTS2-containing matrix protein Pot1p (gPot1p-mRFP) (Figure 5-4 A).

5.7.3 Pex3p, the ER, and *de novo* peroxisome biogenesis: possible mechanisms

How this preperoxisomal compartment actually dissociates itself from the ER remains unknown. The targeting of the membrane proteins Pex2p, Pex3p and Pex16p to peroxisomes was unaffected in mammalian cells blocked in COPI- or COPII-mediated vesicular transport (South *et al.*, 2000; Voorn-Brouwer *et al.*, 2001). However, experiments in *H. polymorpha* showed that a subset of peroxisomal proteins was trapped in the ER in cells treated with Brefeldin A (Salomons *et al.*, 1997). A possible role for COPI and COPII in peroxisome formation has yet to be investigated in *S. cerevisiae*. How g46aa-GFP reaches the ER is also unknown. Pex3p might have intrinsic properties that direct it to the ER, or other proteins might aid in delivering Pex3p to the ER. Inactivation of the ER translocation machinery components Sec61p and Ssh1p did not have an effect on peroxisome biogenesis (South *et al.*, 2001). This result was taken by some researchers as proof that the ER was not involved in peroxisome biogenesis. However, proteins could enter the ER via some undefined mechanism independent of Sec61p or Ssh1p. Future experiments aimed at reconstituting *in vitro* the import of

Pex3p into the ER should clarify this process. Our findings demonstrating a requirement for Pex14p and Pex19p in the formation of peroxisomes from the g46aa-GFP-labeled preperoxisomal compartment and which are capable of matrix protein import from the cytosol (Figure 5-6) are consistent with a scenario in which Pex19p docks to Pex3p to facilitate the import of other peroxisomal membrane proteins such as Pex14p (Fang *et al.*, 2004).

In conclusion, we show that the peroxisomal integral membrane protein Pex3p traffics through the ER and participates in the formation of preperoxisomal vesicles from this endomembrane system. Through the continued activity of Pex3p, these preperoxisomal vesicles can develop into *bona fide* peroxisomes via the import of peroxisomal matrix and membrane proteins. Our findings demonstrate a direct role for the ER in the *de novo* formation of peroxisomes.

CHAPTER 6

PERSPECTIVES

6.1 Synopsis

Three important events in the assembly of peroxisomes are: the formation of the peroxisomal membrane, the import of proteins into peroxisomes and the division of peroxisomes. A summary of the proteins involved in these three events is shown in Figure 6-1. These three events were studied using three different experimental approaches. Pex24p, an integral protein of peroxisomes, was identified by classical genetic screening of yeast mutants and complementation of the mutant by a genomic DNA library. It was shown to be involved in the import of both matrix and membrane proteins into peroxisomes. Pex27p, a peripheral membrane protein of peroxisomes involved in the regulation of peroxisome division, was uncovered by database mining using information from Pex25p which was identified previously by transcriptome profiling. The *de novo* formation of peroxisomes was shown by 4D confocal microscopy. A subdomain of the ER containing a fluorescent chimera of the amino-terminus of Pex3p was shown to develop into functional peroxisomes through the activity of full-length Pex3p.

6.2 Future directions for research related to Pex24p

Pex24p is not involved in the formation of the peroxisomal membrane, as *pex24* mutants contain membrane structures resembling peroxisomes. Alternatively, its primary role might be in the import of peroxisomal matrix and membrane proteins. Since both the PTS1 and PTS2 import pathways are affected in *pex24* mutants, Pex24p might function downstream of Pex14p, which is known to be the point of convergence for both import pathways. Also, since peroxisomal membrane protein import is compromised in *pex24*

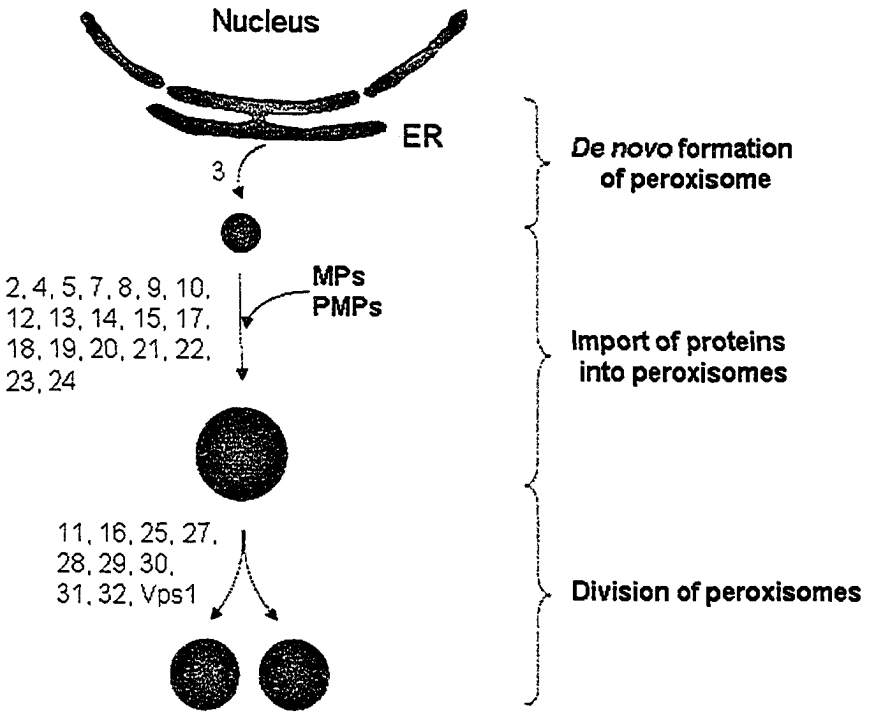

Figure 6-1. Three important events in peroxisome assembly. Peroxisome assembly can be divided into three events, namely the *de novo* formation of peroxisomes, the import of proteins into peroxisomes and the division of peroxisomes. Peroxins involved in each event are shown by their Pex number. Only yeast proteins are shown.

mutants, Pex24p might in fact function mainly in the import of peroxisomal membrane proteins. How membrane proteins are imported is largely unknown, especially in *Y. lipolytica*. Studies in mammalian cells and *S. cerevisiae* suggest that Pex3p acts as a docking factor for Pex19p, which is the receptor and/or chaperone for peroxisomal membrane proteins (Jones *et al.*, 2004; Fang *et al.*, 2004; Rottensteiner *et al.*, 2004). Although Pex3p has been shown to play a role in the *de novo* formation of peroxisomes (Bascom *et al.*, 2003; Chapter 5), one could not rule out its function in the import of peroxisomal membrane proteins. The interactions of Pex24p with Pex19p and Pex3p should be examined. Sequencing of the *Y. lipolytica* genome has recently been completed. It is now possible to isolate Pex24p and its protein complex by immunoprecipitation and to identify its interaction partners by mass spectrometry for a more thorough understanding of the functions of Pex24p.

The *mut1-1* mutant contains a shortened form of Pex24p consisting of the first 117 amino acids. This mutant has reduced, but not abolished, ability to grow on medium containing oleic acid and contains vesicles resembling peroxisomes as seen by electron microscopy. Based on these phenotypes, one could speculate that the shortened form of Pex24p might retain some functions of Pex24p. It is of interest to determine its subcellular localization and interaction partners.

The topology of Pex24p could also provide insight into how Pex24p functions. Pex24p is highly susceptible to degradation during subcellular fractionation. Therefore, protease protection experiments to determine the topology of Pex24p have not been possible. *In vivo* microscopy analysis using tobacco etch virus protease and a GFP

chimera of Pex24p could be performed according to Faber *et al* (2001) to determine the topology of Pex24p.

Membrane structures of density less than that of wild-type peroxisomes but containing peroxisomal proteins were observed in both *pex24* mutants. The origin of these membrane structures and whether they are peroxisomal precursors are of great interest. Isolation of these membrane structures and characterization of their protein composition could be performed.

6.3 Future directions for research related to Pex27p

S. cerevisiae Pex11p was shown to control peroxisome division from inside the organelle (Marshall *et al.*, 1996). The authors isolated mature and proliferating peroxisomes by subcellular fractionation. They showed that Pex11p homodimerizes in mature peroxisomes and stays as monomers in proliferating peroxisomes. By switching between these two protein states of Pex11p, peroxisome division is regulated (Marshall *et al.*, 1996). Pex25p and Pex27p have sequence homology to Pex11p. These three proteins represent members of the Pex11 protein family in *S. cerevisiae*. We showed that Pex25p interacts with itself and Pex27p, Pex27p interacts with itself and Pex25p, and Pex11p interacts only with itself by yeast two-hybrid analysis. Yeast protein-protein interactions determined by yeast two-hybrid analysis could be direct or indirect. Further analysis of the above interactions should be performed to determine if other proteins mediate these interactions. It is possible that Pex25p and Pex27p control peroxisome division in a manner similar to Pex11p. Therefore it is interesting to examine Pex25p and Pex27p

interactions in both mature and proliferating peroxisomes as described by Marshall *et al* (1996).

Synthesis of Pex11p and Pex25p is increased by growing cells in medium containing a peroxisome stimulator such as oleic acid (Marshall *et al.*, 1995, Erdmann and Blobel, 1995; Smith *et al.*, 2002). In contrast, levels of Pex27p are constant in the same type of medium (Chapter 4). Peroxisomes undergo constitutive division in the absence of a peroxisome stimulator and regulated division in the presence of a peroxisome stimulator (Marshall *et al.*, 1996). One would expect the levels of proteins involved in the regulated division of peroxisomes to increase when cells are grown in medium containing a peroxisome stimulator. Pex11p has been shown to promote peroxisome division under both non-stimulating and stimulating conditions (Li and Gould, 2002). In other words, Pex11p is capable of regulating both the constitutive and regulated modes of peroxisome division. Our analysis points to Pex11p being the strongest regulator of peroxisome division among the three members of the Pex11 protein family in *S. cerevisiae* (Chapter 4). It is not surprising that Pex11p can regulate both types of peroxisome division. Since the synthesis of Pex27p is not affected by oleic acid, it is tempting to speculate that Pex27p plays a large role in the constitutive division of peroxisomes. It would be interesting to determine and compare the ability of the Pex11 protein family members to control the constitutive division of peroxisomes.

Both Pex25p and Pex27p are peripheral membrane proteins. Whether they locate to the inside or outside of the peroxisomal membrane has not yet been determined. Since Pex25p interacts with Pex27p, one would expect they are localized to the same side of the

peroxisomal membrane. The topology of Pex25p and Pex27p could reveal from which side of the peroxisomal membrane they act to regulate peroxisome division.

Although Pex11p, Pex25p and Pex27p share sequence similarities in general, Pex25p and Pex27p differ the most from Pex11p at their amino-termini (Figure 4-1). Functional analysis of the amino-terminal regions of Pex25p and Pex27p could lead to a better understanding of how Pex25p and Pex27p might work differently from Pex11p in regulating peroxisome division.

Other proteins including Vps1p, Pex28p, Pex29p, Pex30p, Pex31p and Pex32p are also implicated in peroxisome division (Hoepfner *et al.*, 2001; Vizeacoumar *et al.*, 2003 and 2004). Including members of the Pex11 protein family, there are at least 9 proteins involved in controlling peroxisome size and number. To gain a better picture of how peroxisome division is carried out, both spatial and temporal protein interaction networks among these proteins should be determined.

6.4 Future directions for research related to the *de novo* formation of peroxisomes

Our confocal images show that the amino-terminus of Pex3p is capable of targeting to a subdomain of the ER in the absence of peroxisomes. To complement and provide stronger evidence for this localization information, immunoelectron microscopy could be performed. From the ER compartment containing the amino-terminus of Pex3p, peroxisomes can form upon synthesis of full-length Pex3p. Although we were able to show that newly synthesized Pex3p colocalizes with the amino-terminus of Pex3p by video microscopy, it is essential to show that full-length Pex3p can target to the ER. This could be done by both confocal and immunoelectron microscopy. It might be difficult to

show that Pex3p transits through ER by video microscopy due to the abundance of ER elements in the cell and the small size of a yeast cell. Alternatively, pulse-chase analysis could be performed to show that newly synthesized Pex3p initially colocalizes with an ER marker and later colocalizes with peroxisomal markers.

In *Y. lipolytica*, Pex2p and Pex16p pass through ER on their way to peroxisomes (Titorenko and Rachubinski, 1998). It is still not clear if other peroxisomal membrane proteins traffic to peroxisomes via the ER. The presence of other peroxisomal membrane proteins in the 46aa-GFP compartment should be verified.

What exactly is the nature of this ER compartment? Potential components of this compartment could possibly be identified by immunoprecipitating the amino-terminus of Pex3p in the absence of peroxisomes. Components might include ER translocation machineries for Pex3p and factors involved in the budding of the peroxisomal precursor from the ER. It is not known if COPI and COPII have roles in peroxisome formation in *S. cerevisiae*. Localization of Pex3p in strains bearing mutations in components of COPI and COPII should be examined. Furthermore, previous studies have shown that mutations in either Sec61p or Ssh1p do not affect peroxisome biogenesis (South *et al.*, 2001). Sec61p and Ssh1p are two components of the ER translocation complex in *S. cerevisiae*. Double mutation in both proteins and mutations in other components of the translocation complex should be analyzed for any effect on the formation of peroxisomes. It is also possible that Pex3p translocates into the ER by a different and yet unidentified translocation machinery. Reconstitution of the import of Pex3p into the ER *in vitro* would be of great interest.

Recently, our laboratory has identified *S. cerevisiae* strains defective in the inheritance of peroxisomes. One strain is incapable of retaining peroxisomes in the mother cell during cell division. The other strain is compromised in the insertion of peroxisomes into the bud. Cells devoid of peroxisomes in these strains are good subjects for studying the *de novo* formation of peroxisomes, since all genes related to peroxisome biogenesis are intact in these strains. Video microscopy could be performed to observe any reappearance of peroxisomes. If peroxisomes do recover in these cells, localization of Pex3p and other peroxisomal membrane proteins before the appearance of peroxisomes could shed light on the origin of peroxisomes.

6.5 Concluding remarks

Our understanding of the assembly of peroxisomes is by no means clear enough. Detailed analyses aimed at elucidating the mechanisms operating in all pathways of peroxisome assembly are essential. This thesis provides the identity of several molecular players involved in early to late events in peroxisome assembly. Future research could be built up from this thesis to generate a broad and detailed picture of how peroxisomes are assembled.

CHAPTER 7

REFERENCES

Abe, I. and Y. Fujiki. 1998. cDNA cloning and characterization of a constitutively expressed isoform of the human peroxin Pex11p. *Biochem. Biophys. Res. Commun.* 252:529-533.

Adames, N. R., J. R. Oberle, and J. A. Cooper. 2001. The surveillance mechanism of the spindle position checkpoint in yeast. *J. Cell Biol.* 153:159-168.

Aitchison, J. D. Targeting of *Candida tropicalis* Trifunctional Enzyme to Peroxisomes in Yeast: Identification of a Carboxy-Terminal Tripeptide Peroxisomal Targeting Signal. 1992. Ph.D. Thesis, McMaster University, Hamilton.

Aitchison, J. D., W. W. Murray, and R. A. Rachubinski. 1991. The carboxyl-terminal tripeptide Ala-Lys-Ile is essential for targeting *Candida tropicalis* trifunctional enzyme to yeast peroxisomes. *J. Biol. Chem.* 266:23197-23203.

Aitchison, J. D., R. K. Szilard, W. M. Nuttley, and R. A. Rachubinski. 1992. Antibodies directed against a yeast carboxyl-terminal peroxisomal targeting signal specifically recognize peroxisomal proteins from various yeasts. *Yeast* 8:721-734.

Albertini, M., P. Rehling, R . Erdmann, W. Girzalsky, J. A. Kiel, M. Veenhuis, and W. H. Kunau. 1997. Pex14p, a peroxisomal membrane protein binding both receptors of the two PTS-dependent import pathways. *Cell* 89:83-92.

Argos, P. and J. K. Rao. 1986. Prediction of protein structure. *Methods Enzymol.* 130:185-207.

Ausubel, F.J., R. Brent, R. E. Kingston, D. D. Moore, J. G. Seidman, J. A. Smith, and K. Struhl. 1989. Current Protocols in Molecular Biology. Greene Publishing Associates, New York, NY.

Baerends, R. J., K. N. Faber, A. M. Kram, J. A. Kiel, I. J. van der Klei and M. Veenhuis. 2000. A stretch of positively charged amino acids at the N terminus of *Hansenula polymorpha* Pex3p is involved in incorporation of the protein into the peroxisomal membrane. *J. Biol. Chem.* 275:9986-9995.

Baerends, R. J., S. W. Rasmussen, R. E. Hilbrands, M. van der Heide, K. N. Faber, P. T. Reuvekamp, J. A. Kiel, J. M. Cregg, I. J. van der Klei and M. Veenhuis. 1996.

The *Hansenula polymorpha PER9* gene encodes a peroxisomal membrane protein essential for peroxisome assembly and integrity. *J. Biol. Chem.* 271:8887-8894.

Baird, G. S., D. A. Zacharias, and R. Y. Tsien. 2000. Biochemistry, mutagenesis, and oligomerization of DsRed, a red fluorescent protein from coral. *Proc. Natl. Acad. Sci. U. S. A.* 97:11984-11989.

Baker, A. 1996. In vitro systems in the study of peroxisomal protein import. *Experientia* 52:1055-1062.

Barth, G. and C. Gaillardin. 1997. Physiology and genetics of the dimorphic fungus *Yarrowia lipolytica. FEMS Microbiol. Rev.* 19:219-237.

Bascom, R. A., H. Chan, and R. A. Rachubinski. 2003. Peroxisome biogenesis occurs in an unsynchronized manner in close association with the endoplasmic reticulum in temperature-sensitive *Yarrowia lipolytica* Pex3p mutants. *Mol. Biol. Cell* 14:939-957.

Bevis, B. J. and B. S. Glick. 2002. Rapidly maturing variants of the *Discosoma* red fluorescent protein (DsRed). *Nat. Biotechnol.* 20:83-87.

Bevis, B. J., A. T. Hammond, C. A. Reinke, and B. S. Glick. 2002. *De novo* formation of transitional ER sites and Golgi structures in *Pichia pastoris. Nat. Cell Biol.* 4:750-756.

Brachmann, C. B., A. Davies, G. J. Cost, E. Caputo, J. Li, P. Hieter, and J. D. Boeke. 1998. Designer deletion strains derived from *Saccharomyces cerevisiae* S288C: a useful set of strains and plasmids for PCR-mediated gene disruption and other applications. *Yeast* 14:115-132.

Brade, A. M. Peroxisome Assembly in *Yarrowia lipolytica*. 1992. M.Sc. Thesis, McMaster University, Hamilton.

Bradford, M. M. 1976. A rapid and sensitive method for the quantitation of microgram quantities of protein utilizing the principle of protein-dye binding. *Anal. Biochem.* 72:248-254.

Brickner, D. G., J. J. Harada, and L. J. Olsen. 1997. Protein transport into higher plant peroxisomes. In vitro import assay provides evidence for receptor involvement. *Plant Physiol.* 113:1213-1221.

Broach, J. R., J. N. Strathern, and J. B. Hicks. 1979. Transformation in yeast: development of a hybrid cloning vector and isolation of the *CAN1* gene. *Gene* 8:121-133.

Brocard, C., F. Kragler, M. M. Simon, T. Schuster, and A. Hartig. 1994. The tetratricopeptide repeat-domain of the PAS10 protein of *Saccharomyces cerevisiae* is essential for binding the peroxisomal targeting signal-SKL. *Biochem. Biophys. Res. Commun.* 204:1016-1022.

Brosius, U. and J. Gartner. 2002. Cellular and molecular aspects of Zellweger syndrome and other peroxisome biogenesis disorders. *Cell Mol. Life Sci.* 59:1058-1069.

Brown, T. W. A Study of Peroxisome Biogenesis in the Yeast *Yarrowia lipolytica*. 2000. M.Sc. Thesis, University of Alberta, Alberta.

Brown, T. W., V. I. Titorenko, and R. A. Rachubinski. 2000. Mutants of the *Yarrowia lipolytica PEX23* gene encoding an integral peroxisomal membrane peroxin mislocalize matrix proteins and accumulate vesicles containing peroxisomal matrix and membrane proteins. *Mol. Biol. Cell* 11:141-152.

Burnette, W. N. 1981. "Western blotting": electrophoretic transfer of proteins from sodium dodecyl sulfate-polyacrylamide gels to unmodified nitrocellulose and radiographic detection with antibody and radioiodinated protein A. *Anal. Biochem.* 112:195-203.

Campbell, R. E., O. Tour, A. E. Palmer, P. A. Steinbach, G. S. Baird, D. A. Zacharias, and R. Y. Tsien. 2002. A monomeric red fluorescent protein. *Proc. Natl. Acad. Sci. U. S. A.* 99:7877-7882.

Chang, C. C., S. South, D. Warren, J. Jones, A. B. Moser, H. W. Moser, and S. J. Gould. 1999a. Metabolic control of peroxisome abundance. *J. Cell Sci.* 112 (10):1579-1590.

Chang, C. C., D. S. Warren, K. A. Sacksteder, and S. J. Gould. 1999b. PEX12 interacts with PEX5 and PEX10 and acts downstream of receptor docking in peroxisomal matrix protein import. *J. Cell Biol.* 147:761-774.

Collins, C. S., J. E. Kalish, J. C. Morrell, J. M. McCaffery, and S. J. Gould. 2000. The peroxisome biogenesis factors Pex4p, Pex22p, Pex1p, and Pex6p act in the terminal steps of peroxisomal matrix protein import. *Mol. Cell Biol.* 20:7516-7526.

Crane, D. I., J. E. Kalish, and S. J. Gould. 1994. The Pichia pastoris *PAS4* gene encodes a ubiquitin-conjugating enzyme required for peroxisome assembly. *J. Biol. Chem.* 269:21835-21844.

Crookes, W. J. and L. J. Olsen. 1998. The effects of chaperones and the influence of protein assembly on peroxisomal protein import. *J. Biol. Chem.* 273:17236-17242.

de Duve C. and P. Baudhuin. 1966. Peroxisomes (microbodies and related particles). *Physiol. Rev.* 46:323-357.

Dibrov, E., S. Fu, and B. D. Lemire. 1998. The *Saccharomyces cerevisiae TCM62* gene encodes a chaperone necessary for the assembly of the mitochondrial succinate dehydrogenase (complex II). *J. Biol. Chem.* 273:32042-32048.

Dilworth, D. J., A. Suprapto, J. C. Padovan, B. T. Chait, R. W. Wozniak, M. P. Rout, and J. D. Aitchison. 2001. Nup2p dynamically associates with the distal regions of the yeast nuclear pore complex. *J. Cell Biol.* 153:1465-1478.

Dodt, G., N .Braverman, C .Wong, A. Moser, H. W. Moser, P. Watkins, D. Valle, and S. J. Gould. 1995. Mutations in the PTS1 receptor gene, *PXR1*, define complementation group 2 of the peroxisome biogenesis disorders. *Nat. Genet.* 9:115-125.

Dodt, G. and S. J. Gould. 1996. Multiple PEX genes are required for proper subcellular distribution and stability of Pex5p, the PTS1 receptor: evidence that PTS1 protein import is mediated by a cycling receptor. *J. Cell Biol.* 135:1763-1774.

Douma, A. C., M. Veenhuis, W. de Koning, M. Evers, and W. Harder. 1985. Dihydroxyacetone synthase is localized in the peroxisomal matrix of methanol-grown *Hansenula polymorpha*. *Arch. Microbiol.* 143:237-243.

Dyer, J. M., J. A. McNew, and J. M. Goodman. 1996. The sorting sequence of the peroxisomal integral membrane protein PMP47 is contained within a short hydrophilic loop. *J. Cell Biol.* 133:269-280.

Eckert, J. H. and R. Erdmann. 2003. Peroxisome biogenesis. *Rev. Physiol. Biochem. Pharmacol.* 147:75-121.

Eisenberg, D., E. Schwarz, M. Komaromy, and R. Wall. 1984. Analysis of membrane and surface protein sequences with the hydrophobic moment plot. *J. Mol. Biol.* 179:125-142.

Eitzen, G. A. An Analysis of Peroxisome Assembly Mutants of the Yeast *Yarrowia lipolytica*. 1997. Ph.D. Thesis, University of Alberta, Alberta.

Eitzen, G. A., R. K. Szilard, and R. A. Rachubinski. 1997. Enlarged peroxisomes are present in oleic acid-grown *Yarrowia lipolytica* overexpressing the *PEX16* gene encoding an intraperoxisomal peripheral membrane peroxin. *J. Cell Biol.* 137:1265-1278.

Eitzen, G. A., V. I. Titorenko, J. J. Smith, M. Veenhuis, R. K. Szilard, and R. A. Rachubinski. 1996. The *Yarrowia lipolytica* gene *PAY5* encodes a peroxisomal integral membrane protein homologous to the mammalian peroxisome assembly factor PAF-1. *J. Biol. Chem.* 271:20300-20306.

Elgersma, Y., L. Kwast, M. van den Berg, W. B. Snyder, B. Distel, S. Subramani, and H. F. Tabak. 1997. Overexpression of Pex15p, a phosphorylated peroxisomal integral membrane protein required for peroxisome assembly in *S.*cerevisiae, causes proliferation of the endoplasmic reticulum membrane. *EMBO J.* 16:7326-7341.

Elgersma, Y., C. W. van Roermund, R. J. Wanders, and H. F. Tabak. 1995. Peroxisomal and mitochondrial carnitine acetyltransferases of *Saccharomyces cerevisiae* are encoded by a single gene. *EMBO J.* 14:3472-3479.

Erdmann, R. and G. Blobel. 1995. Giant peroxisomes in oleic acid-induced *Saccharomyces cerevisiae* lacking the peroxisomal membrane protein Pmp27p. *J. Cell Biol.* 128:509-523.

Erdmann, R. and G. Blobel. 1996. Identification of Pex13p a peroxisomal membrane receptor for the PTS1 recognition factor. *J. Cell Biol.* 135:111-121.

Erdmann, R., M. Veenhuis, D. Mertens, and W. H. Kunau. 1989. Isolation of peroxisome-deficient mutants of *Saccharomyces cerevisiae. Proc. Natl. Acad. Sci. U. S. A* 86:5419-5423.

Faber, K. N., A. M. Kram, M. Ehrmann, and M. Veenhuis. 2001. A novel method to determine the topology of peroxisomal membrane proteins in vivo using the tobacco etch virus protease. *J. Biol. Chem.* 276:36501-36507.

Fang, Y., J. C. Morrell, J. M. Jones, and S. J. Gould. 2004. PEX3 functions as a PEX19 docking factor in the import of class I peroxisomal membrane proteins. *J. Cell Biol.* 164:863-875.

Finley, D., E. Ozkaynak, and A. Varshavsky. 1987. The yeast polyubiquitin gene is essential for resistance to high temperatures, starvation, and other stresses. *Cell* 48:1035-1046.

Fransen, M., T. Wylin, C. Brees, G. P. Mannaerts, and P. P. van Veldhoven. 2001. Human Pex19p binds peroxisomal integral membrane proteins at regions distinct from their sorting sequences. *Mol. Cell. Biol.* 21:4413-4424.

Fujiki, Y., A. L. Hubbard, S. Fowler, and P. B. Lazarow. 1982. Isolation of intracellular membranes by means of sodium carbonate treatment: application to endoplasmic reticulum. *J. Cell Biol.* 93:97-102.

Gatto, G. J. Jr., B. V. Geisbrecht, S. J. Gould, and J. M. Berg. 2000. Peroxisomal targeting signal-1 recognition by the TPR domains of human PEX5. *Nat. Struct. Biol.* 7:1091-1095.

Geuze, H. J., J. L. Murk, A. K. Stroobants, J. M. Griffith, M. J. Kleijmeer, A. J. Koster, A. J. Verkleij, B. Distel, and H. F. Tabak. 2003. Involvement of the endoplasmic reticulum in peroxisome formation. *Mol. Biol. Cell* 14:2900-2907.

Ghaedi, K., S. Tamura, K. Okumoto, Y. Matsuzono, and Y. Fujiki. 2000. The peroxin Pex3p initiates membrane assembly in peroxisome biogenesis. *Mol. Biol. Cell* 11:2085-2102.

Ghaemmaghami, S., W. K. Huh, K. Bower, R. W. Howson, A. Belle, N. Dephoure, E. K. O'Shea, and J. S. Weissman. 2003. Global analysis of protein expression in yeast. *Nature* 425:737-741.

Giaever, G., A. M. Chu, L. Ni, C. Connelly, L. Riles, S. Veronneau, S. Dow, A. Lucau-Danila, K. Anderson, B. André, A.P. Arkin, A. Astromoff, M. El Bakkoury, R. Bangham, R. Benito, S. Brachat, S. Campanaro, M. Curtiss, K. Davis, A. Deutschbauer, K. D. Entian, P. Flaherty, F. Foury, D. J. Garfinkel, M. Gerstein, D. Gotte, U. Göldener, J. H. Hegemann, S. Hempel, Z. Herman, D. F. Jaramillo, D. E. Kelly, S. L. Kelly, P. Kötter, D. LaBonte, D. C. Lamb, N. Lan, H. Liang, H. Liao, L. Liu, C. Luo, M. Lussier, R. Mao, P. Menard, S. L. Ooi, J. L. Revuelta, C. J. Roberts, M. Rose, P. Ross-Macdonald, B. Scherens, G. Schimmack, B. Shafer, D. D. Shoemaker, S. Sookhai-Mahadeo, R. K. Storms, J. N. Strathern, G. Valle, M. Voet, G. Volckaert, C. Y. Wang, T. R. Ward, J. Wilhelmy, E. A. Winzeler, Y. Yang, G. Yen, E. Youngman, K. Yu, H. Bussey, J. D. Boeke, M. Snyder, P. Philippsen, R. W. Davis, and M. Johnston. 2002. Functional profiling of the *Saccharomyces cerevisiae* genome. *Nature* 418:387-391.

Gietz, R. D. and R. A. Woods. 2002. Transformation of yeast by lithium acetate/single-stranded carrier DNA/polyethylene glycol method. *Methods Enzymol.* 350:87-96.

Girzalsky, W., P. Rehling, K. Stein, J. Kipper, L. Blank, W. H. Kunau, and R. Erdmann. 1999. Involvement of Pex13p in Pex14p localization and peroxisomal targeting signal 2-dependent protein import into peroxisomes. *J. Cell Biol.* 144:1151-1162.

Glover, J. R., D. W. Andrews, S. Subramani, and R. A. Rachubinski. 1994. Mutagenesis of the amino targeting signal of *Saccharomyces cerevisiae* 3-ketoacyl-CoA thiolase reveals conserved amino acids required for import into peroxisomes in vivo. *J. Biol. Chem.* 269:7558-7563.

Goodman, J. M., S. B. Trapp, H. Hwang, and M. Veenhuis. 1990. Peroxisomes induced in *Candida boidinii* by methanol, oleic acid and D-alanine vary in metabolic function but share common integral membrane proteins. *J. Cell Sci.* 97 (1):193-204.

Götte, K., W. Girzalsky, M. Linkert, E. Baumgart, S. Kammerer, W. H. Kunau, and R. Erdmann. 1998. Pex19p, a farnesylated protein essential for peroxisome biogenesis. *Mol. Cell. Biol.* 18:616-628.

Gould, S. J., G. A. Keller, N. Hosken, J. Wilkinson, and S. Subramani. 1989. A conserved tripeptide sorts proteins to peroxisomes. *J. Cell Biol.* 108:1657-1664.

Gould, S.J., G. A. Keller, and S. Subramani. 1988. Identification of peroxisomal targeting signals located at the carboxy terminus of four peroxisomal proteins. *J. Cell Biol.* 107:897-905.

Gould, S. J., S. Krisans, G. A. Keller, and S. Subramani. 1990. Antibodies directed against the peroxisomal targeting signal of firefly luciferase recognize multiple mammalian peroxisomal proteins. *J. Cell Biol.* 110:27-34.

Gould, S. J., G. V. Raymond, and D. Valle. 2001. The peroxisome biogenesis disorders. *In* The Metabolic and Molecular Bases of Inherited Disease. C. R. Scriver, A. L. Beaudet, D. Valle, and W. S. Sly, editors. McGraw-Hill, New York. 3181-3217.

Gunkel, K., R. van Dijk, M. Veenhuis, and I. J. van der Klei. 2004. Routing of *Hansenula polymorpha* alcohol oxidase: an alternative peroxisomal protein-sorting machinery. *Mol. Biol. Cell* 15:1347-1355.

Guo, T., Y. Y. Kit, J. M. Nicaud, M. T. Le Dall, S. K. Sears, H. Vali, H. Chan, R. A. Rachubinski, and V. I. Titorenko. 2003. Peroxisome division in the yeast *Yarrowia lipolytica* is regulated by a signal from inside the peroxisome. *J. Cell Biol.* 162:1255-1266.

Hammond, A. T. and B. S. Glick. 2000. Raising the speed limits for 4D fluorescence microscopy. *Traffic* 1:935-940.

Harlow, E. and D. Lane. 1988. Antibodies: A Laboratory Manual. Cold Spring Harbor Laboratory, Cold Spring Harbor, NY. 63-70.

Hettema, E. H., B. Distel, and H. F. Tabak. 1999. Import of proteins into peroxisomes. *Biochim. Biophys. Acta* 1451:17-34.

Hettema, E. H., W. Girzalsky, M. van den Berg, R. Erdmann, and B. Distel. 2000. *Saccharomyces cerevisiae* Pex3p and Pex19p are required for proper localization and stability of peroxisomal membrane proteins. *EMBO J.* 19:223-233.

Hoepfner, D., M. van den Berg, P. Philippsen, H. F. Tabak, and E. H. Hettema. 2001. A role for Vps1p, actin, and the Myo2p motor in peroxisome abundance and inheritance in *Saccharomyces cerevisiae*. *J. Cell Biol.* 155:979-990.

Höhfeld, J., M. Veenhuis, and W. H. Kunau. 1991. *PAS3*, a *Saccharomyces cerevisiae* gene encoding a peroxisomal integral membrane protein essential for peroxisome biogenesis. *J. Cell Biol.* 114:1167-1178.

Honsho, M., S. Tamura, N. Shimozawa, Y. Suzuki, N. Kondo, and Y. Fujiki. 1998. Mutation in *PEX16* is causal in the peroxisome-deficient Zellweger syndrome of complementation group D. *Am. J. Hum. Genet.* 63:1622-1630.

Huh, W. K., J. V. Falvo, L. C. Gerke, A. S. Carroll, R. W. Howson, J. S. Weissman, and E. K. O'Shea. 2003. Global analysis of protein localization in budding yeast. *Nature* 425:686-691.

Huhse, B., P. Rehling, M. Albertini, L. Blank, K. Meller, and W. H. Kunau. 1998. Pex17p of *Saccharomyces cerevisiae* is a novel peroxin and component of the peroxisomal protein translocation machinery. *J. Cell Biol.* 140:49-60.

Huynh, T. V., R. A. Young, and R. W. Davis. 1985. DNA Cloning: A Practical Approach. IRL Press, Oxford.

Imanaka, T., G. M. Small, and P. B. Lazarow. 1987. Translocation of acyl-CoA oxidase into peroxisomes requires ATP hydrolysis but not a membrane potential. *J. Cell Biol.* 105:2915-2922.

Innis, M. A. and D. H. Gelfand. 1990. Optimization of PCRs. *In* PCR Protocols: A Guide to Methods and Applications. M. A. Innis, D. H. Gelfand, J. J. Sninsky, and T. J. White, editors. Academic Press, San Diego, 3-12.

Jones, J. M., J. C. Morrell, and S. J. Gould. 2004. PEX19 is a predominantly cytosolic chaperone and import receptor for class 1 peroxisomal membrane proteins. *J. Cell Biol.* 164:57-67.

Jun, Y., R. A. Fratti, and W. Wickner. 2004. Diacylglycerol and its formation by phospholipase C regulate Rab- and SNARE-dependent yeast vacuole fusion. *J. Biol. Chem.* 279:53186-53195.

Kamiryo, T., M. Abe, K. Okazaki, S. Kato, and N. Shimamoto. 1982. Absence of DNA in peroxisomes of *Candida tropicalis*. *J. Bacteriol.* 152:269-274.

Kerscher, S. J., A. Eschemann, P. M. Okun, and U. Brandt. 2001. External alternative NADH:ubiquinone oxidoreductase redirected to the internal face of the mitochondrial inner membrane rescues complex I deficiency in *Yarrowia lipolytica*. *J. Cell Sci.* 114:3915-3921.

Klein, A. T., M.van den Berg, G. Bottger, H. F. Tabak, and B. Distel. 2002. *Saccharomyces cerevisiae* acyl-CoA oxidase follows a novel, non-PTS1, import pathway into peroxisomes that is dependent on Pex5p. *J. Biol. Chem.* 277:25011-25019.

Koch, A., M. Thiemann, M. Grabenbauer, Y. Yoon, M. A. McNiven, and M. Schrader. 2003. Dynamin-like protein 1 is involved in peroxisomal fission. *J. Biol. Chem.* 278:8597-8605.

Koller, A., W. B. Snyder, K. N. Faber, T. J. Wenzel, L. Rangell, G. A. Keller, and S. Subramani. 1999. Pex22p of *Pichia pastoris*, essential for peroxisomal matrix protein import, anchors the ubiquitin-conjugating enzyme, Pex4p, on the peroxisomal membrane. *J. Cell Biol.* 146:99-112.

Kragler, F., A. Langeder, J. Raupachova, M. Binder, and A. Hartig. 1993. Two independent peroxisomal targeting signals in catalase A of *Saccharomyces cerevisiae*. *J. Cell Biol.* 120:665-673.

Krogh, A., B. Larsson, G. von Heijne, and E. L. Sonnhammer. 2001. Predicting transmembrane protein topology with a hidden Markov model: application to complete genomes. *J. Mol. Biol.* 305:567-580.

Kunau, W. H., S. Buhne, M. de la Garza, C. Kionka, M. Mateblowski, U. Schultz-Borchard, and R. Thieringer. 1988. Comparative enzymology of β-oxidation. *Biochem. Soc. Trans.* 16:418-420.

Lambkin, G. R. and R. A. Rachubinski. 2001. *Yarrowia lipolytica* cells mutant for the peroxisomal peroxin Pex19p contain structures resembling wild-type peroxisomes. *Mol. Biol. Cell* 12:3353-3364.

Lazarow, P. B. and Y. Fujiki. 1985. Biogenesis of peroxisomes. *Annu. Rev. Cell Biol.* 1:489-530.

Lazarow, P. B. and H. W. Moser. 1994. Disorders of peroxisome biogenesis. *In* The Metabolic Basis of Inherited Disease. A. L. Beaudet, W. S. Sly, and A. D. Valle, editors. McGraw-Hill, New York. 2287-2324.

Li, X., E. Baumgart, G. X. Dong, J. C. Morrell, G. Jimenez-Sanchez, D. Valle, K. D. Smith, and S. J. Gould. 2002. PEX11α is required for peroxisome proliferation in response to 4-phenylbutyrate but is dispensable for peroxisome proliferator-activated receptor α-mediated peroxisome proliferation. *Mol. Cell. Biol.* 22:8226-8240.

Li, X. and S. J. Gould. 2002. PEX11 promotes peroxisome division independently of peroxisome metabolism. *J. Cell Biol.* 156:643-651.

Lisenbee, C. S., M. Heinze, and R. N. Trelease. 2003. Peroxisomal ascorbate peroxidase resides within a subdomain of rough endoplasmic reticulum in wild-type Arabidopsis cells. *Plant Physiol.* 132:870-882.

Longtine, M. S., A. McKenzie III, D. J. Demarini, N. G. Shah, A. Wach, A. Brachat, P. Philippsen, and J. R. Pringle. 1998. Additional modules for versatile and economical PCR-based gene deletion and modification in *Saccharomyces cerevisiae*. *Yeast* 14:953-961.

Lopez-Huertas, E., J. Oh, and A. Baker. 1999. Antibodies against Pex14p block ATP-independent binding of matrix proteins to peroxisomes in vitro. *FEBS Lett.* 459:227-229.

Lorenz, P., A. G. Maier, E. Baumgart, R. Erdmann, and C. Clayton. 1998. Elongation and clustering of glycosomes in *Trypanosoma brucei* overexpressing the glycosomal Pex11p. *EMBO J.* 17:3542-3555.

Lück, H. 1963. Catalase. *In* Methods of Enzymatic Analysis. H. U. Bergmeyer, editor. Academic Press, New York. 885-888.

Maniatis, T., E. F. Fritsch, and J. Sambrook. 1982. Molecular Cloning: A Laboratory Manual. Cold Spring Harbor Laboratory, Cold Spring Harbor.

Marelli, M., J. J. Smith, S. Jung, E. Yi, A. I. Nesvizhskii, R. H. Christmas, R. A. Saleem, Y. Y. C. Tam, A. Fagarasanu, D. R. Goodlett, R. Aebersold, R. A. Rachubinski, and J. D. Aitchison. 2004. Quantitative mass spectrometry reveals a role for the GTPase Rho1p in actin organization on the peroxisome membrane. *J. Cell Biol.* 167:1099-1112.

Marshall, P. A., J. M. Dyer, M. E. Quick, and J. M. Goodman. 1996. Redox-sensitive homodimerization of Pex11p: a proposed mechanism to regulate peroxisomal division. *J. Cell Biol.* 135:123-137.

Marshall, P. A., Y. I. Krimkevich, R. H. Lark, J. M. Dyer, M. Veenhuis, and J. M. Goodman. 1995. Pmp27 promotes peroxisomal proliferation. *J. Cell Biol.* 129:345-355.

Matsumoto, N., S. Tamura, and Y. Fujiki. 2003. The pathogenic peroxin Pex26p recruits the Pex1p-Pex6p AAA ATPase complexes to peroxisomes. *Nat. Cell Biol.* 5:454-460.

Matsuzono, Y., N. Kinoshita, S. Tamura, N. Shimozawa, M. Hamasaki, K. Ghaedi, R. J. Wanders, Y. Suzuki, N. Kondo, and Y. Fujiki. 1999. Human *PEX19*: cDNA cloning by functional complementation, mutation analysis in a patient with Zellweger syndrome, and potential role in peroxisomal membrane assembly. *Proc. Natl. Acad. Sci. U. S. A.* 96:2116-2121.

McCammon, M. T., J. A. McNew, P. J. Willy, and J. M. Goodman. 1994. An internal region of the peroxisomal membrane protein PMP47 is essential for sorting to peroxisomes. *J. Cell Biol.* 124:915-925.

Needleman, R. B. and A. Tzagoloff. 1975. Breakage of yeast: a method for processing multiple samples. *Anal. Biochem.* 64:545-549.

Nuttley, W. M., A. M. Brade, C. Gaillardin, G. A. Eitzen, J. R. Glover, J. D. Aitchison, and R. A. Rachubinski. 1993. Rapid identification and characterization of peroxisomal assembly mutants in *Yarrowia lipolytica*. *Yeast* 9:507-517.

Okumoto, K., I. Abe, and Y. Fujiki. 2000. Molecular anatomy of the peroxin Pex12p: ring finger domain is essential for Pex12p function and interacts with the peroxisome-targeting signal type 1-receptor Pex5p and a ring peroxin, Pex10p. *J. Biol. Chem.* 275:25700-25710.

Osumi, T., T. Tsukamoto, S. Hata, S. Yokota, S. Miura, Y. Fujiki, M. Hijikata, S. Miyazawa, and T. Hashimoto. 1991. Amino-terminal presequence of the precursor of peroxisomal 3-ketoacyl-CoA thiolase is a cleavable signal peptide for peroxisomal targeting. *Biochem. Biophys. Res. Commun.* 181:947-954.

Otera, H., T. Harano, M. Honsho, K. Ghaedi, S. Mukai, A. Tanaka, A. Kawai, N. Shimizu, and Y. Fujiki. 2000. The mammalian peroxin Pex5pL, the longer isoform of the mobile peroxisome targeting signal (PTS) type 1 transporter, translocates the Pex7p·PTS2 protein complex into peroxisomes via its initial docking site, Pex14p. *J. Biol. Chem.* 275:21703-21714.

Passreiter, M., M. Anton, D. Lay, R. Frank, C. Harter, F. T. Wieland, K. Gorgas, and W. W. Just. 1998. Peroxisome biogenesis: involvement of ARF and coatomer. *J. Cell Biol.* 141:373-383.

Pause, B., R. Saffrich, A. Hunziker, W. Ansorge, and W. W. Just. 2000. Targeting of the 22 kDa integral peroxisomal membrane protein. *FEBS Lett.* 471:23-28.

Pool, M. R. , E. Lopez-Huertas, and A. Baker. 1998. Characterization of intermediates in the process of plant peroxisomal protein import. *EMBO J.* 17:6854-6862.

Pringle, J. R., A. E. Adams, D. G. Drubin, and B. K. Haarer. 1991. Immunofluorescence methods for yeast. *Methods Enzymol.* 194:565-602.

Promega Protocols and Applications Guide. 1989/90.

Purdue, P. E. and P. B. Lazarow. 2001. Peroxisome biogenesis. *Annu. Rev. Cell Dev. Biol.* 17:701-752.

Purdue, P. E., Y. Takada, and C. J. Danpure. 1990. Identification of mutations associated with peroxisome-to-mitochondrion mistargeting of alanine/glyoxylate aminotransferase in primary hyperoxaluria type 1. *J. Cell Biol.* 111:2341-2351.

Purdue, P. E., X. Yang, and P. B. Lazarow. 1998. Pex18p and Pex21p, a novel pair of related peroxins essential for peroxisomal targeting by the PTS2 pathway. *J. Cell Biol.* 143:1859-1869.

Reddy, J. K. and G. P. Mannaerts. 1994. Peroxisomal lipid metabolism. *Annu. Rev. Nutr.* 14:343-370.

Rehling, P., A. Skaletz-Rorowski, W. Girzalsky, T. Voorn-Brouwer, M. M. Franse, B. Distel, M. Veenhuis, W. H. Kunau, and R. Erdmann. 2000. Pex8p, an intraperoxisomal peroxin of *Saccharomyces cerevisiae* required for protein transport into peroxisomes binds the PTS1 receptor Pex5p. *J. Biol. Chem.* 275:3593-3602.

Rhodin, J. Correlation of ultrastructural organization and function in normal and experimentally changed convoluted tubule cells of the mouse kidney. 1954. Ph.D. Thesis, Karolinska Institutet Stockholm, Stockholm.

Rose, M. D., F. Winston, and P. Heiter. 1988. Laboratory Course Manual for Methods in Yeast Genetics. Cold Spring Harbor Laboratory, Cold Spring Harbor.

Rottensteiner, H., A. Kramer, S. Lorenzen, K. Stein, C. Landgraf, R. Volkmer-Engert, and R. Erdmann. 2004. Peroxisomal membrane proteins contain common Pex19p-binding sites that are an integral part of their targeting signals. *Mol. Biol. Cell* 15:3406-3417.

Sacksteder, K. A., J. M. Jones, S. T. South, X. Li, Y. Liu, and S. J. Gould. 2000. PEX19 binds multiple peroxisomal membrane proteins, is predominantly cytoplasmic, and is required for peroxisome membrane synthesis. *J. Cell Biol.* 148:931-944.

Saiki, R. K. 1990. Amplification of genomic DNA. *In* PCR Protocols: A Guide to Methods and Applications. M. A. Innis, D. H. Gelfand, J. J. Sninsky, and T. J. White, editors. Academic Press, San Diego. 13-21.

Sakai, Y., P. A. Marshall, A. Saiganji, K. Takabe, H. Saiki, N. Kato, and J. M. Goodman. 1995. The *Candida boidinii* peroxisomal membrane protein Pmp30 has a role in peroxisomal proliferation and is functionally homologous to Pmp27 from *Saccharomyces cerevisiae*. *J. Bacteriol.* 177:6773-6781.

Salomons, F. A., I. J. van der Klei, A. M. Kram, W. Harder, and M. Veenhuis. 1997. Brefeldin A interferes with peroxisomal protein sorting in the yeast *Hansenula polymorpha*. *FEBS Lett.* 411:133-139.

Sanger, F., S. Nicklen, and A. R. Coulson. 1977. DNA sequencing with chain-terminating inhibitors. *Proc. Natl. Acad. Sci. U. S. A.* 74:5463-5467.

Santos, M. J., T. Imanaka, H. Shio, G. M. Small, and P. B. Lazarow. 1988. Peroxisomal membrane ghosts in Zellweger syndrome-aberrant organelle assembly. *Science* 239:1536-1538.

Scholz, O., A. Thiel, W. Hillen, and M. Niederweis. 2000. Quantitative analysis of gene expression with an improved green fluorescent protein. *Eur. J. Biochem.* 267:1565-1570.

Schrader, M., B. E. Reuber, J. C. Morrell, G. Jimenez-Sanchez, C. Obie, T. A. Stroh, D. Valle, T. A. Schroer, and S. J. Gould. 1998. Expression of PEX11β mediates peroxisome proliferation in the absence of extracellular stimuli. *J. Biol. Chem.* 273:29607-29614.

Shaner, N. C., R. E. Campbell, P. A. Steinbach, B. N. Giepmans, A. E. Palmer, and R. Y. Tsien. 2004. Improved monomeric red, orange and yellow fluorescent proteins derived from *Discosoma sp.* red fluorescent protein. *Nat. Biotechnol.* 22:1567-1572.

Sichting, M., A. Schell-Steven, H. Prokisch, R. Erdmann, and H. Rottensteiner. 2003. Pex7p and Pex20p of *Neurospora crassa* function together in PTS2-dependent protein import into peroxisomes. *Mol. Biol. Cell* 14:810-821.

Sikorski, R. S. and P. Hieter. 1989. A system of shuttle vectors and yeast host strains designed for efficient manipulation of DNA in *Saccharomyces cerevisiae*. *Genetics* 122:19-27.

Smith, J. J. Maintenance of Peroxisomes in the Yeast *Yarrowia lipolytica*. 2000. Ph.D. Thesis, University of Alberta, Alberta.

Smith, J. J., T. W. Brown, G. A. Eitzen, and R. A. Rachubinski. 2000. Regulation of peroxisome size and number by fatty acid β-oxidation in the yeast *Yarrowia lipolytica*. *J. Biol. Chem.* 275:20168-20178.

Smith, J. J., M. Marelli, R. H. Christmas, F. J. Vizeacoumar, D. J. Dilworth, T. Ideker, T. Galitski, K. Dimitrov, R. A. Rachubinski, and J. D. Aitchison. 2002. Transcriptome profiling to identify genes involved in peroxisome assembly and function. *J. Cell Biol.* 158:259-271.

Smith, J. J. and R. A. Rachubinski. 2001. A role for the peroxin Pex8p in Pex20p-dependent thiolase import into peroxisomes of the yeast *Yarrowia lipolytica*. *J. Biol. Chem.* 276:1618-1625.

Snyder, W. B., A. Koller, A. J. Choy, and S. Subramani. 2000. The peroxin Pex19p interacts with multiple, integral membrane proteins at the peroxisomal membrane. *J. Cell Biol.* 149:1171-1178.

South, S. T., E. Baumgart, and S. J. Gould. 2001. Inactivation of the endoplasmic reticulum protein translocation factor, Sec61p, or its homolog, Ssh1p, does not affect peroxisome biogenesis. *Proc. Natl. Acad. Sci. U. S. A.* 98:12027-12031.

South, S. T. and S. J. Gould. 1999. Peroxisome synthesis in the absence of preexisting peroxisomes. *J. Cell Biol.* 144:255-266.

South, S. T., K. A. Sacksteder, X. Li, Y. Liu, and S. J. Gould. 2000. Inhibitors of COPI and COPII do not block *PEX3*-mediated peroxisome synthesis. *J. Cell Biol.* 149:1345-1360.

Stein, K., A. Schell-Steven, R. Erdmann, and H. Rottensteiner. 2002. Interactions of Pex7p and Pex18p/Pex21p with the peroxisomal docking machinery: implications for the first steps in PTS2 protein import. *Mol. Cell. Biol.* 22:6056-6069.

Subramani, S. 1998. Components involved in peroxisome import, biogenesis, proliferation, turnover, and movement. *Physiol. Rev.* 78:171-188.

Subramani, S. 1993. Protein import into peroxisomes and biogenesis of the organelle. *Annu. Rev. Cell Biol.* 9:445-478.

Subramani, S., A. Koller, and W. B. Snyder. 2000. Import of peroxisomal matrix and membrane proteins. *Annu. Rev. Biochem.* 69:399-418.

Swartzman, E. E., M. N. Viswanathan, and J. Thorner. 1996. The *PAL1* gene product is a peroxisomal ATP-binding cassette transporter in the yeast *Saccharomyces cerevisiae*. *J. Cell Biol.* 132:549-563.

Swinkels, B. W., S. J. Gould, A. G. Bodnar, R. A. Rachubinski, and S. Subramani. 1991. A novel, cleavable peroxisomal targeting signal at the amino-terminus of the rat 3-ketoacyl-CoA thiolase. *EMBO J.* 10:3255-3262.

Swinkels, B. W., S. J. Gould, and S. Subramani. 1992. Targeting efficiencies of various permutations of the consensus C-terminal tripeptide peroxisomal targeting signal. *FEBS Lett.* 305:133-136.

Szilard,R. K. Identification and Characterization of *Yl*Pex5p, a Component of the Peroxisomal Tranlocation Machinery of *Yarrowia lipolytica*. 2000. Ph.D. Thesis, University of Alberta, Alberta.

Szilard, R. K. and R. A. Rachubinski. 2000. Tetratricopeptide repeat domain of *Yarrowia lipolytica* Pex5p is essential for recognition of the type 1 peroxisomal targeting signal but does not confer full biological activity on Pex5p. *Biochem. J.* 346 (1):177-184.

Szilard, R. K., V. I. Titorenko, M. Veenhuis, and R. A. Rachubinski. 1995. Pay32p of the yeast *Yarrowia lipolytica* is an intraperoxisomal component of the matrix protein translocation machinery. *J. Cell Biol.* 131:1453-1469.

Tabak, H. F., I. Braakman, and B. Distel. 1999. Peroxisomes: simple in function but complex in maintenance. *Trends Cell Biol.* 9:447-453.

Tam, Y. Y. C. and R. A. Rachubinski. 2002. *Yarrowia lipolytica* cells mutant for the *PEX24* gene encoding a peroxisomal membrane peroxin mislocalize peroxisomal proteins and accumulate membrane structures containing both peroxisomal matrix and membrane proteins. *Mol. Biol. Cell* 13:2681-2691.

Tam, Y. Y. C., J. C. Torres-Guzman, F. J. Vizeacoumar, J. J. Smith, M. Marelli, J. D. Aitchison, and R. A. Rachubinski. 2003. Pex11-related proteins in peroxisome dynamics: a role for the novel peroxin Pex27p in controlling peroxisome size and number in *Saccharomyces cerevisiae*. *Mol. Biol. Cell* 14:4089-4102.

Tanaka, A., K. Okumoto, and Y. Fujiki. 2003. cDNA cloning and characterization of the third isoform of human peroxin Pex11p. *Biochem. Biophys. Res. Commun.* 300:819-823.

Terlecky, S. R. and M. Fransen. 2000. How peroxisomes arise. *Traffic* 1:465-473.

Thieringer, R., H. Shio, Y. S. Han, G. Cohen, and P. B. Lazarow. 1991. Peroxisomes in *Saccharomyces cerevisiae*: immunofluorescence analysis and import of catalase A into isolated peroxisomes. *Mol. Cell. Biol.* 11:510-522.

Titorenko, V. I., H. Chan, and R. A. Rachubinski. 2000. Fusion of small peroxisomal vesicles *in vitro* reconstructs an early step in the *in vivo* multistep peroxisome assembly pathway of *Yarrowia lipolytica*. *J. Cell Biol.* 148:29-44.

Titorenko, V. I., G. A. Eitzen, and R. A. Rachubinski. 1996. Mutations in the *PAY5* gene of the yeast *Yarrowia lipolytica* cause the accumulation of multiple subpopulations of peroxisomes. *J. Biol. Chem.* 271:20307-20314.

Titorenko, V. I., D. M. Ogrydziak, and R. A. Rachubinski. 1997. Four distinct secretory pathways serve protein secretion, cell surface growth, and peroxisome biogenesis in the yeast *Yarrowia lipolytica*. *Mol. Cell. Biol.* 17:5210-5226.

Titorenko, V. I. and R. A. Rachubinski. 2001. The life cycle of the peroxisome. *Nat. Rev. Mol. Cell Biol.* 2:357-368.

Titorenko, V. I. and R. A. Rachubinski. 1998. The endoplasmic reticulum plays an essential role in peroxisome biogenesis. *Trends Biochem. Sci.* 23:231-233.

Titorenko, V. I., J. J. Smith, R. K. Szilard, and R. A. Rachubinski. 1998. Pex20p of the yeast *Yarrowia lipolytica* is required for the oligomerization of thiolase in the cytosol and for its targeting to the peroxisome. *J. Cell Biol.* 142:403-420.

Towbin, H., T. Staehelin, and J. Gordon. 1979. Electrophoretic transfer of proteins from polyacrylamide gels to nitrocellulose sheets: procedure and some applications. *Proc. Natl. Acad. Sci. U. S. A.* 76:4350-4354.

Tsukamoto, T., S. Miura, and Y. Fujiki. 1991. Restoration by a 35K membrane protein of peroxisome assembly in a peroxisome-deficient mammalian cell mutant. *Nature* 350:77-81.

Tsukamoto, T., S. Yokota, and Y. Fujiki. 1990. Isolation and characterization of Chinese hamster ovary cell mutants defective in assembly of peroxisomes. *J. Cell Biol.* 110:651-660.

van Roermund, C. W., H. F. Tabak, M. van den Berg, R. J. Wanders, and E. H. Hettema. 2000. Pex11p plays a primary role in medium-chain fatty acid oxidation, a process that affects peroxisome number and size in *Saccharomyces cerevisiae. J. Cell Biol.* 150:489-498.

van der Klei, I. J., R. E. Hilbrands, J. A. Kiel, S. W. Rasmussen, J. M. Cregg, and M. Veenhuis. 1998. The ubiquitin-conjugating enzyme Pex4p of *Hansenula polymorpha* is required for efficient functioning of the PTS1 import machinery. *EMBO J.* 17:3608-3618.

van der Klei, I. J. and M. Veenhuis. 1997. Yeast peroxisomes: function and biogenesis of a versatile cell organelle. *Trends Microbiol.* 5:502-509.

Veenhuis, M. and W. Harder. 1987. Metabolic significance and biogenesis of microbodies in yeasts. *In* Peroxisomes in Biology and Medicine. H. D. Fahimi and H. Sies, editors. Springer-Verlag, Berlin. 436-458.

Veenhuis, M., M. Mateblowski, W. H. Kunau, and W. Harder. 1987. Proliferation of microbodies in *Saccharomyces cerevisiae. Yeast* 3:77-84.

Vizeacoumar, F. J., J. C. Torres-Guzman, D. Bouard, J. D. Aitchison, and R. A. Rachubinski. 2004. Pex30p, Pex31p, and Pex32p form a family of peroxisomal integral membrane proteins regulating peroxisome size and number in *Saccharomyces cerevisiae. Mol. Biol. Cell* 15:665-677.

Vizeacoumar, F. J., J. C. Torres-Guzman, Y. Y. C. Tam, J. D. Aitchison, and R. A. Rachubinski. 2003. *YHR150w* and *YDR479c* encode peroxisomal integral membrane proteins involved in the regulation of peroxisome number, size, and distribution in *Saccharomyces cerevisiae*. *J. Cell Biol.* 161:321-332.

Voorn-Brouwer, T., A. Kragt, H. F. Tabak, and B. Distel. 2001. Peroxisomal membrane proteins are properly targeted to peroxisomes in the absence of COPI- and COPII-mediated vesicular transport. *J. Cell Sci.* 114:2199-2204.

Walton, P. A., P. E. Hill, and S. Subramani. 1995. Import of stably folded proteins into peroxisomes. *Mol. Biol. Cell* 6:675-683.

Wang, H. J., M. T. Le Dall, Y. Wach, C. Laroche, J. M. Belin, C. Gaillardin, and J. M. Nicaud. 1999. Evaluation of acyl coenzyme A oxidase (Aox) isozyme function in the n-alkane-assimilating yeast *Yarrowia lipolytica*. *J. Bacteriol.* 181:5140-5148.

Ward, W. W. 1998. Green Fluorescent Protein: Properties, Applications, and Protocols. Wiley, New York. 45-75.

Waterham, H. R., V. I. Titorenko, P. Haima, J. M. Cregg, W. Harder, and M. Veenhuis. 1994. The *Hansenula polymorpha PER1* gene is essential for peroxisome biogenesis and encodes a peroxisomal matrix protein with both carboxy- and amino-terminal targeting signals. *J. Cell Biol.* 127:737-749.

Weibel, E .R. and P. Bolender. 1973. Stereological techniques for electron microscopic morphometry. *In* Principles and Techniques of Electron Microscopy. M. A. Hayat, editor. Van Nostrand Reinhold, New York. 237-296.

Weller, S., S. J. Gould, and D. Valle. 2003. Peroxisome biogenesis disorders. *Annu. Rev. Genomics Hum. Genet.* 4:165-211.

Winzeler, E. A., D. D. Shoemaker, A. Astromoff, H. Liang, K. Anderson, B. André, R. Bangham, R. Benito, J. D. Boeke, H. Bussey, A. M. Chu, C. Connelly, K. Davis, F. Dietrich, S. W. Dow, M. El Bakkoury, F. Foury, S. H. Friend, E. Gentalen, G. Giaever, J. H. Hegemann, T. Jones, M. Laub, H. Liao, N. Liebundguth, D. J. Lockhart, A. Lucau-Danila, M. Lussier, N. M'Rabet, P. Menard, M. Mittmann, C. Pai, C. Rebischung, J. L. Revuelta, L. Riles, C. J. Roberts, P. Ross-MacDonald, B. Scherens, M. Snyder, S. Sookhai-Mahadeo, R. K. Storms, S. Veronneau, M. Voet, G. Volckaert, T. R. Ward, R. Wysocki, G. S. Yen, K. Yu, K. Zimmermann,

P. Philippsen, M. Johnston and R. W. Davis. 1999. Functional characterization of the *S. cerevisiae* genome by gene deletion and parallel analysis. *Science* 285:901-906.